*UNIVERSITY OF NAPLES FEDERICO II*

*DEPARTMENT OF PHARMACY*

*PhD programme in Pharmaceutical Sciences*

# *Role of Sphingolipids in the development of chronic lung diseases*

*Elisabetta Granato*

**Coordinator**

**Prof.**

**ROSARIA MELI**

**Tutor**

**Prof. Fiorentina Roviezzo**

**Co-Tutor**

**Prof. Giuseppe Cirino**

*XXXVI CYCLE (2021-2023)*

## Table of contents

## Chapter 1

# Chapter 1

# 1. Introduction

## 1.1 Respiratory disease

The respiratory disease group includes any diseases and disorders of the lungs and the airway that affect human respiration.

Respiratory diseases usually affect any structures and organs implicated in breathing, like the nasal cavities, the pharynx, the trachea, the larynx, the bronchi and bronchioles, the lungs and all the respiratory muscles of the chest cage [1].

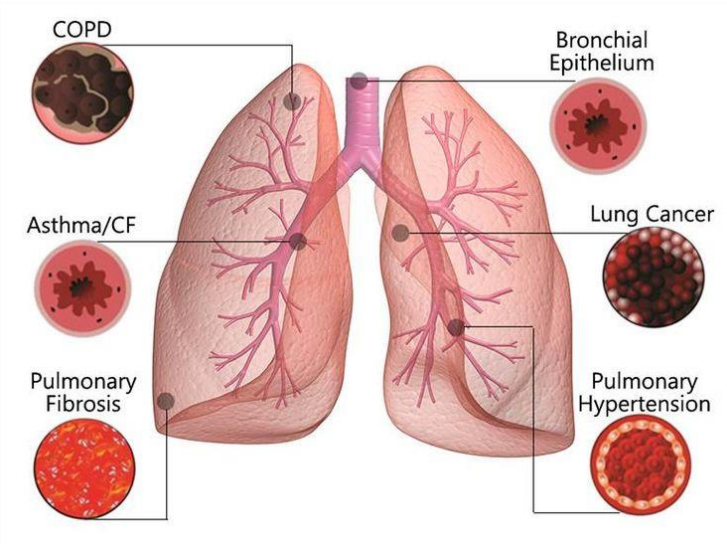


***Figure 1.1: respiratory disease***. diseases and disorders of the lungs and the airway that affect human respiration. *American lung association*.

The respiratory tract is very highly exposed to a large range of disorders for different reasons: first, it is exposed to the environment by inhaling dust, gases, or organisms. Then, it possesses a large network of capillaries, which means that diseases that affect the small blood vessels are likely to affect the lungs. And it could be the site of "sensitivity" or allergic reaction that may affect the functionality and the structure.

The main symptoms that characterize the respiratory disease are **cough**, an important sign of all diseases that affect any part of the bronchial tree. The cough productive of sputum is the most important manifestation of severe inflammatory disease of major airways (bronchitis for example).

The **dyspnea**, the second most important symptom of lung disease, is essentially shortness of breath; this kind of symptom may arise acutely with the onset of a severe attack of asthma. Dyspnea varies in severity in the different diseases, but in pulmonary emphysema, with irreversible lung damage, and lung fibrosis, with an invasion of lung elastic tissue with connective tissues, it is constantly severe and present.

**Chest pain** could be an early symptom of lung diseases, and is usually associated with pneumonia attack, due to a pleura inflammation.

In addition to these major symptoms, we can remember the wheeziness, caused by the narrowing of the airways, such as occur in asthma. Again, we can have a symptom associated with the swelling of fingertips commonly called "clubbing"; it could be a feature of bronchiectasis, fibrosis, and lung cancer [1].

### 1.1.1 Defenses of the respiratory system

The respiratory tract possesses a complicated series of defenses against inhaled material, as a defence from the outside environment. First, the air passes through the nose, in which the large particles are filtered out by cilia

and mucus secreted from the mucous membranes of the nasal cavity. The air then travels through the pharynx, the last part of the upper airway, through the larynx, the beginning part of the lower airways, and through the trachea. A second filtration of air is made from the mucus and the cilia in the trachea. Furthermore, the lymphatic vessels in the wall of the trachea bring the cells of the immunity system like macrophages and lymphocytes, that can destroy the remaining particles. Also, the muscle of the trachea plays a key role in the defence mechanism of the airways, expelling substances inhaled from the respiratory tract with sputum and cough. Reaching the bronchial tree, the cilia move in unison in one direction, moving substances up and out of the airways. In bronchioles and small bronchi there is a thin layer of fluid covering the cilia, this layer increases in thickness in the large bronchi, and the cilia transport the substance along the fluid toward the exit. This system is known as a mucociliary escalator.

The first line of defence in the smaller branches of the airways is the macrophages, immune cells located within the alveoli of the lungs that can destroy and remove bacteria, viruses, and small particles. They are also able to release chemical agents that retrieve other immune cells, like lymphocytes, on the site of infection, in this way, they can start the inflammatory response in the lung. The particles attacked by macrophages are then carried to the lymphatic system of the lung and removed through lung lymph nodes [1].

### 1.1.2 Chronic respiratory diseases

Asthma and Chronic obstructive pulmonary disease (COPD) are two of the most common chronic respiratory diseases. Both affect the airway in the lungs, in particular, asthma is characterized by recurrent attacks of breathlessness and wheezing due to airway narrowing, this symptom can vary in severity and frequency from person to person. On the other hand, COPD only affects adults

and usually becomes worse with time, the most common symptoms are breathlessness with the need for air, sputum production, and a chronic cough. In asthma, most of the time, the airway obstruction is reversible with inhaled medicines, conversely in COPD it is mostly fixed.

The main risk factors for both chronic respiratory diseases include tobacco smoking (including second-hand smoke), air pollution, allergens, and occupational risks. There are also common causes, outdoor air pollution and indoor air pollution (often caused by cooking with solid fuels). Asthma and COPD may be prevented by reducing or avoiding exposure to these risk factors [2].

## 1.2 Asthma

Asthma is a common chronic respiratory disease associated with inflammation of the lower respiratory tract [3].

The National Institute of Health Guidelines on Asthma (NIH Guidelines) define asthma as follows: “Asthma is a chronic inflammatory disorder of the airways in which many cells and cellular elements play a role: in particular, mast cells, eosinophils, T lymphocytes, macrophages, neutrophils, and epithelial cells.

In susceptible individuals, this inflammation causes recurrent episodes of wheezing, breathlessness, chest tightness, and coughing, particularly at night or in the early morning. These episodes are usually associated with widespread but variable airflow obstruction that is often reversible either spontaneously or with treatment. The inflammation also causes an associated increase in the existing bronchial hyperresponsiveness to a variety of stimuli. Reversibility of airflow limitation may be incomplete in some patients with asthma.”

This definition underlines the presence of inflammation and resulting symptoms without reference to cause, which is not fully known, or natural history, which is variable [4].

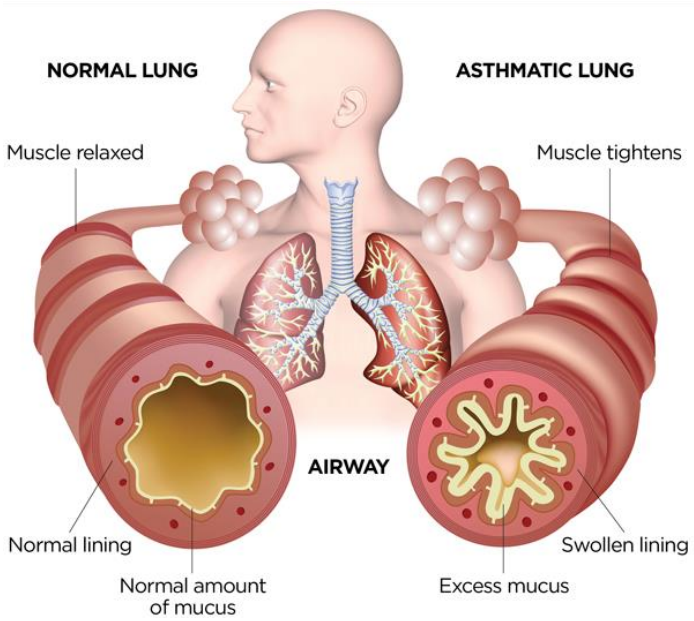


***Figure 1.2: Asthma***. Schematic representation of what happens in the airway with asthma disease. *Source: American Thoracic Society*.

### 1.2.1 Asthma etiology

The causes of asthma are not known but have been identified the principal risk factors and gene-environment interactions that could underly the disease [5]. Genetics are known to play an important role in asthma susceptibility, ranging between 35% and 95%. Different genetic studies have identified hundreds of genetic variants associated with an increased risk of asthma. Also, epigenetic variations, which are the translation of the genetic code, have a role in the development of asthma [6].

Respiratory infections, especially viral infections early in life, airborne environmental exposure (including tobacco smoke, pollutants, and ozone), atopic conditions, and sensitization to inhalant allergens are also associated with developing asthma. Other factors have been theorized to play a role in asthma development, among which: effects of the microbiome and metabolites, chemical exposure, vitamin D, dietary changes, and stress [7].
Therefore, current asthma understanding involves a broad amount of genetic diversity, which is variably translated and environmentally influenced via epigenetic and transcriptional factors, bringing less diverse histopathological features with resulting fundamental asthmatic symptoms.

### 1.2.2 Asthma pathophysiology

Understanding asthma pathophysiology can help to understand how to diagnose and treat the condition. Our knowledge of asthma pathogenesis has changed in the last 25 years, as researchers have found various asthma phenotypes. Asthma involves many pathophysiologic factors, including bronchiolar inflammation with airway constriction and resistance that manifests as episodes of coughing, shortness of breath, and wheezing. Asthma can affect the trachea, bronchi, and bronchioles. Bronchospasms, edema, excessive mucus, and epithelial and muscle damage can lead to bronchoconstriction with bronchospasm. Defined as strong contractions of bronchial smooth muscle, bronchospasm causes the airways to narrow; edema from microvascular leakage contributes to airway narrowing. Airway capillaries may dilate and leak, increasing secretions, which in turn causes edema and impairs mucus removal [8].

- **Bronchoconstriction.** In acute exacerbations of asthma, bronchoconstriction (the bronchial smooth muscle contraction) occurs quickly to narrow the airways in response to exposure to a variety of

stimuli including allergens or pollutants. Allergen-induced acute bronchoconstriction results from an IgE-dependent release of mediators from mast cells that includes histamine, tryptase, leukotrienes, and prostaglandins that directly contract airway smooth muscle [9]. Other agents, like nonsteroidal anti-inflammatory drugs, can also cause acute airflow obstruction, this is a non-IgE-dependent response that also involves the mediators released from airway cells [10]. In addition, other stimuli (including exercise, cold air, stress, and irritants) can cause acute airflow obstruction. The mechanisms regulating the airway response to these factors are not clear, but the intensity of the response appears related to underlying airway inflammation [11].

- **Airway hyperresponsiveness.** Airway hyperresponsiveness, which is an exaggerated bronchoconstrictor response to a variety of stimuli, is the major feature of asthma. The intensity of airway hyperresponsiveness can be defined by contractile responses to methacholine correlates with the clinical severity of asthma. The mechanisms underlying airway hyperresponsiveness are multiple and include inflammation and structural changes; inflammation seems to be a major factor in determining airway hyperresponsiveness for which, treatment for reducing inflammation can also reduce airway hyperresponsiveness and improve asthma control [11].
- **Airway edema.** when the disease becomes more persistent and inflammation more aggressive, other factors limit airflow, these include edema, inflammation, mucus hypersecretion and the formation of inspissated mucus plugs, as well as structural changes including hypertrophy and hyperplasia of the airway smooth muscle. These changes could not respond to usual treatment [11].

- **Airway remodeling.** The airflow limitation, in some patients with asthma, may be only partially reversible. That is because some permanent structural changes can occur in the airway; these alterations are collectively referred to as tissue remodeling and are associated with a progressive loss of lung function that is not fully reversible by current therapy. Airway remodeling involves the activation of many of the structural cells, with permanent changes in the airway that increase airflow obstruction and airway responsiveness [12]. These structural changes primarily occur in the mucosa and submucosa. Pathological changes in the mucosa include epithelial hyperplasia and metaplasia of goblet cells with increased mucus production. The submucosal change includes smooth muscle hypertrophy, collagen deposition, and larger mucous glands leading to narrower airways and increased mucous production during asthma episodes [13]. Regulation of the repair and remodeling process is not well established, but both are likely to be key events in explaining the persistent nature of the disease and limitations to a therapeutic response [11].
- **Cellular inflammation**. Asthma is a chronic inflammatory disease, so many of the principal symptoms are caused by the chronic inflammation of the lower airway. This inflammation is caused by a combination of genetic predisposition, environmental exposures, and possibly alterations in the microbiome and metabolite. We can have three different types of inflammatory responses, although the most common is type 2 [14].

-Th1 Response

The Th1 response is typically activated in infections, particularly viruses. Viruses upregulate interferon-γ and interleukin (IL) 27, which aid in eliminating the pathogen but also are involved in airway inflammation. Th1 responses are involved in the pathogenesis of organ-specific autoimmune disorders, Crohn's disease, sarcoidosis, and acute kidney allograft rejection [15].

-Th2 Response

In most cases, the asthmatic has type 2 inflammation, mediated by the type 2 T helper cell lymphocyte. Dendritic cells in the airway present inhaled allergens to naïve T-cells, which activate the production of Th2 cells [14]. Type 2 inflammation is associated with a specific cytokine profile including IL-4, IL-5, IL-9, and IL-13, IL-4, IL-9, and IL-13. The cytokines stimulate B cells to release IgE and other inflammatory cells, (eosinophils, mast cells, basophils, type 2 T helper lymphocytes). IgE then instigates mast cell degranulation and mediator release (histamine and leukotrienes) causing bronchoconstriction. These mechanisms are perpetuated by cytokines such as IL-25, IL-33, and thymic stromal lymphopoietin (TSLP). IL-25 induces expression of IL-4, IL-5, IL-9, and IL-13, while IL-33 activates dendritic cells to produce IL-5 and IL-13. IL-5 is important for maintaining eosinophils, while IL-9 and IL-13 contribute to mucous production [16].

This time of inflammation is commonly seen in allergic diseases, eosinophilic disorders, and parasite infections. Airway epithelial cells have also been identified to play an important role in regulating type 2 inflammation via cytokines (IL-25, IL-33, and thymic stromal lymphopoietin). Asthmatics without a strong bias toward type 2

inflammation often exhibit poor response to corticosteroids and can be difficult to manage [14].

-Th17 Response

Th17 cells produce IL-17 and IL-22, which induce asthma airway remodeling. IL-17 promotes neutrophilic airway infiltration and induces the airway epithelial to mesenchymal morphological transition, while IL-22 increases smooth muscle mass [16].

- **Biomarkers**. Traditional asthma biomarkers include eosinophils, neutrophils, IgE, periostin, fraction of exhaled nitric oxide (FeNO), and leukotrienes. Many other biomarkers are being studied in asthma such as cytokines, dipeptidyl peptidase 4, and volatile organic compounds. The evaluation of these biomarkers in patients with asthma is important because can help in endotype diagnosis [16].

  FeNO is most used as a marker for allergic asthma [15]. However, FeNO has also been shown to decrease with Omalizumab treatment and with adherence to inhaled corticosteroids [17]. FeNO might be useful to follow in patients on Dupilumab, as IL-4 and IL-13 promote nitric oxide formation. The American Thoracic Society has advocated that FeNO is useful for identifying Th2-type asthma with eosinophilic airway inflammation, and there is evidence that FeNO can predict asthmatics at risk of progressive loss of lung function [18].

  Leukotrienes are also common asthma biomarkers. Cys-LT is one of the leukotrienes released by intracellular 5-lipoxygenase within inflammatory cells, such as mast cells. The production of leukotrienes activates a Th2 response by the immune system.

Despite the differences that exist in the asthma disease outcome, the results of all the studies consistently suggest that there are approximately 4 primary phenotypes of asthma. These include (1) early-onset mild allergic asthma, (2) early-onset allergic moderate-to-severe remodeled asthma, (3) late-onset nonallergic eosinophilic asthma, and (4) late-onset non-eosinophilic nonallergic asthma [19].

### 1.2.3 Asthma treatments

The GINA, Global Initiative for Asthma, has published guidelines, generalized for all patients, for asthma therapy. Treatment of asthma focuses on rescue and control of the disease. In the upcoming years, step-up therapy for patients with moderate-persistent asthma will be tailored according to their asthma endotype, pathophysiology, and biomarkers [20].

- Corticosteroids. Inhaled corticosteroids (ICS) are usually the first-line asthma controller medication for all diagnoses of asthma [20]. From the moment that the dosage of inhaled corticosteroids is low and the absorption for inhalation is not always enough, systemic corticosteroids can be used for acute asthma exacerbations. However long-term treatment with systemic corticosteroids could cause potential side effects, like suppression of the hypothalamic-pituitary-adrenal axis in children, with a small reduction in linear growth velocity [21].

  Inhaled corticosteroid treatment decreases airway inflammation by reducing inflammatory cell infiltration in the airways, swelling, and mucus production. Corticosteroids are also able to repair epithelial damage by increasing ciliated cells in the airway, and prompting cell-

cell adhesion; so, corticosteroids are helpful in asthmatic endotypes where the mechanism is endothelial damage.

Corticosteroids are particularly recommended for treating the allergic and Th2 asthma exacerbations- type, though Th1 and Th17 responses are steroid-resistant. Also genetic, race, and ethnicity factors could influence steroid responsiveness. For example, a cross-sectional study showed that African Americans have no significant response to inhaled corticosteroids with no change in the forced expiratory volume in one second (FEV1) after bronchodilator administration [22].

Also, different asthma endotypes could change the response to the ICS therapy In fact, there have been identified single nucleotide polymorphisms (SNPs) that influence inhaled corticosteroid response in children, likely through a mechanism with eosinophilic inflammation [23].

These differences in responsiveness to ICS are important to evaluating a correct patient's therapeutic response and step-up strategy.

- Long-acting Beta Agonists. Long-acting beta agonists (LABA) directly activate beta-adrenergic receptors to decrease bronchoconstriction through smooth muscle relaxation of the airways. LABAs can be used for patients with frequent exacerbations on inhaled corticosteroids [20]. LABAs should only be used in combination with ICS, as there is an increased risk of asthma and related death, particularly in children, when using LABAs alone [20]. Conversely to ICS given alone, there is no increased risk of side effects using inhaled corticosteroids with LABA [24]. However, several pieces of evidence show how the use of a combined inhaled corticosteroid and LABA could have different efficacy in various asthma endotypes.

- Anti-Leukotriene. This class of drugs is defined as Leukotriene modifiers, and includes all the competitive antagonists of Cys-LT. This kind of drug can decrease inflammation and the Th2 response. Anti-leukotriene is less effective when given alone for patients with mild to moderate asthma, so is usually associated with other drugs like the ICS [20].

  Leukotriene modifiers are useful in preventing type Th2 and Th17 asthma but are ineffective in Th1 pathways. Furthermore, leukotriene modifiers are effective also in patients who smoke or have smoke exposure, and in asthmatics with small airway disease [25].

- Long-acting Muscarinic Agents. Long-acting muscarinic agents (LAMAs) are recommended by GINA as potential additional therapy to inhaled corticosteroids, LABA, and leukotriene [20].

  LAMAs alleviate bronchoconstriction by blocking acetylcholine release. Acetylcholine is released by cholinergic nerves and stimulates bronchoconstriction. As we know LAMAs are effective in the treatment of chronic obstructive pulmonary disease (COPD), and so could be helpful in COPD/asthma overlap syndrome. So, LAMA could be efficacy in neutrophilic asthma caused by tobacco smoke but there is no clinical evidence that demonstrates the effectiveness of this class of drugs in the different asthma endotypes [20].

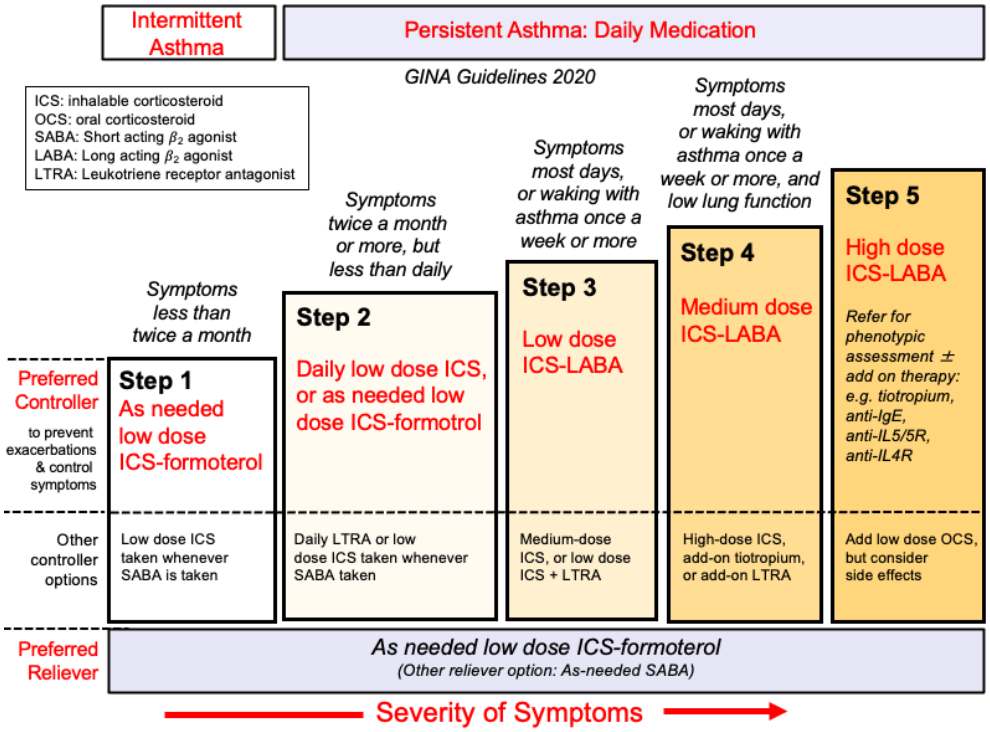


***Figure 1.3: Asthma treatment and management***. Stepwise approach for managing asthma in adults, divided in 6 steps for severity of symptoms. *Adapted from Reddel et al (2019).*

### 1.2.4 Asthma treatment limitation

Despite advancements in treatment, the incidence of asthma, asthma-related deaths and hospitalizations for asthma have increased significantly during the past decade. These unexpected changes in asthma severity have sparked renewed interest in research into the pathogenesis and treatment of the condition. $\beta_2$-Adrenergic agonists are the most used class of drugs for the treatment of asthma. Recent concerns about safety issues for beta-agonists caused a revaluation of prescribing practices and using them on an as-needed basis is now more frequently accepted and recommended. In acute asthma, a $\beta_2$-Adrenergic agonist is still the medication of choice. Long-acting salmeterol

and formoterol, administered only twice daily, can decrease symptoms of asthma during the day and nighttime [26]. Unfortunately, prolonged use of these drugs induces a reduction in receptor responsiveness, this process is known as desensitization is caused by a prolonged stimulation of $\beta_2$ -agonists or by the interaction of many pro-inflammatory mediators with $\beta_2$ -AR [27].
Corticosteroids, including inhaled steroids, are the second principal drug of choice for asthma treatment, they have measurable effects on symptoms, lung function, bronchial responsiveness, and inflammation associated with asthma. The chronic use of corticosteroids (especially the oral one) could cause systemic side effects including osteoporosis, bone fractures, diabetes, ocular disorders, and respiratory infections; these suggest the need to develop new therapeutic strategies that aim to reduce the dose of corticosteroids to be taken, as much as possible, obtaining the same therapeutic result [26].

## 1.3 Chronic obstructive pulmonary disease (COPD)

Chronic obstructive pulmonary disease (COPD) is a chronic respiratory disorder that progresses slowly and is characterized by an obstructive ventilatory pattern, with structural lung changes due to chronic inflammation, which is rarely reversible, very often related to tobacco smoking and which can lead to chronic respiratory failure. Chronic inflammation causes airway narrowing and decreased lung recoil. The principal symptoms of this disease are cough, dyspnea, and sputum production [28].
COPD is primarily present in smokers and those greater than age 40. Prevalence increases with age, and it is currently the third most common cause of morbidity and mortality worldwide. In 2015, the prevalence of COPD was 174 million and there were approximately 3.2 million deaths due to COPD

worldwide. However, the prevalence is likely to be underestimated due to the underdiagnosis of COPD [29].

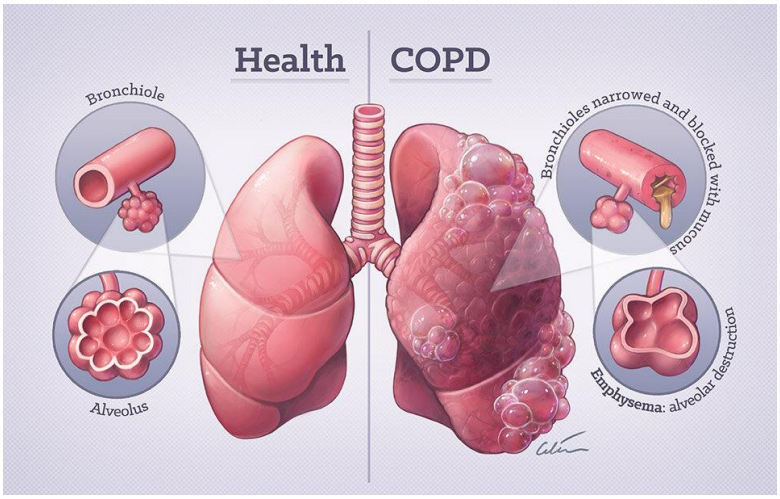


***Figure 1.4: COPD***. Schematic representation of what happens in the airway with COPD focused on the two major symptoms: Emphysema and chronic bronchitis. *COPD Medical Illustration by Dr Ciléin Kearns*.

### 1.3.1 COPD etiology

COPD is caused very often by prolonged exposure to harmful particles or gases; cigarette smoking is the most common cause of COPD worldwide [28]. Although the most common cause of COPD is tobacco smoke, several other factors can cause or make COPD worse, including environmental exposures and genetic risk. For example, heavy exposure to certain dust at work, chemicals, and indoor or outdoor air pollution (including wood smoke or biomass fuels) can contribute to COPD, as well as second-hand smoke and alpha-1 antitrypsin deficiency (AATD). Some people have none of these exposures and still get COPD. Some people smoke but never develop COPD

and never smoke that get the COPD; this is probably associated with hereditary (genetic) factors that play a key role in the development of the disease [30].

### 1.3.2 COPD pathophysiology

COPD is a complex pathology that can involve different degrees of airway obstruction, chronic inflammation (bronchiolitis) and/or emphysema [31]. **Emphysema** is one of the structural changes seen in COPD, characterized by the destruction of the alveolar air sacs (gas-exchanging surfaces of the lungs) leading to obstructive physiology. In emphysema, an irritant exposure (smoking) causes an inflammatory response in the lung. Neutrophils and macrophages are recruited and release multiple inflammatory mediators that contribute to alveolar destruction. In particular, during inflammation, an increase in oxidants and an excess of proteases lead to the destruction of the air sacs. Indeed, two of the main processes involved in the pathogenesis of COPD are represented by the protease/ anti-protease imbalance and between oxidants and antioxidants. Cigarette smoke, and inflammation itself, produce oxidative stress, which primes several inflammatory cells to release a combination of proteases and inactivates several antiproteases by oxidation.
The protease-mediated destruction of elastin causes a loss of elastic recoil and results in airway collapse during exhalation [29].
Chronic inflammation due to cigarette smoke exposure could also lead to **chronic bronchitis.** Chronic bronchitis is characterized by mucous hypersecretion that results in a chronic productive cough. This is not necessarily associated with airflow obstruction, and not all patients with COPD have symptomatic mucous hypersecretion. Mucus hypersecretion is due to an increase in goblet cell number (hyperplasia) and size (hypertrophy)

and an increase in their function in response to chronic irritation. Furthermore, the presence of areas of squamous metaplasia results in ciliary dysfunction characterized by a decrease in ciliate cells, abnormal cilia, and/or deciliation. All that results in abnormal or loss of mucociliary clearance and difficulty expectoration. [32].

The remodeling of the airways (typical of chronic obstructive bronchitis) and the destructive alveolar damage (typical of emphysema) associated with chronic inflammation represents obstructive pulmonary conditions characterized by a limitation to airflow, not completely reversible, by a progressive impairment of gas exchange and functionally, by a decrease in forced expiratory volume (FEV1). Hyperinflation of the lungs is often seen in imaging studies and occurs due to air trapping from airway collapse during exhalation. The inability to fully exhale also causes elevations in carbon dioxide (CO2) levels. Respiratory muscle fatigue and alveolar hypoventilation can contribute to hypoxemia, hypercapnia, and respiratory acidosis, and lead to severe respiratory failure and death. Hypoxia and respiratory acidosis can induce pulmonary vasoconstriction [32]. As the disease progresses, impairment of gas exchange is often seen. The reduction in ventilation or increase in physiologic dead space leads to CO2 retention. Pulmonary hypertension may occur due to diffuse vasoconstriction from hypoxemia [29].

### 1.3.3 COPD evaluation

COPD is evaluated in patients with relevant symptoms and risk factors. The diagnosis is confirmed by spirometry which is always accompanied by different routine tests.

- **Pulmonary function testing (PFT)** is essential in the diagnosis, staging, and monitoring of COPD. This test consists of a spirometry measurement

before and after administration of an inhaled bronchodilator, which may be a short-acting beta2-agonist (SABA), short-acting anticholinergic, or a combination of both. A ratio of the forced expiratory volume in one second to forced vital capacity (FEV1/FVC) less than 0.7 confirms the diagnosis of COPD [33].

- The Global Initiative for Chronic Obstructive Lung Disease (**GOLD**) is a program initiated by the World Health Organization (WHO) and the National Heart, Lung, and Blood Institute (NHLBI) to provide updated and detailed reports on the recommendations for the diagnosis and management of COPD. The GOLD recommendations are often used to assess disease severity and choice of therapy. The 2019 GOLD reports on a simplified method of evaluating and choosing the initial treatment for patients with COPD. It defines how to identify the severity of the disease in the patients and the GOLD group classification from 1 to 4: once the diagnosis of COPD is confirmed by spirometry (FEV1/FVC <0.7), the FEV1 is used to determine the severity (GOLD 1-4) [29]. Symptom severity is usually evaluated using the modified British Medical Research Council (mMRC) questionnaire and the COPD Assessment Test (CAT). The mMRC questionnaire assesses the degree of breathlessness on a scale of 0-4 with 4 being the most severe. The COPD Assessment Test (CAT) provides a score on eight functional parameters to measure the impact of the disease on a patient's daily life [29].
- A **walk test** of 6 minutes, performed indoors on a flat and straight surface, is commonly performed to assess the submaximal functional capacity of a patient. The length of the walk is usually 100 feet, and the test measures the distance the patient walks over in 6 minutes [34].
- **Laboratory testing** is also often required for a complete COPD diagnosis, are usually made a complete blood count to assess for infection, anemia,

and polycythemia or Alpha-1 antitrypsin levels should be checked for other causes of COPD.

- **Radiographic imaging** includes a chest x-ray and computed tomography (CT). Chest X-rays are useful to see hyperinflation, flattening of the diaphragm, and increased anterior-posterior diameter. In cases of chronic bronchitis, bronchial wall thickening may be present. CT imaging may be useful in patients with bronchiectasis, malignancy, or if planning surgical procedures. CT of the chest in patients with COPD will be significant for centrilobular emphysema [35].

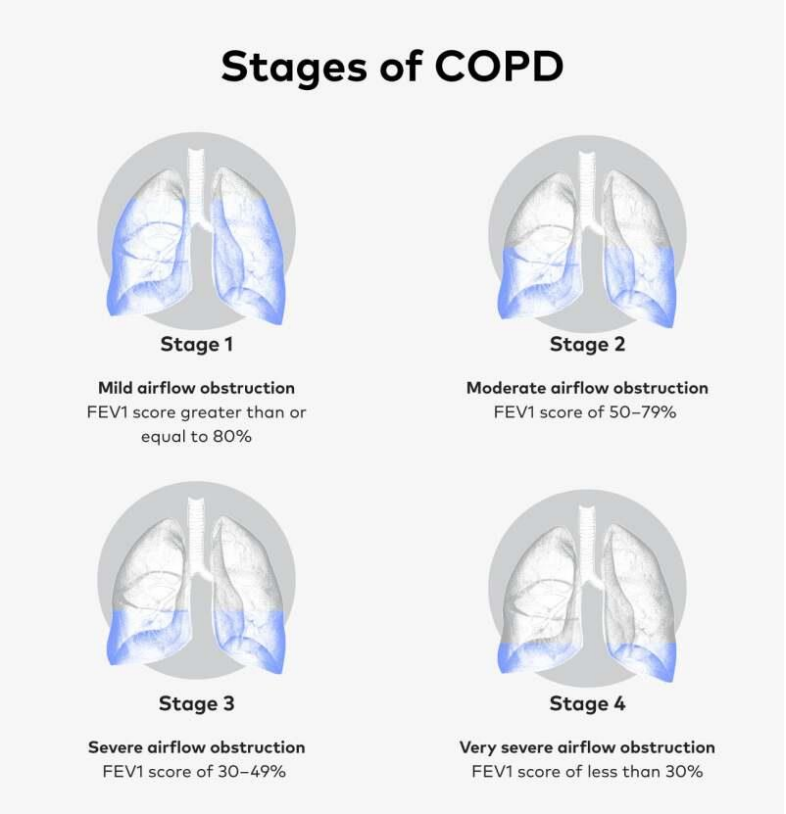


***Figure 1.5: Stages of COPD***. Classification of the 4 different stages of COPD, defined by severity of symptoms and airflow obstruction. *Healtgrades*.

### 1.3.4 COPD treatments

The first line of therapy is to control the symptoms, reduce exacerbation and mortality, improve the quality of life and the smoking cessation with pulmonary rehabilitation.
The classes of drugs commonly used in COPD include bronchodilators (beta2-agonists, antimuscarinics, methylxanthines), inhaled corticosteroids (ICS), systemic glucocorticoids, phosphodiesterase-4 (PDE4) inhibitors, and antibiotics.

- Beta2-agonists. These drugs work by relaxing the smooth muscle in the airways. SABAs and long-acting beta2-agonists (LABA) are commonly used in treatment. SABAs are used as needed to provide immediate relief. LABAs are typically used for maintenance therapy.
- Antimuscarinics work by blocking the M3 muscarinic receptors in the smooth muscle and in this way preventing bronchoconstriction. Short-acting antimuscarinic agents (SAMA) like SABAs provide a rapid onset of action and are used on an as-needed basis. Long-acting antimuscarinic agents (LAMA), like LABAs, are used as maintenance therapy [36].
- Methylxanthines are used in maintenance therapy, usually after LABA or LAMA treatment as additional relief. Methylxanthines work by relaxing the smooth muscle in the airways causing mild bronchodilation. The mechanism of action is not completely elucidated however, it may be due to the inhibition of phosphodiesterase (PDE) III and IV. Theophylline is a methylxanthine commonly used and when used in combination with salmeterol provides significantly greater improvement in FEV1 compared to salmeterol alone [37].

- Inhaled corticosteroids (ICS) are often used in combination with LABAs and LAMAs to decrease inflammation. A combination of ICS and LABA is more beneficial than either of the drugs when used alone. Oral glucocorticoids are not indicated for long-term use and can have multiple side effects [38].
- Phosphodiesterase-4 inhibitors work by inhibiting the reduction of intracellular cyclic AMP and in this way reduce inflammation. Roflumilast is a PDE4 inhibitor used for patients with severe disease and has been shown to decrease the number of exacerbations in COPD patients [39].
- Recently, Azithromycin has been shown to reduce the number of exacerbations in patients with COPD. Physicians should use caution as this practice may promote bacterial resistance [40].

Acute exacerbations of COPD can be managed in different ways depending on the severity. Mild cases can be treated in the outpatient setting with bronchodilators, corticosteroids, and antibiotics. For moderate and severe cases, hospitalization is indicated. Hospitalized patients often require oxygen therapy and bronchodilator therapy with SABA and sometimes with SAMA. Long-acting bronchodilators are typically used when the patient becomes stable and ready for discharge. Antibiotics should be considered if there is suspicion of a bacterial infection [28],[29].

Severe cases may require surgical intervention including bullectomy, lung volume reduction surgery, or lung transplantation. Surgical intervention is indicated in severe conditions where symptoms are not controlled with medical therapy alone and may improve quality of life.

Pulmonary rehabilitation is indicated in all stages of COPD. It is a comprehensive plan that is tailored to patients and may involve therapies such

as exercise training, education, and behavioral changes. It aims to improve a patient's physical function and psychological condition [28].

## 1.4 Sex and Gender Differences in Respiratory Disease

Sex differences in the anatomy and physiology of the respiratory system have been widely known and reported by various studies. From birth to adult life, significant differences exist between male and female lungs. Changes in sex hormone levels during development, puberty, and physiological events such as pregnancy and menopause, also influence lung function and health.

During childhood female sex hormones are beneficial in promoting lung development and maturation, conversely, androgens appear to have the opposite effect [41]. After puberty, the situation is reversed, for example in diseases such as severe asthma, where improvement is observed with increasing androgen levels, and fluctuations of female hormones (such as estrogen and progesterone) promote asthma exacerbations. Anyhow, several studies show that the effect of sex hormones on lung health depends on the timing of exposure and affects males and females differently throughout the lifespan, based on the lung disease [42].

In neonates, the male disadvantage in developing lung disease is a well-established clinical fact, especially in the preterm population; indeed, guidelines have been adopted to predict outcomes for extremely preterm birth outcomes, including sex as a critical biological variable, from the National Institutes of Child Health and Disease (NICHD) and Neonatal research network (NRN) [43]. Instead, in children and adults, some lung conditions are more frequent in women and men, respectively, and can present with different degrees of severity and symptoms. Overall, different studies show that some

lung diseases, like asthma, are more commonly found, or present with a higher degree of severity, exacerbation rate, hospitalizations, and mortality in women than men. On the other hand, diseases like chronic obstructive pulmonary disease (COPD), and some types of lung cancer such as adenocarcinoma present with a higher degree of severity, in men [33].

### 1.4.1 Sex differences in asthma

Asthma is a complex and heterogeneous disease that affects more than 339 million people worldwide, with different prevalence ranges from as low as 1% in some countries to as high as 18% in others [44].

Asthma prevalence and severity are different between males and females during the lifespan. During childhood, boys are more susceptible to developing asthma. During puberty, this trend reverses, and women have an increased prevalence and severity of asthma. This shift in asthma prevalence over time suggests a role of sex hormones, genetic and epigenetic variations, immune mechanisms, response to therapies, environmental factors, socioeconomic factors, differential access to resources (*e.g.*, nutrition and air quality), comorbidities and healthcare in the sex differences observed in asthma incidence, prevalence, and severity.

Sex hormones (*e.g.*, estrogen, ER-α, testosterone, AR, DHEA-S) are key mediators of the transition of differences in asthma prevalence across sexes from childhood into adulthood. these changes occur during adolescence and result in a higher prevalence of asthma in adult women compared with adult men: indeed, for women, fluctuations in sex hormone levels during puberty, the menstrual cycle and pregnancy are associated with asthma pathogenesis [45].

Also, the response to asthma therapeutics shows an important difference between the two sexes: asthma is a heterogeneous disease with different

phenotypes and responses to current therapeutics. Multivariate cluster analyses on adults with asthma or controls determined that different phenotypes of asthma require different utilization of primary or secondary healthcare. Sex differences are seen in these various clusters, with female predominance in less atopic, less corticosteroid-responsive patients, with increased asthma symptoms [46].

Immune mechanisms are also associated with different asthma phenotypes and gender differences. Th2 type (T2) asthma is often characterized by allergies and/or inflammation consisting of the production of interleukins (IL) IL-4, IL-5, IL-13, and IL-9 from type 2 innate lymphoid cells (ILC2s), and/or CD4+ T-helper type 2 cells (Th2). The increased production of type 2 cytokines leads to increased IgE, mast cell activation, mucus, and exhaled nitric oxide fraction ($F_{ENO}$) production, eosinophil infiltration and activation, and airway hyperresponsiveness (AHR). Non-T2 inflammation is present in some endotypes of asthma with increased neutrophil infiltration, mucus production and AHR that is mediated by increased interferon-gamma (IFN-γ) or IL-17A production from T-cells or IL-6, tumor necrosis factor (TNF) and IL-1β. Children with asthma primarily manifest the T2 eosinophilic or allergic asthma phenotypes [47]. T2, non-T2 or mixed endotypes of asthma are seen in adults. Estrogen signaling through estrogen receptor (ER)-α increased AHR, IL-33 production, type 2 cytokine production and eosinophil infiltration into the airway while estrogen signaling through ER-β decreased AHR and eosinophil infiltration [48]. Testosterone and other androgens signaling through the androgen receptor (AR) decreased ILC2 proliferation, eosinophil infiltration, IL-33 and thymic stromal lymphopoietin (TSLP) production, and type 2 cytokine production [48],[49],[50].

Environmental factors interact with airway architecture, immunology and hormones and could contribute to sex and gender differences in asthma

development. The economy, geography, maternal parity, environmental smoke and pollution, urbanization and other factors contribute to the balance between T2-mediated and non-T2-mediated inflammation in males and females [48].

### 1.4.2 Sex differences in COPD

Chronic obstructive pulmonary disease (COPD) affects an estimated 174 million people and is a major cause of morbidity and mortality worldwide.
Several studies demonstrate that the clinical presentation of COPD is different in women and men, which has led to better and more accurate diagnoses in women in the past few decades. It has been shown that women with COPD have different disease burdens, symptoms, and clinical trajectories than men, and that women tend to develop COPD earlier in life and have more frequent respiratory exacerbations than men [41].
Given the same amount of exposure to tobacco smoke, women are more likely to develop more severe airflow limitation and inflammation at an earlier age than men. Importantly, at all stages of COPD severity, men have more severe computed tomography–defined emphysema than women [31].
Epidemiological data show that since the year 2000, the number of women in the US dying from COPD has surpassed the number of men. Some studies have suggested that both asthma and the so-called “Asthma COPD Overlap” (ACOS), which are more common among adult women than men, can predispose women to develop COPD [41].
Recently, several clinical and experimental studies aimed to understand the contribution of sex to the biological pathogenesis of COPD. Levels of pro-inflammatory cytokines, including C reactive protein, interleukin-6 (IL-6), tumor necrosis factor-alpha (TNFa), matrix metalloproteinase 9 (MMP-9), pulmonary and activation-regulated chemokine (PARC), and vascular

endothelial growth factor (VEGF), have been identified to contribute to the development of COPD. VEGF helps regulate the growth of new vessels and vascular leaks and was found to be elevated in patients with COPD. In patients with COPD, statistically higher levels of VEGF and IL-6 have been found in men vs. women [51]. Additionally, studies in mouse models of chronic cigarette smoke have indicated that sex hormones may contribute to the greater COPD susceptibility in females. Exposure to cigarette smoke in female mice results in higher peripheral airway inflammation and airway remodeling, but less emphysema than in male mice: this effect is mediated by estrogens [52].

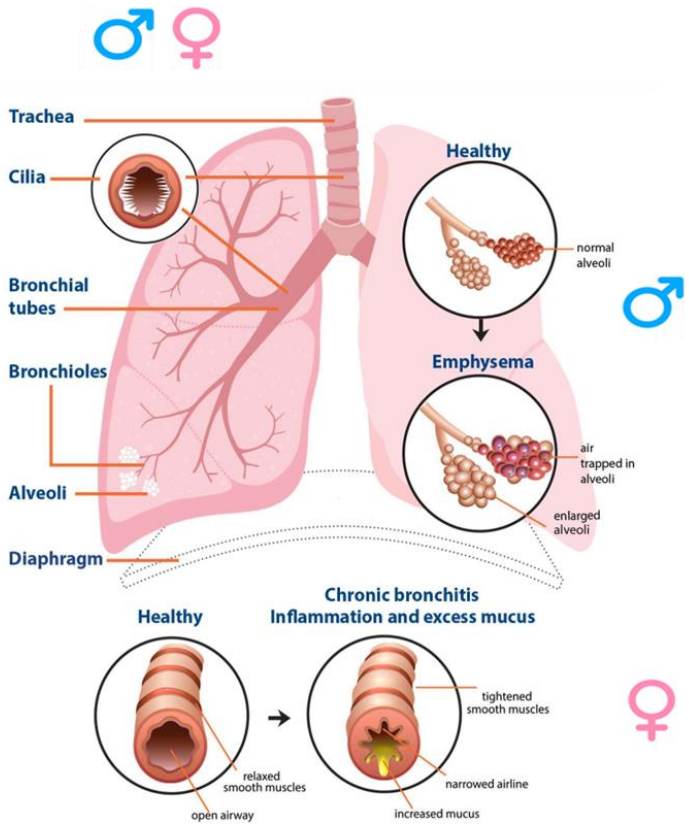

***Figure 1.6: sex differences in COPD.*** sex differences in COPD are associated with sexual hormones and define different symptoms and exacerbations in the development of the disease.

## 1.5 Sphingolipids

Sphingolipids are a complex class of lipids component of the membranes of the cells. They are key structural elements in cellular membranes and are essential signaling molecules for a wide range of cellular functions including growth and differentiation, signal transduction, immune response, cell proliferation, and apoptosis [53].

Sphingolipids are usually classified as sphingomyelins (which are true phospholipids (PLs)), or glycolipids (i.e., ceramide-containing gluco- and galactocerebrosides, sulfatides, globosides, and gangliosides), each of which possesses one or more monosaccharide residue linked to the sphingosine backbone rather than phosphate.

Ceramide is the basic structural unit of all sphingolipids and sphingosine is the precursor of ceramide, and it shows us a long-chain amino alcohol formed from palmitoyl-CoA and serine. Sphingosine is one of 30 or more different long-chain amino alcohols found in nature. It is the major base of mammalian sphingolipids.

Ceramide (N-acylsphingosine) is formed in the endoplasmic reticulum through the amide linkage of a long-chain fatty acid moiety to the amino group of sphingosines. It has two hydroxyl groups, one attached to C3 that remains unsubstituted, and the other attached to C1 that is substituted in the formation of sphingomyelins and the glycolipids.

The sphingolipids generated from ceramide are generally classified as either sphingomyelins (sphingophospholipids), or the nonphosphate-containing glycosphingolipids (or glycolipids). Both groups contain ceramide as their basic structural component.

Both sphingomyelins and the glycolipids contribute to the development of rigidity of membranes and are implicated in several cellular functions mediated at the level of the cell surface. They:

• Provide antigenic chemical markers for cells.

• Act as chemical markers identifying various stages of cell differentiation.

• Regulate normal growth patterns of cells.

• Allow cells to react with other bioactive substances such as bacterial toxins.

Typically, very long-chain fatty acids occur in ceramides, particularly those found in glycosphingolipids of the brain. There is also evidence that ceramide may act as a second messenger or lipid mediator, activating a protein kinase that opposes some actions of diacylglycerol (DAG).

Sphingomyelins, instead, are formed by the addition of phosphocholine to the C1 of ceramide, which can occur following transfer from either CDP-choline, or phosphatidylcholine (PTC). This process occurs mainly in the Golgi apparatus.

Cerebrosides (which are glycolipids including the glyco-and galactocerebrosides, globosides, gangliosides, and sulfatides) are formed through the glycosidic linkage of either Glc or Gal to the C1 of ceramide. Galactocerebrosides are formed through the glycosidic linkage of either glucose (Glc) or galactose (Gal) to the C 1 of ceramide [54].

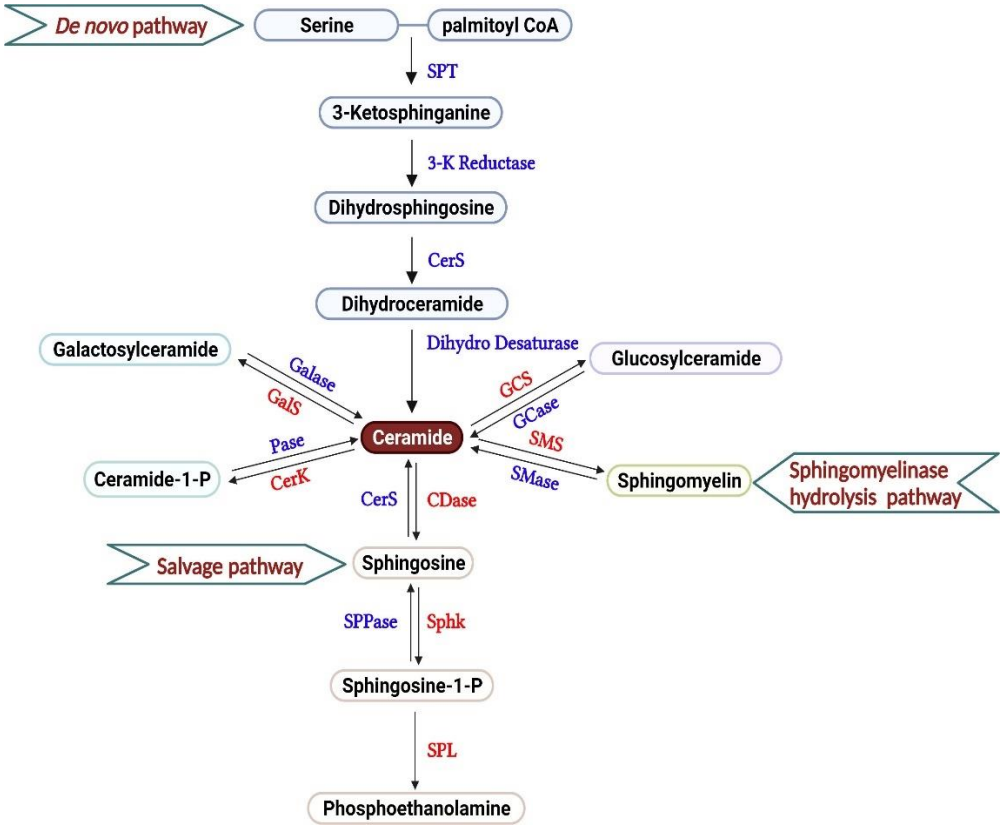


***Figure 1.7: Sphingomyelin and glycolipid production:*** Schematic representation of the sphingolipid's pathway from Palmitoyl-CoA to Sphingomyelin and glycolipids formation. *https://doi.org/10.3389/fimmu.2022.904823*

**Ceramides.** Ceramides are central molecules of sphingolipid metabolism, composed of a sphingosine base and an amide-linked fatty acid chain varying in length within the range C14:0–C26:0. They are produced in the endoplasmic reticulum (ER) before being transported to the Golgi apparatus by the ceramide transport protein (CERT) or vesicular transport and can be converted to sphingomyelin. The two main pathways of ceramide synthesis are the de novo pathway or the recycling of sphingosine through the salvage pathway. The de novo pathway commences with the condensation of serine and palmitoyl coenzyme A (catalyzed by serine palmitoyl transferase) to

generate 3-keto-dihydrosphinganine. Subsequently, 3-keto-dihydrosphinganine is reduced to form dihydro-sphinganine. Six mammalian genes that encode ceramide synthases (CerSs) generate dihydroceramides of specific fatty acyl chain lengths. Dihydroceramides are then desaturated by dihydroceramide desaturase, which generates a 4,5-trans-double bond to form ceramides with different acyl chain lengths. Ceramides have fundamental roles in biological processes, including cancer development, obesity, type 2 diabetes mellitus, lung disease, lipid storage, and neurological disorders. As such, understanding how the individual CerSs and the ceramides they synthesize interrupt cellular homeostasis to promote disease progression has the potential to enable the generation of novel and highly selective therapeutics that would bypass the detrimental effects of global ceramide inhibition [55].

**Sphingosine-1-Phosphate.** The metabolism of sphingolipids generates a polar lipid mediator such as sphingosine 1-phosphate (S1P). In vertebrates, S1P is found in the extracellular matrix and interacts with cell-surface receptors to regulate an array of cellular responses, including cell migration, differentiation, and survival [56]. S1P is formed in multiple cell types in response to numerous stimuli including antigens and cytokines. S1P is involved in various cellular processes, including cell growth, differentiation, proliferation, signal transduction, and immune response [57].

Sphingolipid turnover, which is initiated by the action of sphingomyelinase, leads to the formation of ceramide, which is further processed into sphingosine by the enzyme ceramidase. Sphingosine is then phosphorylated by the sphingosine kinase (Sphk1,2) isoenzymes, giving rise to S1P. The levels of S1P in the cell are regulated not only by S1P biosynthetic enzymes but also by degradative enzymes such as S1P phosphatases and S1P lyase. Once

produced inside the cell, S1P is exported by specific transporters, such as spinster 2 (Spns2), which was recently shown to be involved in establishing a vascular S1P gradient in mice. Blood plasma thus contains high levels of S1P (′1 μM), whereas interstitial fluid levels of S1P are low, giving rise to a gradient of this lipid mediator, which plays an important role in driving S1P function [56]. In plasma, S1P is bound to its chaperones, apolipoprotein-M containing high-density lipoprotein ($ApoM^+$ HDL) and albumin. Extracellular S1P can also be degraded by lysophospholipid phosphatase 3 (LPP3) into sphingosine, which can then be taken up by cells for further metabolism [58]. S1P receptors are G protein-coupled receptors (GPCRs). Five S1P receptors, $S1P_{1-5,}$ have been described, and most cells express one or more subtypes of S1P receptor. All bind to S1P with high affinity and induce cellular responses. S1P receptors exhibit unique properties. For example, $S1P_1$ couples exclusively to the $G_{i/o}$ family, whereas $S1P_2$ is capable of coupling to $G_{i/o}$, to $G_{12/13}$ as well as to the $G_q$ family. This coupling results in the activation of small GTPases such as Rho, Rac, and Ras. Further downstream effectors of S1P receptors include adenylate cyclase, PI-3-kinase, phospholipase C, protein kinase C, and intracellular calcium [56].

Changes in S1P levels have been associated with harmful effects in pulmonary inflammatory disease.

### 1.5.1 Sphingolipids in the Pathobiology of Lung Inflammation

Pulmonary physiology relies on lipids for important extracellular activity ensured by surfactants and consisting of a sphingolipid/glycerolipid network [59].

In the pathobiology of pulmonary inflammation, characterized by loss of barrier functions, bronchial hyperreactivity, airway remodeling, pro-

inflammatory markers, and cytokines recruitment, sphingolipids are critically involved in the disease process. They expedite inflammation by promoting chemotaxis (neutral sphingomyelinase), increased endothelial permeability (acid sphingomyelinase, S1P3-receptors), increased epithelial permeability (S1P2- and S1P3-receptors), and delaying neutrophil apoptosis (neutral sphingomyelinase, S1P1-receptors). They extenuate inflammation by attenuating chemotaxis (S1P) and by stabilizing the endothelial and the epithelial barrier (S1P1-receptor) [60].

### 1.5.2 Sphingolipids and Asthma

The risk for asthma is determined in childhood, it is highly heritable, and the phenotypes are conferred by both genetic susceptibility and environmental exposures. Asthma exacerbations are triggered by environmental stimuli, most often respiratory viruses, and allergens. For most asthma types, a genetic predisposition is present and essential for the "asthmatic reaction" to environmental stimuli [61].

Over 100 genes have been identified in association with asthma among them, the orosomucoid-like 3 gene (ORMDL3) and the associated 17q21 locus have emerged through genome-wide association studies as likely contributors to the genetic susceptibility and underlying pathogenesis of asthma. While the functions of ORMDL3 are incompletely understood, it is known to be involved in sphingolipid metabolism and de novo sphingolipid synthesis, suggesting altered sphingolipid metabolism as a contributing factor in asthma [62].

The de novo pathway of sphingolipid synthesis which originates in the endoplasmic reticulum (ER) is an important key regulator of ceramide cellular level and other sphingolipids like S1P. ORMDL proteins act as inhibitors of

serine palmitoyl-CoA transferase (SPT), the rate-limiting enzyme for de novo sphingolipid synthesis and regulate cellular ceramide levels. Alteration in de novo sphingolipid synthesis has emerged as a contributing factor in airway hyperreactivity, a cardinal feature of all asthma types [62].

Ceramides and S1P have been the most extensively studied sphingolipids and are important bioactive signaling molecules [53]. They play an important role in asthma development and exacerbation. S1P is derived from sphingosine through phosphorylation by two sphingosine kinases (SphK1 and SphK2) which are widely expressed, including in bronchial epithelium and airway smooth muscle cells [63]. Most studies show that the sphingolipid mediator S1P is involved in asthma inflammatory and allergic mechanisms.

Through the activation of different signaling pathways, S1P mediates a diverse set of biological processes, acting as both an intracellular second messenger and as an extracellular ligand for specific cell surface G protein-coupled receptors, S1P 1–S1P 5 [62]. S1P and SphK have been implicated in airway smooth muscle cell hyperresponsiveness, lung inflammation, and mast cell activation, all key features in the pathogenesis of asthma. S1P and the SphK pathways have therefore been targeted for the development of sphingolipid-based therapeutic agents, though the role of S1P and its receptors remains incompletely understood. For example, the immunomodulating agent FTY720 (Fingolimod), approved for the treatment of multiple sclerosis, attenuates allergen-induced inflammation, as well as airway hyperreactivity in mouse models of asthma [64].

Exogenous systemic administration of S1P resulted in increased contraction of the bronchi, increased airway resistance, as well as mast cell and eosinophil recruitment to the lung in the mouse, [65]. S1P has also been shown to be important in immunoglobulin E (IgE) mediated mast cell migration and degranulation, allergic asthma, and secretion of pro-inflammatory cytokines.

Mast cells play a central role in the development of asthma, and cross-linking of FCεR1, the high-affinity IgE receptor, induces SphK activation and S1P secretion [66].

S1P levels are significantly increased in bronchioalveolar lavage (BAL) fluid from subjects with asthma following segmental allergen challenge compared to control subjects [67]. In addition, ceramide (C16) levels were noted to be increased in the exhaled breath collection of subjects with severe asthma, compared to healthy controls [68].

### 1.5.3 Sphingolipids and COPD

Altered sphingolipids and sphingolipid metabolism have been suggested as a possible mechanism in COPD susceptibility [62]. Lung ceramide levels were shown to be higher in human subjects with emphysema (a specific phenotype of COPD) compared to those without, and the expression of multiple species of ceramides, dihydroceramide, glycosphingolipids, and sphingomyelins were shown to be significantly higher in smokers with COPD than those in non-smokers. The accumulation of ceramide depended on its de novo synthesis [69]. In another recent study looking at the association between sphingolipid species and different COPD phenotypes, plasma sphingolipids were shown to be inversely related to emphysema severity and positively associated with severe COPD exacerbations [70].

### 1.5.4 Sphingolipids and sexual hormone

Steroid hormones like testosterone, progesterone, cortisol, aldosterone, and estradiol are important endocrine chemical messengers that are involved in a

vast number of physiological processes including metabolism, inflammation, electrolyte and fluid balance, and secondary sex differentiation.

Sphingolipids have recently been identified as important bioactive molecules involved in a variety of cellular processes, including steroidogenesis.

Sphingolipids such as ceramide (Cer), sphingosine (SPH), sphingosine-1-phosphate (S1P), sphingomyelin (SM), and gangliosides (GMs) have been shown to modulate the steroidogenic pathway at multiple levels including regulating steroidogenic gene expression and activity as well as acting as secondary messengers in signaling cascades [71].

Thus, there is a clear connection between sexual hormones and sphingolipids. Recent studies have demonstrated that estrogen signaling is not limited by the genomic pathway; estrogens have been shown to interact with multiple cytoplasmic signaling networks, including the recently recognized participants, sphingolipids. Both estrogen and S1P are reported as important mediators of different inflammatory lung diseases and in the development of major symptoms. Accordingly, plasma S1P levels are significantly higher in women than that in men [72].

# Chapter 2

# 2. Aim of the study

This project aims to investigate the molecular mechanism involved in the development of chronic lung diseases, such as asthma and COPD, and to develop new therapeutic strategy.

We focused on:

- Role of sphingolipids metabolism in the development of lung diseases.
- Role of sexual hormones in modulation of sphingolipids metabolism.
- Identification of new pharmacological targets for lung disease treatments.

# Chapter 3

# 3. Materials and Methods

## 3.1 Animal studies

### 3.1.1 Mice

Female and male BALB/c and C5//Bl6 mice, and male CD1 mice, were purchased from Charles River Laboratories (Italy). All mice, aged 8-9 weeks, were housed in a controlled environment with a 12-hour light/dark cycle under specific pathogen-free conditions and received water ad libitum. All experiments were conducted during daylight according to Italian regulations on the protection of animals used for experiments and other scientific purposes (D.Lgs. 26/2014) as well as with the European Economic Community regulations (EU Directive 2010/63/EU). Animal studies are reported in compliance with the ARRIVE guidelines [73].

### 3.1.2 Ovalbumin Sensitization Protocol

**Protocol 1:** Female BALB/c mice received subcutaneous (s.c) administration of Ovalbumin ((from chicken egg white, Sigma-Aldrich, Milan, Italy) OVA, 100µg) absorbed to 3.3 mg of aluminium hydroxide gel (Merck KGaA, Darmstadt, Germany) or saline (control group) on days 0 and 7. On 21 and 22 days, mice were subjected to aerosol administration of OVA 3% for 15 minutes and after 24h mice were killed by an overdose of enflurane, and lung, bronchi, and blood were collected.

**Protocol 2:** Female BALB/c mice received subcutaneous (s.c) administration of Ovalbumin ((from chicken egg white, Sigma-Aldrich, Milan, Italy) OVA,

100µg) absorbed to 3.3 mg of aluminum hydroxide gel (Merck KGaA, Darmstadt, Germany) or saline (control group) on days 0 and 7. On day 21, mice were killed by an overdose of enflurane, and lung, bronchi, and blood were collected [74].

### 3.1.3 Mouse paw edema

CD1 male mice (Charles River; weight 25-30g) were divided into groups (n=6) and lightly anesthetized with enflurane. Each group of animals received sub-plantar administration of 50µl of a physiologic solution containing carrageenan (1%). Paw volume was measured using a hydroplethismometer specially modified for small volumes (Ugo Basile Milan Italy) immediately before the sub plantar injection and 0.5, 1, 2, 3, 4 and 24, 48, and 72h thereafter. The control group received intraplantar administration of the vehicle. The increase in paw volume was evaluated as the difference between the paw volume at each time point and the basal paw volume. To assess in vivo the synergistic effect of montelukast formoterol salt, mice received 30 minutes before intraplantar injection of carrageenin intraperitoneal administration of vehicle, formoterol (0.3mg/Kg), montelukast (0.3mg/Kg), or montelukast formoterol salt (MFS 0.3mg/Kg) [74].

### 3.1.4 Estradiol treatment protocol

Male BALB/c received a subcutaneous injection (25µg/kg) of β-estradiol (Sigma E8875) or vehicle every day for one week. Mice were sacrificed 7 days after the first administration of estradiol. All the mice were anesthetized and subjected to euthanasia. Blood, main bronchi, and lungs were collected and processed for functional and molecular studies. Each lung was divided into two parts: the right lobes were immediately frozen, stored at -80 °C, and

successively homogenated, while the left lobes were fixed in 10% formalin buffer for histopathological analysis.

### 3.1.5 Tamoxifen treatment protocol

Female BALB/c received a subcutaneous injection (0.4mg/kg) of the anti-estrogen tamoxifen (Sigma T5648) or vehicle every day for one week. Mice were sacrificed 7 days after the first administration of tamoxifen. Blood, main bronchi, and lungs were collected and processed for functional and molecular studies. Each lung was divided into two parts: the right lobes were immediately frozen, stored at -80 °C, and successively homogenated, while the left lobes were fixed in 10% formalin buffer for histopathological analysis.

### 3.1.6 S1P exposure

Female BALB/c received a subcutaneous (s.c) injection of S1P (10 ng) dissolved in sterile saline containing bovine serum albumin (BSA 0.001%). S1P was administered at 0 and 7 days. Mice were sacrificed on day 14 or 21 for molecular and functional studies. In another set of experiments, mice were pretreated with the antagonist of receptor type I and II of TGF-β LY2109761 (50 $mg \cdot kg^{-1}$) 15 min before S1P administration [75].

## 3.2 Bronchial reactivity measurements

### 3.2.1 Isolated organ bath

The main bronchi were rapidly dissected and cleaned from fat and connective tissue. Rings of 1-2 mm in length were cut and mounted in a 2.5 mL organ

bath containing Krebs solution (Mm: 118NaCl, 4.7 KCl, 1.2 $MgCl_2$, 1.2 $KH_2PO_4$, 2.5 $CaCl_2$, 25$NaHCO_3$, and 11 glucose), at 37°C, oxygenated (95% O2 and 5% CO2) and connected to an isometric force transducer (type 7006, Ugo Basile, Comerio, Italy) associated to a PowerLab 800 (AD Instruments). Rings were initially stretched until a resting tension of 0.5 g and allowed to equilibrate for at least 30 min. In each experiment bronchial rings were previously challenged with carbachol ($10^{-6}$ M) until a reproducible response curve was obtained. Then, after tissue washing, a cumulative concentration-response curve to carbachol ($10^{-9}$ -3x$10^{-6}$ M) was performed to evaluate bronchial contractility [76]. To analyze $\beta_2$-adrenoceptor-mediated relaxation, bronchial tissue was subjected to a cumulative concentration-response curve to salbutamol ($10^{-8}$ -3x$10^{-5}$ M). Bronchi were preincubated with different substances to study the pathophysiology and the mechanism of different pathways in the development or treatment of lung disease.

### 3.2.2 Desensitization Protocol.

Rings were initially stretched until a resting tension of 0.5 g and allowed to equilibrate for at least 30 min. In each experiment bronchial rings were previously challenged with carbachol ($10^{-6}$ M) until a reproducible response curve was obtained. To assess the drug effect on homologous $\beta_2$ desensitization two consecutive concentration-response curves to salbutamol ($10^{-9}$ -3x$10^{-6}$ M; Tocris Cat. No. 0634) were performed. The second curve was performed after washing and leaving the rings to equilibrate for 30 minutes [74].

### 3.3 Plasma IgE level measurement

Blood was collected by intracardiac puncture from male and female BALB/c mice using citrate (3.8%) as an anticoagulant. Then plasma was obtained by centrifugation at 12.000 rpm at 4°C for 10 minutes and immediately frozen at–80°C. Total IgE levels were measured with enzyme-linked immunosorbent416assay (ELISA) using matched antibody pairs (BD Biosciences Pharmingen San Jose, CA [77].

### 3.4 Lung cytokines level measurement

Lungs, harvested from male and female BALB/c mice, were isolated and homogenized in PBS (Sigma Aldrich, Milan, Italy). The homogenate was centrifuged (4° C, 6000 × *g*, 10 min). The pulmonary levels of IL-5 (Affymetrix eBioscience San Diego, CA), IL-33 (Affymetrix eBioscience San Diego, CA), IL-4 (R&D system, Biotechne) were measured with commercially available ELISA kits according to the manufacturer's instructions) and expressed as pg $mg^{-1}$ of tissue [77].

### 3.5 Lung Histology and Immunohistochemistry (IHC)

**Histology**: Lung was collected, fixed in formalin 4%, and embedded in paraffin. Lung slices were processed to remove paraffin and were rehydrated. Sections (7µm) were stained for hematoxylin & eosin (H&E) or periodic acid-Schiff ($PAS^{+}$) for the assessment of bronchial epithelium, pulmonary cells infiltration, and mucus production [77]. Inflammation severity was visually scored in a blinded fashion on hematoxylin-and-eosin-stained slides using a subjective semi-quantitative four-point scale, in which 0= normal lung (no

inflammatory infiltrate), 1= minimal disease (infrequent sparsely scattered inflammatory cells), 2= mild (light perivascular/peribronchiolar involvement), 3= moderate (many vessels and airways affected by substantial numbers of inflammatory cells), and 4 = severe (generalized accumulations of perivascular/peribronchiolar inflammatory cells with frequent circumferential and/or bridging infiltrates). Pulmonary cell infiltration was quantified by using ImageJ software. $PAS^+$ staining was graded with scores of 0 to 4 to describe low to severe lung inflammation as follows: 0: <5%; 1: 5-25%; 2: 25-50%; 3: 50-75%; 4: <75% positive staining/total lung area [78].

**IHC**: Lung slides were processed as described above and incubated with 3% hydrogen peroxide (Sigma-Aldrich H1009) for 15 min to quench the endogenous peroxidase activity. Antigen retrieval was performed by incubating the slices with a pre-heated retrieval solution (Citrate Buffer, 10mM Citric Acid, 0.05% Tween 20, pH 6.0) for 20 min [79]. Tissue sections were then incubated with 2% BSA (Sigma-Aldrich A9418) for 1h to reduce non-specific antibody interactions. Sections were incubated overnight at 4°C with primary antibodies diluted in 2% BSA. After rinsing with PBS 0.01M, slides were incubated with Peroxidase AffiniPure Goat anti-Rabbit or Mouse IgG (Jackson ImmunoResearch, 1:500) for 1h at room temperature. Colour development was performed using 3,3'-Diaminobenzidine Chromogen Solution (SIGMAFAST$^{TM}$-DAB) and sections were analyzed by using Leica Microsystem with a magnification of 20x. Semi-quantitative determination of protein expression was obtained with ImageJ/Fiji software. For antibodies details see Table 1.

## 3.6 Quantitative RT-PCR

Mouse bronchial tissues were homogenized by using FastPrep in Purezol Reagent (Bio-Rad, Hercules, CA) and RNA was extracted according to the manufacturer's instructions. The quantification and quality analysis of RNA was ascertained by using NanoDrop™ One/OneC Microvolume UV-Vis Spectrophotometer (ThermoFisher Scientific, Monza, Italy). Retro-transcription was performed by using the High-Capacity cDNA Reverse Transcription Kit (Applied Biosystem, Carlsbad, CA). Reverse transcription polymerase chain reaction (qRT–PCR) was performed by using Fast SYBR Green Master Mix (Applied Biosystem, Carlsbad, CA) and reactions were performed and analyzed on CFX Connect Real-Time PCR Detection System (Bio-Rad, Hercules, CA). Target gene expression calculations were normalized on reference housekeeping gene GAPDH (glyceraldehyde-3-phosphate dehydrogenase) and expressed by using the 2-ΔΔCt formula.

## 3.7 Quantification of S1P and Sphingosine

Extraction of sphingosine (S) and sphingosine-1-Phosphate (S1P) from lung tissue homogenates was performed by the following method: Briefly, 1mL of mixture *i*–PrOH–Water–EtOAc (30:10:60) was added to 0.5 mg of total proteins measured by Bradford assay in each lung tissue homogenate. Samples were stirred for 30 min, sonicated for 15 min, and centrifuged at 21000 g for 15 min. The supernatant was transferred to a new centrifuge tube and evaporated to dryness at 40 °C in the vacuum rotator. Samples were reconstituted in 50 µL MeOH, vortexed for 5 min, sonicated for 10 min, and

centrifuged for 10 min at 10000 g and 10 µL were loaded on the UPLC-MSMS system.

Sph and S1P were quantified by liquid chromatography coupled to tandem mass spectrometry detection (LC-MS/MS) on Shimadzu LC-20A and Auto Sampler systems and QTRAP 6500 instrument from AB-Sciex. C18 chromatographic column (Kinetex C18, 50 x 2.1 mm, 5µm, Phenomenex) was used for chromatographic separation. The mobile phase was composed of water 0.1% formic acid (mobile phase A) and methanol 0.1% formic acid (mobile phase B). The flow rate was set at 400 µL/min. The mass spectrometer was set in the positive ion mode (ESI+) with an electrospray voltage of 5500 V at 400°C of the heated capillary temperature. The multiple reaction monitoring (MRM) mode and the Analyst 1.6.2 software have been used. S was analyzed with the mass transition 300 m/z to 282 m/z and it was observed at the rt of 7.18 min. S1P was analysed with the mass transition 380 m/z to 264 m/z and it was observed at the rt of 8.30 min. Nitrogen was used as the air curtain gas (20psi), atomizing gas (30psi), auxiliary gas (60psi) and collision gas (4psi). Dwell time was 100ms, DP was 74v, EP was 10v, CE was 22v and CXP was 15v. For quantitative analysis, a standard curve with S and S1P amounts of 250 pg, 100 pg, 25 pg, 10 pg and 2.5pg has been run.

### 3.8 cAMP assay

Mice were sacrificed and bronchi were dissected from the lungs and placed at 37°C in oxygenated Krebs solution, to perform different incubation. Samples were incubated with Krebs solution as a vehicle (for 10 minutes), Salbutamol (10 µM for 10 minutes), IBMX (0,1 µM for 10 minutes) plus salbutamol (10 µM for 10 minutes), L-NAME (100 µM for 10 minutes) plus salbutamol (10

μM for 10 minutes). After incubation, all tissues were quickly frozen at -80° Afterwards, bronchi were homogenated with TCA 5% and centrifugated at 1.500 g for 10 min. After three washes with ether, samples were placed in termo-block for 5 minutes at 70°C. Cyclic-AMP level in bronchi was measured with a commercially available enzyme-linked immunosorbent assay kit (Cayman Cyclic AMP ELISA kit) according to manufacturer's instructions. Levels of the mediator were expressed as pmoli/mg tissue.

## 3.9 Flow cytometry

Main bronchi were excised in sterile conditions by using a digestive solution containing a mixture of collagenase, trypsin, and hyaluronidase. Markers such as CD326 also known as an epithelial cell adhesion molecule (EpCAM) and mesenchymal markers such as CD90 were analyzed using flow cytometry (Camerlingo et al., 2011). After digestion, cell suspension was incubated with CD90 PE mouse and rat (Milteny iBiotec, Calderara di Reno, Bologna, Italy), CD326 APC mouse (Milteny iBiotec, Calderara di Reno, Bologna, Italy). After incubation, the samples were analyzed by FACS AriaII (Becton Dickinson, Franklin Lakes, NJ, USA). All data were analyzed by Diva 6.1 Software (Becton Dickinson, Franklin Lakes, NJ, USA) [75].

## 3.10 Cellular studies

### 3.10.1 J774 cell culture

The murine monocyte/macrophage J774 cell line was obtained from the American Type Culture Collection (ATTC TIB 67). The cell line was grown

in adhesion in Dulbecco's modified Eagles medium (DMEM) supplemented with glutamine (2 mM, Aurogene Rome, Italy), Hepes (25 mM,358Aurogene Rome, Italy), penicillin (100 U/mL, Aurogene Rome, Italy), streptomycin (100 μg/mL,359Aurogene Rome, Italy), fetal bovine serum (FBS, 10%, Aurogene Rome, Italy) and sodium pyruvate (1.2%, Aurogene Rome, Italy) (DMEM completed). The cells were plated at a density of $1 \times 10^6$ cells in 75 $cm^2$ culture flasks and maintained at 37 °C under 5% CO2 in a humidified incubator until 90% confluence. The culture medium was changed every 2 days. Before a confluent monolayer appeared, the sub-culturing cell process was carried out.

### 3.10.2 BEAS-2B cell culture

BEAS- 2B cells (Epithelial cells from human bronchial epithelium, ATCC-CRL-9609) were cultured under a 5%CO2/air atmosphere at 37°C in a 24-well tissue culture plate containing Roswell Park Memorial Institute Medium (RPMI), supplemented with glutamine (2 mM, Aurogene, Rome, Italy), penicillin (100 U/mL, Aurogene, Rome, Italy), streptomycin (100 μg/mL, Aurogene, Rome, Italy), fetal bovine serum (FBS, 10%, Aurogene Rome, Italy). The cells were plated at a density of $1 \times 10^6$ cells in 75 cm2 culture flasks and maintained at 37 ◦C under 5% CO2 in a humidified incubator until 90% confluence. The culture medium was changed every 2 days.

### 3.10.3 A549 cell culture

A549 (human lung epithelial cells) were obtained from the American Type Culture Collection (ATTC). A549 cell line was grown in adhesion in Dulbecco's modified Eagles medium (DMEM), supplemented with glutamine (2 mM, Aurogene, Rome, Italy), penicillin (100 U/mL, Aurogene, Rome,

Italy), streptomycin (100 µg/mL, Aurogene, Rome, Italy), fetal bovine serum (FBS, 10%, Aurogene Rome, Italy). The cells were plated at a density of 1 × $10^6$ cells in 75 cm2 culture flasks and maintained at 37 ◦C under 5% CO2 in a humidified incubator until 90% confluence. The culture medium was changed every 2 days.

### 3.10.4 HBSM cell culture

Human Bronchial Smooth Muscle Cells (BMSC) line was obtained from LONZA. The cells were isolated from the major bronchial normal tissue from male donor. All cells test negative for mycoplasma, bacteria, yeast, and fungi. HIV-1, Hepatitis B and Hepatitis C are not detected for all donors and/or cell lots.

The cell line was grown with Smooth Muscle Cell Growth Medium -2 BulletKit™ (SmGM #CC-3182) containing Smooth muscle basal medium (SmBM) and all supplement required for growth smooth muscle cells: FBS (Fetal bovine serum) 5%; Insulin, 0,50mL; hFGF-B, 1mL; GA1000, 0,5mL; hEGF, 0,5mL. The cells were plated at a density of 5 × $10^5$ cells in 75 cm2 culture flasks and maintained at 37 ◦C under 5% CO2 in a humidified incubator. The culture medium was changed every 2 days.

## 3.11 Cellular viability measurement

Mitochondrial activity, an indicator of cell viability, was assessed by the mitochondrial-dependent reduction of 3-(4,5-dimethylthiazol-2-yl)-2,5-diphenyltetrazolium bromide (MTT; Sigma Aldrich,Milan, Italy) to formazan. Cells were plated to a seeding density of 1.0 × $10^5$ in 96 multiwells. After stimulation with test compounds for 24 h, cells were incubated in 96-well plates with MTT (0.2380mg/mL), for 1 h. The medium was removed by

aspiration and the cells were lysed in DMSO (0.1 mL). The extent of reduction of MTT to formazan within cells was quantified by the measurement of OD550 [80].

### 3.12 Nitric oxide assay

The nitrite concentration in the samples was measured by the Griess reaction, by3 adding 100 μL of Griess reagent (0.1% naphthylethylenediamide dihydrochloride in H2O and 1% sulphanilamide in 5% concentrated H2PO4; vol. 1:1; Sigma Aldrich, Milan, Italy) to 100 μL samples. Theoptical density at 540nm (OD540) was measured immediately after Griess reagent addition, using ELISA microplate reader (Thermo Scientific, Multiskan GO). Nitrite concentration was calculated by comparison with OD540 of standard solutions of sodium nitrite prepared in a culture medium. IC50 analysis for PS, TBZ, and PS-TBZ has been performed with GraphPad 9 software [80].

### 3.13 Cell contraction assay

The cells are mixed in Rat tail collagen Type I by mixing 6 parts of cell at density of $2x10^5$ cells for dish, 2.5 parts of rat tail collagen and 0.046 part of NaOH. A quantity of 0.5 mL of the cell-collagen mixture was added per well in a 24-well plate, and incubate 1h at 37ºC. After collagen polymerization, 0.5 mL of culture medium was added in each collagen gel, with the treatments (+/- OEA10uM and +/_ CSE2%) and Carbachol as contracturant, at concentration of 10-6 M in each well. Only rat tail collagen and cell medium were plated as control. Images were taken using Chemi Doc chemiluminescent detection system after 6h, 24h and 48h. The collagen gel diameter size change was measured at various times with ImageJ/Fiji software.

## 3.14 Scratch assay

The cells were seeded into 12-well tissue culture plate at a density that after 24h growth, they reached 70-80% confluence. Once at confluence the cell layer was scraped in a straight line using a 1 mm pipette tip. After scratch, the cell monolayer was gently washed to remove detached cells, then replenished with fresh medium with the treatments (+/- OEA10uM and +/_ CSE2%). Images were taken using a phase contrast microscope on 4x magnification after 6h, 24h and 48h at the same point coordinates.

## 3.15 Western blot

Lung and bronchi from female and male C57/Bl6, BEAS, A549 and HBSM cells were homogenates, the total protein content was measured in each sample, WB was performed using different polyclonal primary antibodies, incubated overnight, and following using secondary antibodies anti-Mouse or anti-Rabbit HRP conjugated. Membranes were detected with ECL (Bio-Rad) immunoblotting detection reagents. Bands were quantified using a Chemi Doc chemiluminescent detection system and densitometrical analyzed using ImageQuant-400 (GE Healthcare, USA). The target protein band intensity was normalized over the intensity of the housekeeping protein GAPDH (1:5000, Invitrogen). For antibodies details see Table 1.

## 3.16 Human Study

### 3.16.1 Human lung sections

Lung tissue sections from never smoker control (NSC), smoker control (SC) and COPD (GOLD 1-4) patients male and female were obtained from archival lung specimens from lung explants obtained at the time of lung transplantation or wedge resections/lobectomies performed for clinical indications. Normal lung tissue sections were identified by a clinical expert (S.O.V.) from surgical tissue obtained from patients without COPD or other underlying primary lung diseases.

## 3.17 Immunofluorescence (IF)

**Human lung**: Formalin-fixed and paraffin-embedded (5 μm-thick) lung sections from explants or lung resections from patients never smoker control (NSC) (n= 4Female/5Male), smoker control (SC) (n=5Female/5Male) and COPD (GOLD 1-4) (n= 6Female/6Male) obtained during surgical resections were deparaffinized, and antigen retrieval was performed by boiling the slides immersed in 0.01 M sodium citrate and 2 mM citrate buffer (pH 6.0) in a microwave. These lung slices were stained for different primary antibodies. As secondary antibody was using Alexa 488 Goat anti-Rabbit, and Alexa 568 Goat anti-Mouse, both at dilution 1:100 purchased from Invitrogen.
Sections were analyzed by using Leica Microsystem with a magnification of 20x. Semi-quantitative determination of protein expression on bronchi was obtained with ImageJ/Fiji software measuring fluorescence intensity [81].

**HBSM and BEAS2-B Cell**: HBSM cells were plated at the density of $3x10^4$ on 8 chamber polystyrene vessel tissue Culture glass slide (Falcon). Then the

cells were fixed with glacial methanol 100% for 20 minutes and stained for different primary antibodies. As secondary antibody was using Alexa 488 Goat anti Rabbit, at dilution 1:100 and Alexa 568 Goat anti-Mouse purchased from Invitrogen.

The staining was analyzed by using Leica Microsystem with a magnification of 20x. Semi-quantitative determination of protein expression on cells and the determination of cell confluency was obtained with ImageJ/Fiji software measuring fluorescence intensity [81]. For antibodies details see Table 1.

## 3.18 Statistical Analysis

The results are expressed as mean ± S.E.M of n observations, where n represents the number of animals, cell groups or patients. Statistical evaluation was performed by one-way or two-way ANOVA using GraphPad InStat (Graphpad Software Inc., San Diego, CA) followed by a Bonferroni post-hoc test for multiple comparisons. Post hoc tests were run only if F achieved $P < 0.05$ and if there was no significant variance in the homogeneity. Correlations were calculated using the Spearman correlation test (r). A P value $< 0.05$ was used to define statistically significant differences between mean values. Outliers were identified by Grubbs' test.

## 3.19 Materials and Drugs

The compounds used were provided by the following suppliers: OVA, OEA, carbachol, Estradiol, Tamoxifen, IBMX, H89 by Sigma Aldrich (Milan, Italy), S1P by Enzo Life Science (Rome, Italy), TY52156, JTE-013, SK-I and salbutamol by Tocris Bioscience (United Kingdom), DHT by Sigma Aldrich (Milan, Italy).

**Cigarette smoke extract preparation:** One full-strength Marlboro cigarette (Philip Morris USA, Richmond, VA, USA) without the filter was directly connected to one end of a tube, and the other end of the tube emerged in 10 mL of culture media in a vacuum glass vessel. The cigarette was ignited, and the smoke was allowed to permeate the media by the application of a vacuum to the vessel. The CSE-media solution was filtered through a 0.22-μm filter (Millipore, Bedford, MA, USA). The CSE was prepared immediately before each experiment. The final product was defined as 100% CSE [82].

# Chapter 4

# 4. Role of Sphingolipids in the development of asthma and their interaction with sexual hormones.

## 4.1 Sphingosine-1-phosphate/TGF-β axis is involved in epithelial-mesenchymal transition in asthma.

Epithelial-mesenchymal transition (EMT) represents an important source of myofibroblasts, contributing to airway remodeling, which is a critical feature of chronic lung diseases. Here, we investigated the sphingosine-1-phosphate (S1P) role in EMT and its involvement in asthma-related airway dysfunction.

### 4.1.1 Rationale

Sphingosine 1-phosphate (S1P) is a potent bioactive molecule involved in a variety of cellular processes, including cell differentiation, proliferation, and migration. In animal models of asthma or mild chronic obstructive pulmonary disease, inhibition of S1P signaling reduces symptoms underling a key role for S1P in driving molecular mechanisms involved in pulmonary diseases [83]. Systemic administration of S1P to mice induces asthma-like disease characterized by a dose and time-dependent airway hyperresponsiveness and lung inflammation [84],[65]. These features are mediated by a clear cellular activity, with an obligatory role for the Th2-like adaptive immunity [84].

Airway dysfunction is a common denominator of chronic lung diseases. The airway epithelium constitutes the first barrier to the external environment and plays a key role in the protection of the internal milieu of the lung. In this scaffolding, the epithelial-mesenchymal trophic unit ensures lung homeostasis. In pulmonary inflammatory diseases, alteration of this homeostatic mechanism leads to changes in airway structure and in lung function decline. This phenomenon is generally defined as airway remodeling. This includes subepithelial fibrosis, hyperplasia of myofibroblasts and myocytes and an increase in smooth muscle fibers. These events cause down-regulation of epithelial cell–cell adhesion and mesenchymal gene expression programs promotion providing the background for Th2-biased lung inflammation. This interaction among structural changes, altered immunity and inflammation allows the persistence of chronic airway inflammation also in the absence of environmental stimulation. Clinical studies have demonstrated a significant positive correlation between S1P levels and epithelial-mesenchymal transition (EMT) in lung diseases [75].

### 4.1.2 Aim

Sphingolipid metabolism represents a pathway influencing airway function in physiological and pathological conditions. The link between S1P, TGF-β (TGFβ1), EMT and the development of airway diseases has not been clearly defined yet. Here, we aim to investigate the contribution of S1P as an inducer of EMT through the regulation of TGF-β signaling in asthma-feature development.

### 4.1.3 Materials and Methods

Material and methods, and statistical analysis related to these experiments are reported in Chapter3.

### 4.1.4 Results

***TGF-β is involved in S1P-induced EMT.***

The role of S1P in EMT was evaluated by using A549 cells. Epithelial cells cultured in absence of TGF-β maintained a classic epithelial morphology and growth pattern (Figure 4. A). A549 cells following incubation for 72 h with TGF-β or S1P assumed an elongated shape and many cells lost contact with their neighbor and displayed a spindle-shape, acquiring a fibroblast-like morphology. These effects were reversed by incubation of cells with TGF-β receptor antagonist LY2109761 (Figure 4.1A). A549 cells exposed to S1P show also an up-regulation of the mesenchymal marker CD90 and a down-regulation of the epithelial marker CD326 (Figure 4.1B). Incubation with LY2109761 before TGF-β or S1P induces either CD90 up-regulation or CD326 down-regulation (Figure 4.1B). The alteration in the expression and distribution of vimentin and cytokeratin has been confirmed by immunofluorescence assay (Figure 4.1C).

Immunofluorescence studies show that both S1P (Figure 4.1C, panels B and G) or TGF-β (panels D and I) induce a down-regulation of cytokeratin (Figure 4.1C, left panels) and up-regulation of vimentin (Figure 4.1 C, right panels) when compared to vehicle (panels A and F) and the cells acquire a fibroblast-like morphology (panel G and I). Pretreatment of cells with

LY2109761 before S1P (panels C and H) or TGF-β (panels E and L) reverses both the downregulation of cytokeratin (left panels) and up-regulation of vimentin (right panels) and the cells maintain their classic cobblestone epithelial morphology. This data was confirmed by colocalization staining of vimentin and α-SMA (Figure 4.2). Immunofluorescence staining was examined for the mesenchymal markers, α-SMA (green fluorescence, Figure 4.2 A.III, B.III, C.III, D.III, E.III) and vimentin (red fluorescence, A.II, B.II, C.II, D.II, E.II), while in the right panels the co-expression of markers (Figure 4.2 A.IV, B.IV, C.IV, D.IV, E.IV) were reported. Both S1P and TGF-β induced up-regulation of vimentin and α-SMA (Figure 4.2 panel B. II, B.III, C. II and C.III.) and the cells showed structural features with myofibroblast differentiation (B.IV and C.I).

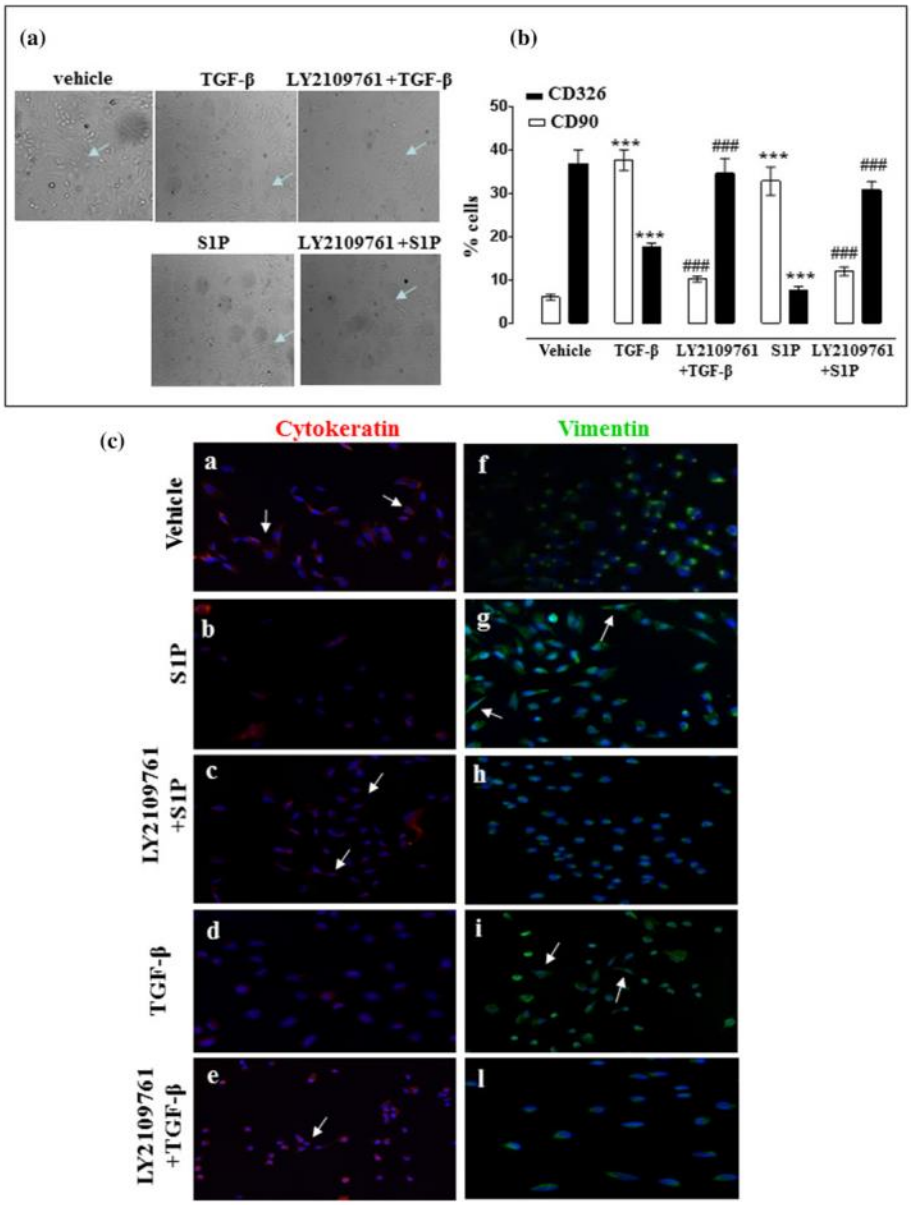


***Figure 4.1: S1P induces EMT in a TGF-β dependent manner.*** A549 cells were exposed to vehicle, TGF-β or S1P in the presence or absence of LY2109761 (TGF-β antagonist of both type I and II receptors). Morphological changes were assessed by light microscopy ×10 magnification (a). A flow cytometry analysis of CD326+ (epithelial marker,) and CD90+ (mesenchymal marker) cells was performed. (b) Data are expressed as mean ± SEM as assessed by one-way ANOVA followed by Tukey's

multiple comparison test $p <$ ***$p < 0.001$ vs. vehicle. ###$p < 0.001$ vs. S1P or TGF-β. Immunofluorescence staining (c) was examined for the following markers: cytokeratin the epithelial marker (red fluorescence, left panels A–E) and vimentin the mesenchymal markers (green fluorescence, right panels F–L). Cells were photographed at ×20 magnification. The arrows in panels G and I indicate cells undergoing to mesenchymal transition displaying an increased staining for vimentin (green) and downregulation of cytokeratin. Panels A, C and E indicate the epithelial phenotype.

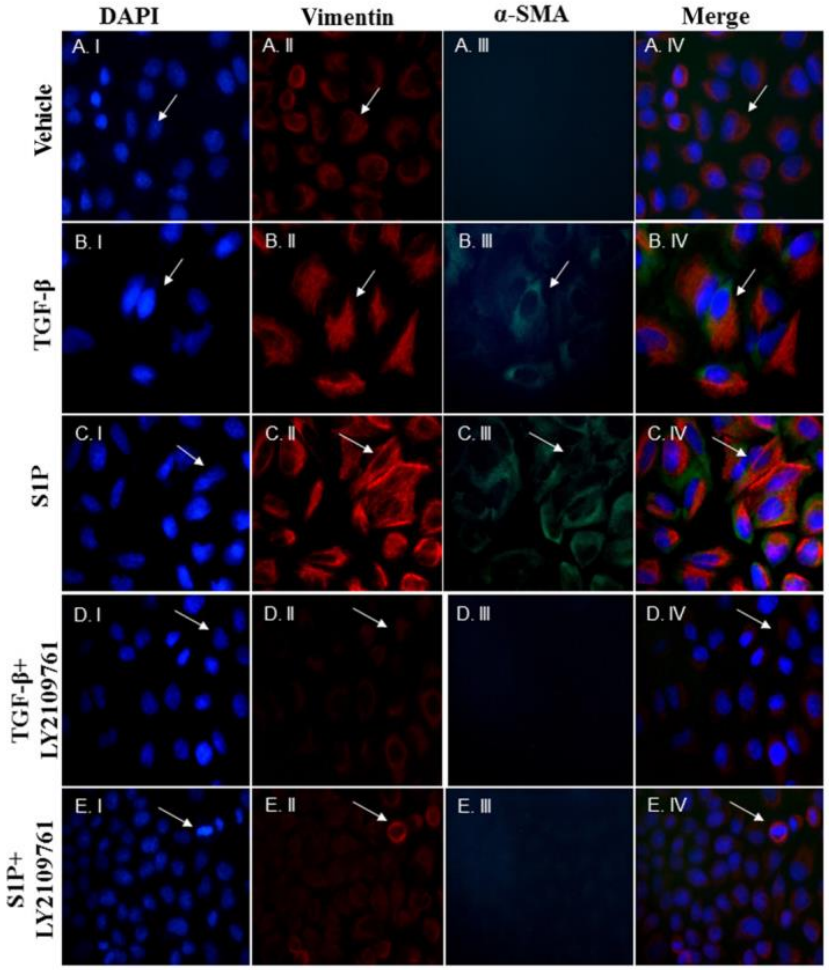


***Figure 4.2: TGF-β and S1P-induce expression of mesenchymal markers.*** A549 cells were exposed to TGF-β or S1P in the presence or absence of LY2109761 (TGF-β antagonist of both types I and II receptors). Immunofluorescence staining was examined for the mesenchymal markers, α-SMA (green fluorescence, A.III, B.III, C.III, D.III, E.III) and vimentin (red fluorescence, A.IV, B.IV, C.IV, D.IV, E.IV), in the right panels the co-expression of markers (A.V, B.V, C.V, D.V, E.V). Nuclear DAPI staining (A.I, B.I, C.I, D.I, E.I). Cells were photographed at 40× magnification. The arrows indicate a single cell undergoing each staining performed, that is, DAPI or Vimentin or α-SMA and the staining MERGE (column IV) for each treatment.

***S1P induces EMT in a fibroproliferative environment within the lung.***

Subcutaneous administration of S1P (Figure 4.3A) to mice induces a time and dose-dependent airway hyperresponsiveness and lung inflammation. These symptoms are mediated by cellular activity, with an essential role for the Th2-like adaptive immunity. Lungs harvested from S1P-treated mice display a time-dependent increase of TGF-β in the lung (Figure 4.3B), IL-33 (Figure 4.3 C) and FGF-2 (Figure 4.3 D). At the same time, bronchi harvested from S1P-treated mice show a shift in the expression from an epithelial to a mesenchymal structure as confirmed by the two key markers analyzed by flow cytometry (Figures 4.3E). CD90, a mesenchymal marker, is more expressed in bronchial tissues harvested from S1P-treated mice than in vehicle-treated mice. Conversely, the expression of CD326, an epithelial marker, is elevated in bronchi harvested from vehicle-treated mice and decreases in S1P-treated mice (Figure 4.3E). These results matched with the different morphology (Figure 4.4A) of fibroblasts isolated from lungs of vehicle or S1P treated mice. Also, a significant increase in the proliferation rate occurs in the fibroblasts harvested from S1P treated mice compared to the vehicle (Figure 4.4B). As clearly shown in Figure 4.4C, a significant up-regulation of α-SMA occurs in fibroblasts harvested from S1P-treated mice.

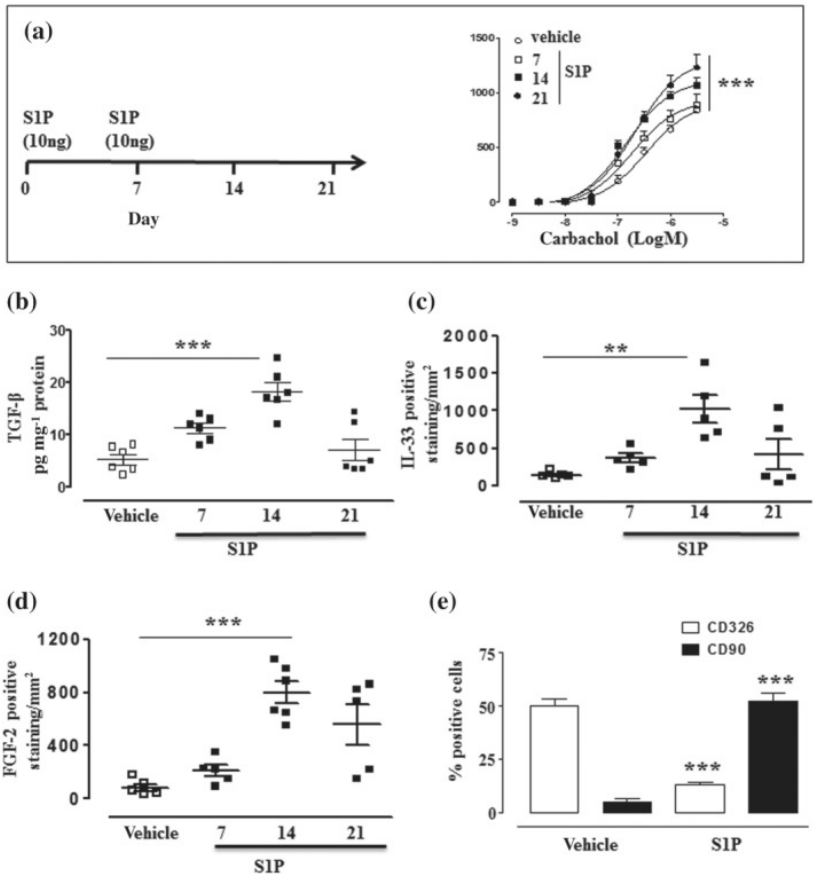


***Figure 4.3: Systemic administration of S1P induces a fibroproliferative environment within the lung.*** BALB/c mice received subcutaneous administration of S1P (10 ng) at days 0 and 7 (a). Mice were killed at 7, 14 and 21 days and bronchial reactivity was assessed (a) $***p < 0.001$ vs. vehicle as assessed by two-way ANOVA followed by Bonferroni post-test. TGF-β (b), IL-33 (c) and FGF-2 (d) were measured in lung homogenate. Data are expressed as mean ± SEM. $**p < 0.01$ vs. vehicle; $***p < 0.001$ vs. vehicle as assessed by one-way ANOVA followed by Tukey's multiple comparison test. Bronchi were harvested after 14 days from vehicle or S1P treated mice and a flow cytometry analysis (e) of CD326+ (epithelial marker) and CD90+ (mesenchymal marker) cells were performed. $n = 6$; data are expressed as mean ± SEM. $**p < 0.01$ vs. vehicle; $***p < 0.001$ vs. vehicle as assessed by the Student's *t*-test.

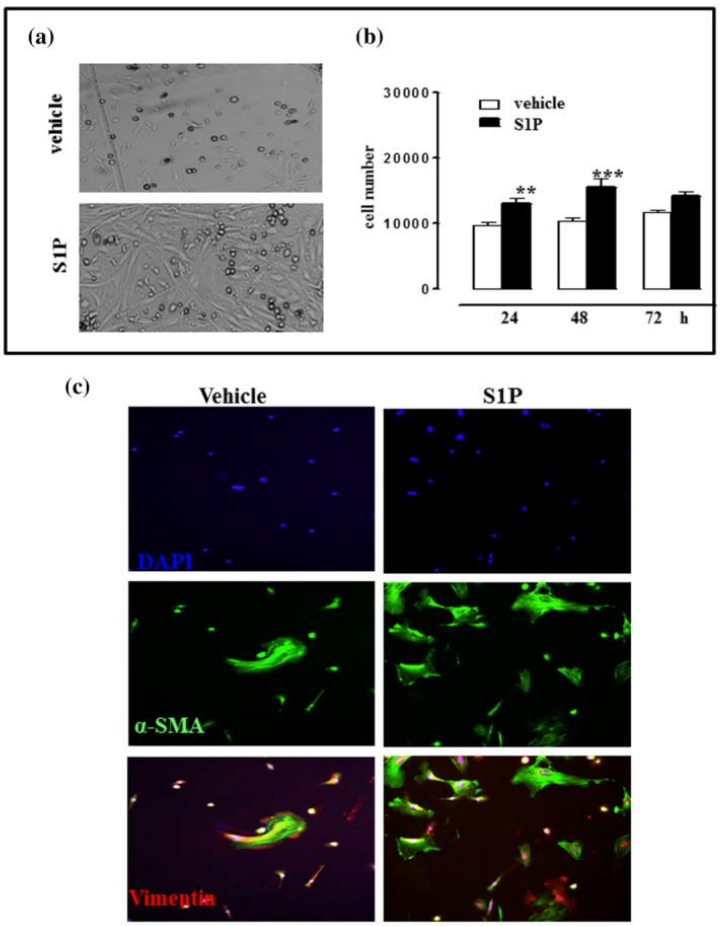


***Figure 4.4: Systemic administration of S1P primes pulmonary fibroblasts.*** Pulmonary fibroblasts were harvested from mice ($n = 6$) treated with either vehicle or S1P. Morphological changes were assessed by light microscopy ×10 magnification (a). Fibroblast proliferation was assessed by MTT assay (b). Data are expressed as mean ± SEM. $^{**}p < 0.01$ vs. vehicle; $^{***}p < 0.001$ vs. vehicle as assessed by two-way ANOVA followed by Bonferroni post-test. Fibroblast differentiation was evaluated by immunofluorescence analysis by using a mouse monoclonal antibody against α-SMA (c).

***S1P shifts the epithelial-mesenchymal repertoire in airways.***

EMT induction by S1P in vivo was further analyzed by RT-PCR performed on bronchi harvested from both vehicle and S1P treated mice. The EMT regulators Twist and Snail (Figure 4.5 A, B) increase in S1P treated mice on day 14. The expression of type I (COL2A1) and type III (COL3A1) collagens have been analyzed as myofibroblast and EMT markers, respectively. The increase in mRNA levels of COL1A1 and COL3A1 genes (Figure 4.5C, D) correlates to the development of asthma-like features induced by S1P. Furthermore, we have also measured other markers that have been identified as characteristic of epithelial or mesenchymal cells. Bronchi harvested from S1P treated mice showed a decrease in the epithelial marker E-cadherin (Figure 4.5E) in a time-dependent manner. On the other hand, there was an increase in the expression of mesenchymal markers: vimentin (Figure 4.5F), alpha-smooth muscle actin (α-SMA) (Figure 4.5G) and fibronectin 1 (Figure 4.5H).

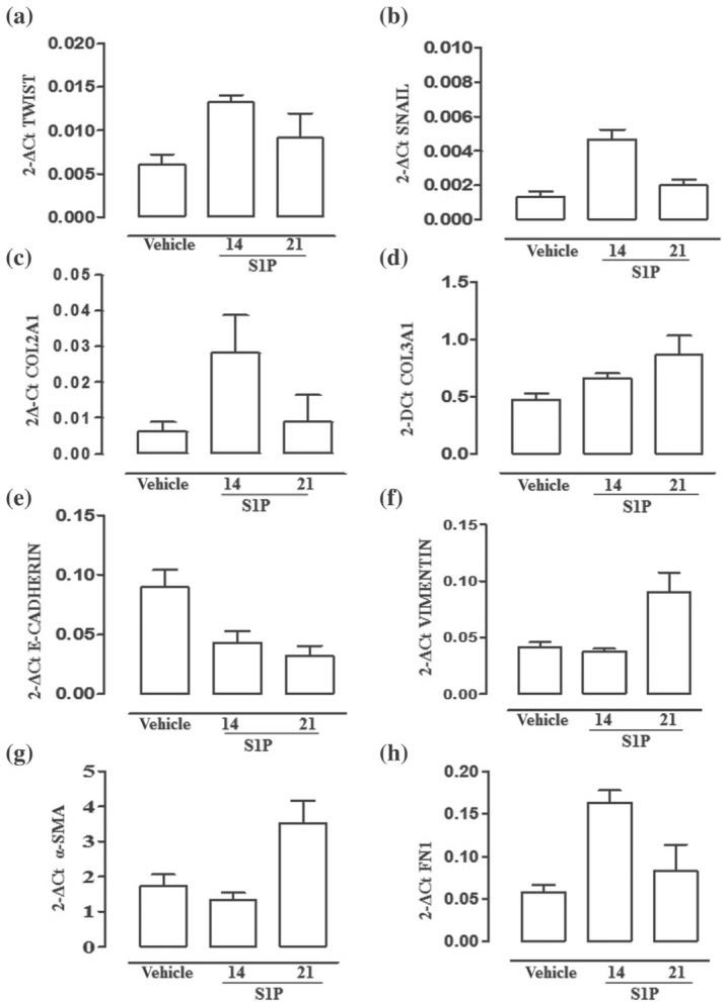


***Figure 4.5: S1P promotes EMT in the bronchi***. Bronchi were harvested from mice ($n = 6$) treated with vehicle or S1P and sacrificed at 14 days. mRNA expression levels of TWIST (a), SNAIL 1 (b), COL2A1 (c) and COL3A1 (d) E-cadherin (e), vimentin (f), alpha-smooth muscle actin (α-SMA) (g) and fibronectin 1 (h) were measured by quantitative reverse-transcription polymerase chain reaction (qRT-PCR) on samples expressed as media of the triplicates. Data are expressed as mean ± SEM, and the results were normalized to GAPDH mRNA by using the $2^{-\Delta Ct}$ formula.

***The S1P/TGF-β axis promotes asthma-like features.***

To assess the contribution of TGF-β signaling in the S1P-induced effect also in vivo, S1P-treated mice were pretreated with LY2109761. TGF-β blockade blunts the development of S1P-induced AHR (Figure 4.6A) and mucus hyperproduction as showed by PAS staining (Figure 4.6B). Accordingly, the immunohistochemical analysis of pulmonary sections showed a significant reduction of S1P-induced cell infiltration in mice treated with LY2109761(Figure 4.6C). Also, LY2109761 reverses both CD90 up-regulation and CD326 down-regulation induced by S1P (Figure 4.6D).

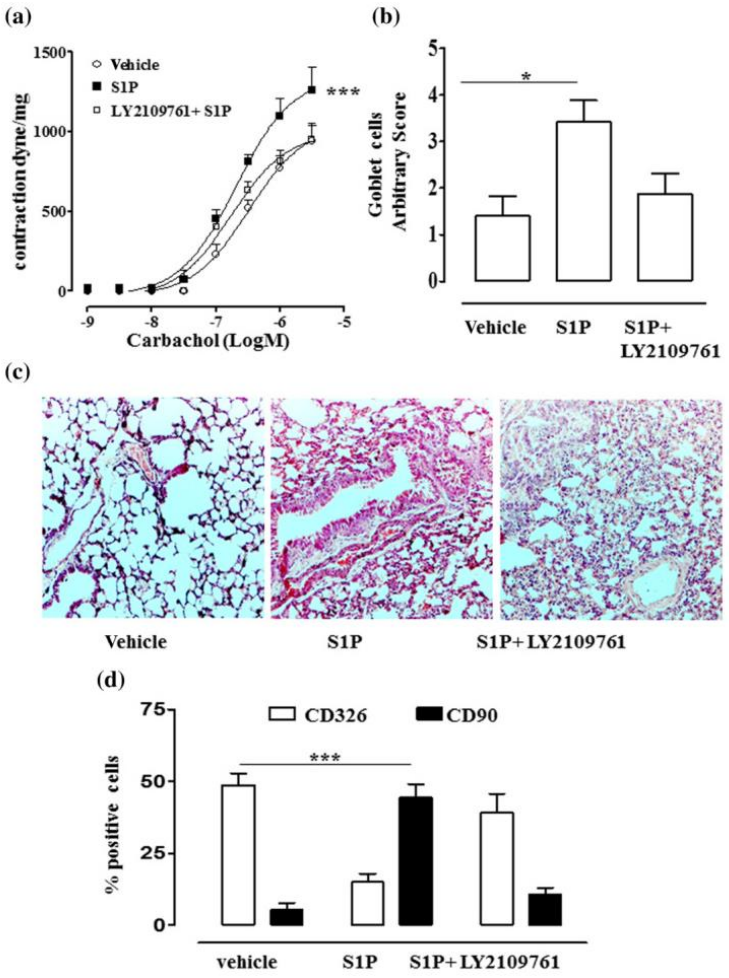


***Figure 4.6: TGF-β essential role for lung effects induced by S1P in vivo.*** Mice were treated in vivo with the vehicle, S1P or LY2109761 + S1P. Reactivity to carbachol (a) was evaluated using isolated bronchi. Data are expressed as mean ± SEM, ***$p < 0.001$ vs. vehicle as assessed by two-way ANOVA followed by Bonferroni post-test. The degree of inflammation was scored by blinded observers by using PAS staining (b). PAS-positive cryosections were graded with scores 0 to 4 to describe low to severe lung inflammation as follows: 0: <5%; 1: 5–25%; 2: 25–50%; 3: 50–75%; 4: <75% PAS-positive staining/total lung area. *$p < 0.05$ vs. vehicle as assessed by one-way ANOVA followed by Tukey's post-test. Representative H&E staining of the pulmonary sections photographed under light microscopy at ×10 magnification

(c). Flow cytometry analysis (d) of CD326 (epithelial markers) and CD90 (mesenchymal markers) was performed on bronchi. $n = 6$; data are expressed as mean ± SEM, ***$p < 0.001$ vs. vehicle as assessed by one-way ANOVA followed by Tukey's post-test.

***Blocking of the S1P/TGF-β axis blunts EMT and asthma features in OVA-sensitized mice.***

To further assess the essential role of the S1P/TGF-β axis in EMT and asthma, we used the mouse model of OVA-induced asthma (Figure 4.7A). As shown in Figure 4.7B, pretreatment with SK1-II abrogates OVA-induced AHR to carbachol at 21 days (Figure 4.7B) and TGF-β expression at 14 days (Figure 4.7C). In addition, SK1-II also inhibits EMT. Indeed, the flow cytometry analysis performed at 14 days on bronchi showed an up-regulation of the mesenchymal marker CD90 and a down-regulation of the epithelial marker CD326 (Figure 4.7D) that is reversed by the pretreatment in vivo with SK1-II (Figure 4.7D). SK1-II pretreatment also reverses OVA-induced fibroblast differentiation in myofibroblasts (Figure 4.7E, panels A–F).

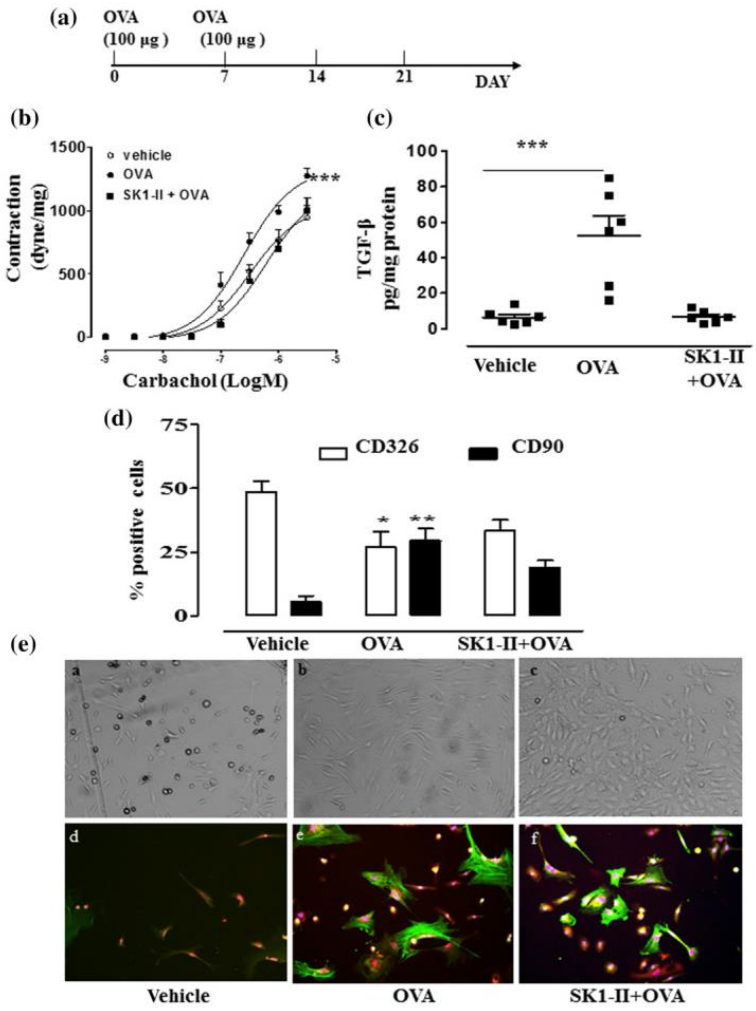


***Figure 4.7: Sphingosine kinase blockade inhibits changes in airway hyperreactivity, EMT and TGF-β triggered by OVA.*** Mice received subcutaneous (s.c) injection of 0.4 ml of 100-µg ovalbumin (OVA) absorbed to 3.3 mg of aluminum hydroxide gel in sterile saline on days 0 and 7 (a). A group of mice were treated with SKI-II (sphingosine kinases inhibitor; 3 mg/kg) prior to OVA challenge. Airway reactivity to carbachol was assessed at 21 days on isolated bronchi in vitro (b); ***$p < 0.001$ vs. vehicle. TGF-β secretion (c) was measured at 14 days in lung homogenates by ELISA; ***$p < 0.01$ vs. vehicle assessed by one-way ANOVA followed by Tukey's multiple comparison test. The epithelial marker CD326 (d) and

the mesenchymal marker CD90 (d) were assessed in bronchi by using flow cytometry analysis. $n = 6$; data are expressed as mean ± SEM; $*p < 0.05$ and $***p < 0.001$ vs. vehicle as assessed by one-way ANOVA followed by Tukey's post-test. Pulmonary fibroblasts were harvested from treated mice and their differentiation (e) was assessed as evident by light microscopy (panels A–C) and immunofluorescence analysis by using a monoclonal antibody against α-SMA (panels D–F).

### 4.1.5 Discussion and Conclusion

EMT has been recognized to play a key role in chronic respiratory diseases. TGF-β is an essential mediator of fibrotic and remodeling responses. Besides its role in regulating both Th17 and Treg activity, TGF-β modulates lung tissue morphogenesis and differentiation. Therefore, we aimed to investigate if TGF-β could act as a cytokine rheostat that mediates S1P effects within the lung. For this purpose, we have used the A549 cell line and two different experimental asthma models by exposing mice to S1P or to OVA. Following exposure to either S1P or TGF-β, A549 cells acquire a fibroblast-like morphology characterized by an increase of the mesenchymal marker CD90 and a decrease in the epithelial CD326 expression. The immunofluorescence analysis confirms the presence of an epithelial transition characterized by an increase in vimentin-positive staining and a reduction in cadherin. Thus, either S1P or TGF-β causes a similar EMT profile in A549 cells. The experiments performed pretreating A549 cells with LY2109761, an antagonist of TGF-β receptor type I and II, demonstrated that S1P-induced EMT is dependent on TGF-β as downstream signaling.

Following this evidence, we evaluated if this mechanism is also relevant in vivo. To this purpose, we used our previously characterized experimental model, where asthma-like features are triggered by a systemic administration

of S1P to BALB/c mice. In this model, S1P by itself promotes AHR, collagen deposition, and mucus secretion as well as an increase in serum IgE. In these experimental conditions, we found in the early phase, after 7 days, a pulmonary profibrotic environment characterized by a significant increase in TGF-β expression. This fibrotic environment is further characterized by the increased expression of two other remodeling biomarkers of asthma severity such as FGF-2 and IL-33. FGF-2 is required for pulmonary fibrosis and collagen production, implying a possible synergic action with TGF-β. IL-33 acts as an endogenous "danger signal" (alarmin), alerting the immune system to damaged cells/tissues and promoting repair mechanisms. The flow cytometry analysis of the bronchi harvested from S1P-challenged mice further confirmed the presence of a shift in epithelial-mesenchymal pattern. Indeed, in bronchi harvested from S1P-treated mice, there is an up-regulation of the mesenchymal marker CD90 and a concomitant down-regulation of the epithelial marker CD326. Accordingly, the two transcriptional regulators of EMT, Twist and Snail, are up regulated. E-cadherin, an epithelial marker, is down-regulated while up-regulation of the mesenchymal markers such as vimentin, fibronectin 1 and α-smooth muscle actin occurs. Thus, this altered pattern favors a fibroproliferative environment as also demonstrated by the significant increase in the expression of type I and type III collagens.

In the S1P model, the molecular data were confirmed by the structural changes observed in bronchi. Indeed, the histological analysis shows an increase in myofibroblasts around bronchi as confirmed by α-SMA evaluation, suggesting a functional impact of EMT on lung function. S1P-treated mice also develop AHR in a time-dependent manner and this functional change correlates well with the EMT markers such as cadherin and collagen.

To confirm the obligatory role of TGF-β in the S1P-induced effect already observed in A549 cells, we treated mice with the TGF-β antagonist before the

S1P challenge. LY2109761 treatment reduced EMT, airway hyperresponsiveness and pulmonary inflammation induced by S1P. Thus, the activation of the S1P/TGF-β axis is also essential to promote S1P-induced EMT in vivo.

S1P acts through different subtypes of receptors that are expressed in the lung. The contribution of S1P receptors in lung disease is confirmed by data obtained with FTY720, which binds to all S1P receptors except $S1P_2$. Treatment with FTY720 suppressed both Th1- and Th2-driven lung inflammation. FTY720 also inhibited the OVA-induced AHR and EMT in human lung cancer cells.

To further confirm the role of the S1P/TGF-β axis in asthma-associated EMT and to define the therapeutic relevance of this axis, we used an allergen-induced asthma model. OVA-sensitization triggers S1P signaling that participates in the molecular mechanisms underlying AHR and lung inflammation. Pretreatment with an inhibitor of sphingosine kinase, SK1-II, of OVA-sensitized mice caused a reduction of the bronchial hyperreactivity as well as of the TGF-β expression. In addition, bronchi, collected from OVA-sensitized mice, display morphological alterations typical of EMT such as down-regulation of the epithelial marker CD326 and up-regulation of mesenchymal markers CD90. Treatment of mice with SK1-II also prevents changes in epithelial and mesenchymal markers and as well blunts fibroblast differentiation.

In conclusion, our study provides direct evidence for a crosstalk between the SPK/S1P and TGF-β pathways in airways in vivo. Thus, targeting the S1P/TGF-β axis may hold promise as a feasible therapeutic target to prevent lung dysfunction in pulmonary diseases associated with EMT such as asthma [75].

## 4.2 Sphingosine-1-phosphate signaling is involved in female asthma susceptibility.

Genome-wide association studies have identified a link between asthma susceptibility and the ORMDL sphingolipid biosynthesis regulator 3 (ORMDL3). This study aimed to define the role of sphingosine-1-phosphate (S1P), the core structure of sphingolipids, in asthma susceptibility and sexual dimorphism in asthma features.

### 4.2.1 Rationale

Asthma phenotypes are determined by genetic susceptibility, but are also influenced by environmental exposures, as indicated by genome-wide association studies conducted in the last decade (2). Atopic asthma is considered the most common form of asthma, with a high incidence of 70-90% in children and 50% in adult patients [85].

Sex hormones play a crucial role in shaping the differences in asthma prevalence between males and females during the transition from childhood to adulthood. While boys during childhood exhibit a higher prevalence of asthma (65%), conversely during adulthood the rates become higher in adult women (also 65%) compared to adult men [85],[86]. The prevalence and severity of asthma appear to align with important phases in a woman's reproductive life and are strongly influenced by hormonal fluctuations during the menstrual cycle [87].

Sphingolipids, particularly sphingosine-1-phosphate (S1P), have been identified as significant contributors to asthma. S1P is involved in various cellular processes, including cell growth, differentiation, proliferation, signal

transduction, and immune response. Interestingly, S1P plasma levels are considerably higher in women compared to men during adulthood and associated with estrogen, with a noticeable decline after menopause [88].
Polymorphisms in orosomucoid-like 3 (ORMDL3) proteins, which play a crucial role in sphingolipid homeostasis and synthesis, have been associated with an increased risk of childhood asthma. The expression of ORMDL3 significantly increases during Th2-mediated allergic asthma in mouse models that mimic the key features of human asthma [89].

### 4.2.2 Aim

The aim of the study is to investigate sex-related differences in S1P signaling in the airways and it contributes to asthma susceptibility. To explore this hypothesis, we employed both animal and human studies.

### 4.2.3 Materials and Methods

Material and methods, and statistical analysis related to these experiments are reported in Chapter3.

### 4.2.4 Results

***S1P pathway is upregulated in female BALB/c mice.***

Female BALB/c mice show higher plasma IgE levels (Figure 4.8a) as well as pulmonary IL-5 expression (Figure 4.8b) when compared to males. Female bronchi display an increased contractility to carbachol (Figure 4.8c) compared to males. Immunohistochemical analysis of pulmonary sections shows upregulation of both α-SMA and ORMDL3 in bronchi harvested from females when compared to males (Figure 4.8e). However, no difference in peri-bronchial and parenchymal collagen deposition between sexes was evident through Sirius red staining (Figure 4.8d).

Western blot analysis on bronchi shows a higher expression in females of ceramidases (ASAH1; Figure 4.9a) a key enzyme in rheostat mechanisms of balance between S1P and its precursor ceramide. HPLC-SM analysis confirms higher levels of both pulmonary sphingosine and S1P in females when compared to males (Figure 4.9b). Accordingly, immunohistochemistry shows upregulation of transporter proteins SpnS2 in bronchi harvested from male mice when compared to female ones (Figure 4.9c). An increased expression of S1P receptors such as S1P1 (Figure 4.9d), S1P2 (Figure 4.9e), S1P3 (Figure 4.9g), as well as of both sphingosine kinases involved in sphingosine activation such as SPK1 (Figure 4.9g) and SPK2 (Figure 4.9h) is evident in bronchi harvested from females as well.

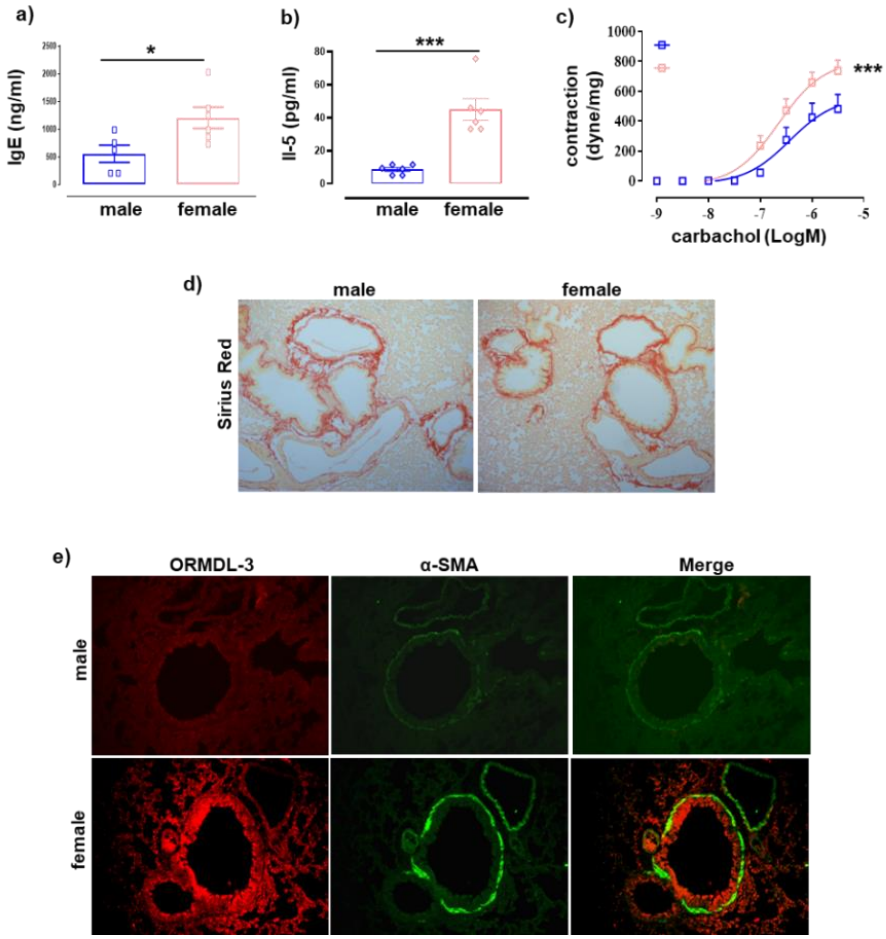


***Figure 4.8: Sex dimorphism in bronchial reactivity is associated with upregulation in α-SMA and ORMDL3.*** a) Plasma IgE levels and (b)pulmonary expression of IL-5 were measured in female and male BALB/c mice (n=6). c)Airway reactivity was assessed in isolated bronchi by exposure to cumulative administration of carbachol. In vitro study showed a higher reactivity of bronchi harvested from female BALB/c mice compared to males. (d) Collagen determination was assessed by Sirius Red staining performed on lung sections. Representative histological staining showed a more compact peri-bronchial collagen deposit in females. e) ORMDL3 (AlexaFluor 594) andα-SMA (AlexaFluor 488) expression was evaluated by immunohistochemical analysis that showed a higher expression of both in pulmonary sections obtained by female BALB/c mice. Scale bar= d) 169,6μm, e) 85,6μm. Data are presented as means±SEM; *p<0.05; ***p<0.01 versus male group.

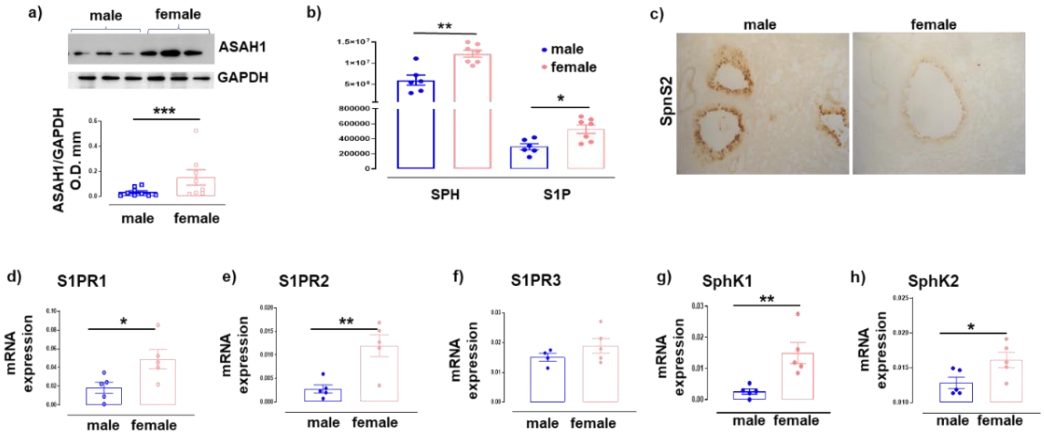


***Figure 4.9: S1P signaling is upregulated in female BALB/c mice***. Bronchi harvested from male and female BALB/c mice were processed for molecular studies. a) Expression of ceramidases (ASAH1) was assessed by western blot showing an increased expression in females. b) levels of both pulmonary sphingosine and S1P were measured by HPLC-SM. c) S1P transporter proteins SpnS2 was quantified by immunohistochemistry performed on lung sections and showed a peribronchial upregulation in male mice. d-h) expression of S1P receptors such as S1PR1 (d), S1PR2 (e), S1PR3 (f), as well as of both sphingosine kinases such as SphK1 (g) and SphK2 (h)were measured by RT-PCR. Data are expressed as mean±SEM; * $p<0.05$; $p<0.01$; $p<0.001$; versus male group.

***Pharmacological modulation of S1P signaling abrogates sexual dimorphism in bronchial reactivity.***

Bronchial tissues from female and male mice were treated with receptor antagonists of $S1P_2$ (JTE-013) or $S1P_3$ (TY52156) or the inhibitor of sphingosine kinases (SK-II), to assess the contribution of S1P signaling in the sex-related airway reactivity difference.

JTE-013, TY52156 and SK-II significantly inhibited carbachol-induced bronchial contractions in females (figures 4.10a, b and c). Conversely in bronchi harvested from male mice, pharmacological inhibition of S1P signaling did not affect bronchial contractility (figures 4.10d, e, and f). Thus, pharmacological modulation of S1P signaling abrogates sexual dimorphism in BALB/c mice, reporting female reactivity to the values observed in males (Figure 4.10g, h and i).

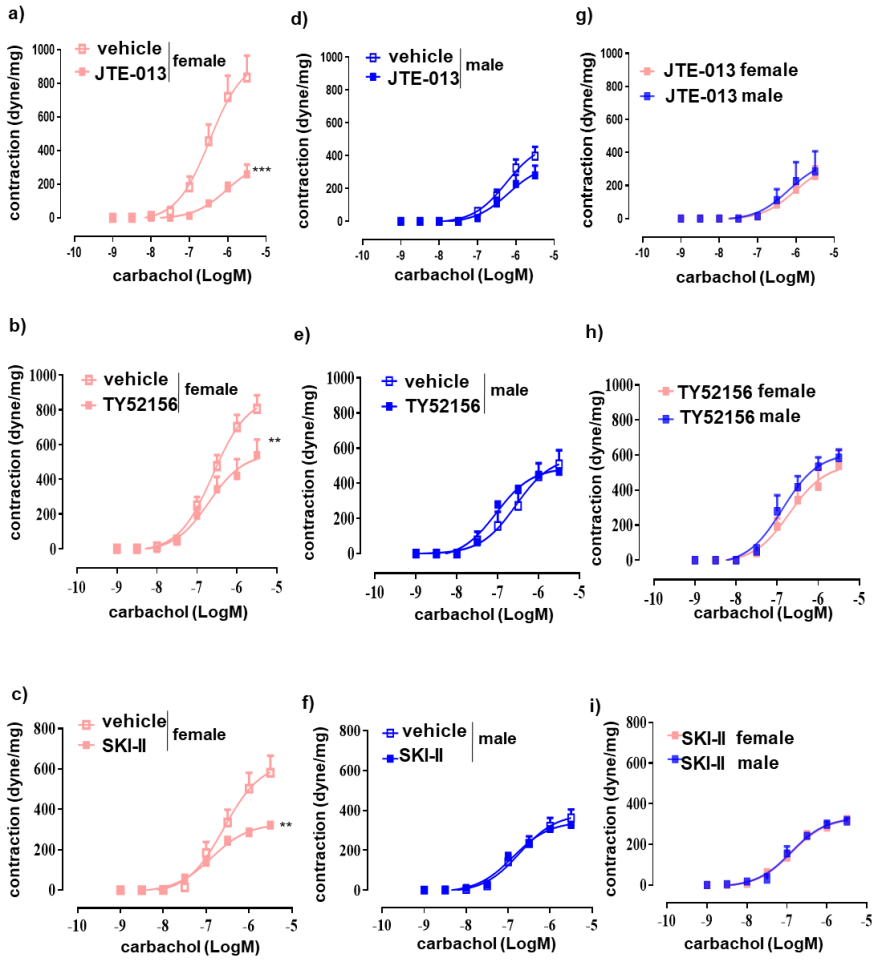


***Figure 4.10**: **S1P signaling blockage blunts sexual dimorphism in bronchial reactivity.*** Bronchial tissues harvested from female (a,b,c) and male (d,e,f) BALB/c mice (n=6) were exposed to cumulative administration of carbachol in presence of a S1PR2 antagonist (a, d; JTE-01310μM, 30 min) or a S1PR3 antagonist (b, e; TY52156 10μM, 30 min) or a non-selective inhibitor of SphKs (c, f; SKI-II, 100 μM, 1h). Pharmacological treatment reduced bronchial reactivity only in female mice abrogating sex dimorphism (g,h,i). Data are expressed as media± SEM; **: $p<0.01$***: $p<0.001$ versus vehicle.

***17β-estradiol supplementation enhances S1P signalling and increases bronchial reactivity in male mice.***

Administration of 17β-estradiol (25μg/kg every day for 7 days) to male mice (Figure 4.11a) promotes a significant increase in contractility abrogating the sex differences in bronchial reactivity as evident in Figure 4.11b. Male bronchial hyperreactivity induced by 17β-estradiol is coupled to a significant rise in plasma IgE levels (Figure 4.11c) as well as in pulmonary IL-5 expression (Figure 4.11d). RT-PCR analysis performed on bronchi shows that 17β-estradiol induces in the male mice a significant increase in all S1P receptors evaluated such as S1P1, S1P2, and S1P3 (Figure 4.11e-g). Incubation of bronchial tissues harvested from 17β-estradiol-treated male mice with S1P2 or S1P3 antagonists abrogates the 17β-estradiol-induced effect on bronchial reactivity (Figures 4.11h and i). 17β-estradiol supplementation also induces bronchial SPhK2 upregulation (Figure 4.12a, b, and c). HPLC/SM performed on pulmonary tissues shows an increase in both sphingosine and S1P levels (Figure 4.12d and e), abrogating sex differences bias of SPH/S1P expression. In perfect tune with the functional and analytical data, western blot shows a significant increase of ASAH1 in bronchi of estradiol-treated male mice when compared to vehicle male mice (Figure 4.12f).

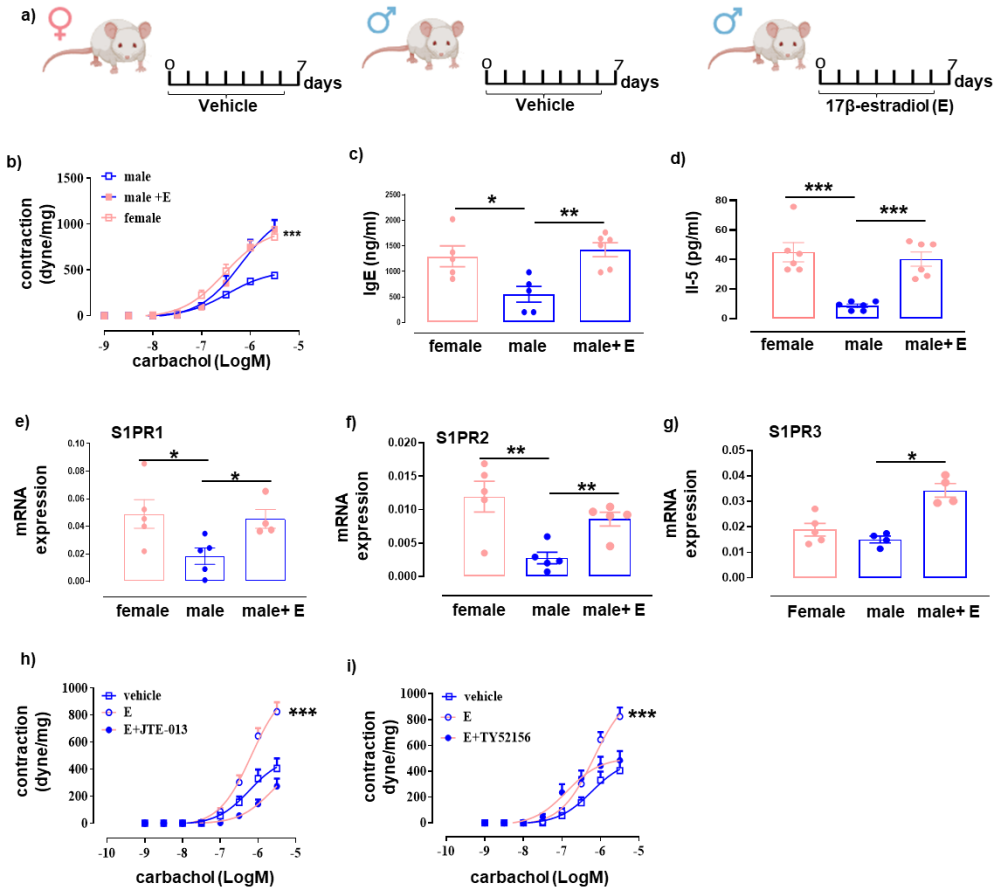


***Figure 4.11: 17-β-estradiol (E) supplementation promotes AHR and S1P upregulation in male mice.*** a) male BALB/c mice received subcutaneous administration of 17-β-estradiol (25µg/kg every day for 7 days). 17-β-estradiol increased b) bronchial reactivity to carbachol, c) IgE plasma levels and d) IL-5 pulmonary expression. e) S1PR1, f) S1PR2 and g) S1PR3 expression were assessed by RT–PCR. AHR of bronchi harvested from 17-β-estradiol treated male mice was abrogated by (h) S1P2 antagonist (JTE-013 10µM, 30 min) or (i) S1P3 antagonist (TY52156 10µM, 30 min) Data are expressed as mean ± SEM n=6. *: $p<0.05$, **: $p<0.01$, ***: $p<0.001$ versus male group.

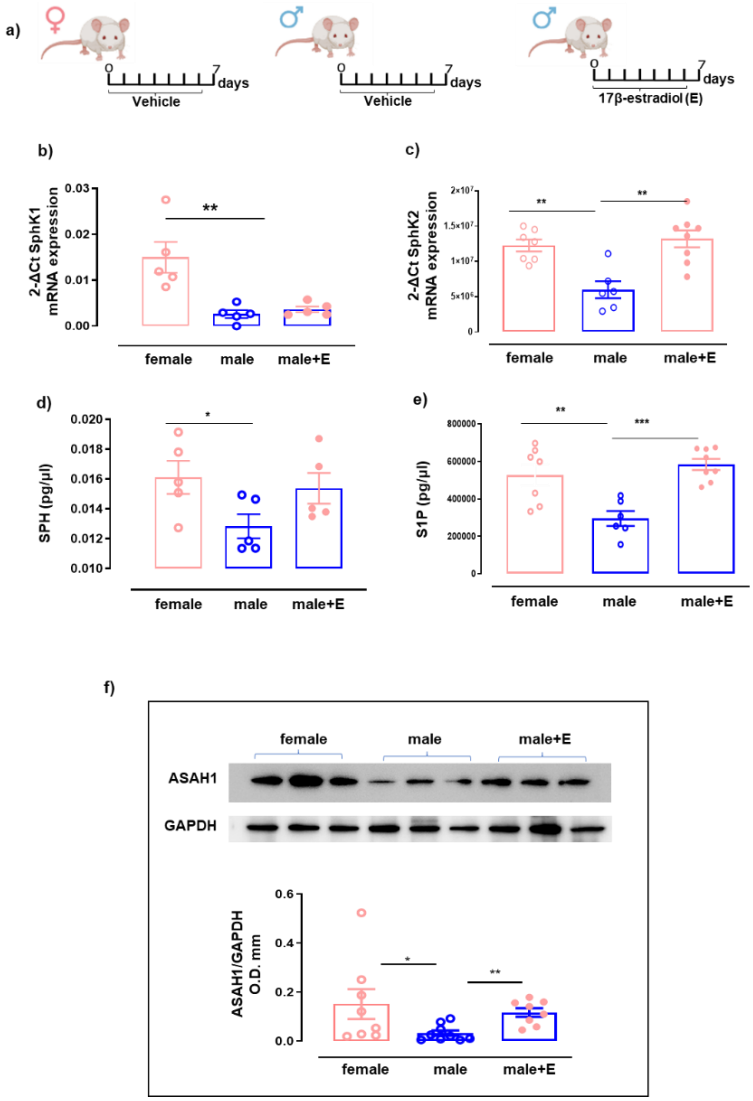


***Figure 4.12: 17-β-estradiol (E) supplementation in male mice abrogates sexual dimorphism in S1P signaling***. a) BALB/c male mice received subcutaneous injections of E (25µg/kg every day for 7 days). b) SphK1 and c) SphK2 expression were assessed by RT–PCR in bronchial tissue of male, female and E-treated male BALBc mice Both d) SPH and e) S1P levels were measured by HPLC-SM in the lung and were increased in male mice following E supplementation. f) bronchial ASAH1 expression was quantified by western blot. Data are expressed as mean±SEM. b) n=5; c) n=6-8; d) n=5; e) n=6-8; f) n=8. *: $p<0.05$, **: $p<0.01$, ***: $p<0.001$ versus male group.

***Tamoxifen supplementation to female mice abrogates sex dimorphism in bronchial reactivity.***

Female mice received systemic administration of tamoxifen, a specific estradiol receptor antagonist (figure 4.13a). Tamoxifen treatment induced a significant reduction in bronchial reactivity in females, (figure 4.13b). Tamoxifen did not affect plasma IgE levels (figure 4.13c), nor IL-5 expression in the lung (figure 4.13d). However, tamoxifen reduced sexual differences in sphingosine and S1P pulmonary levels (figures 4.13e and f).

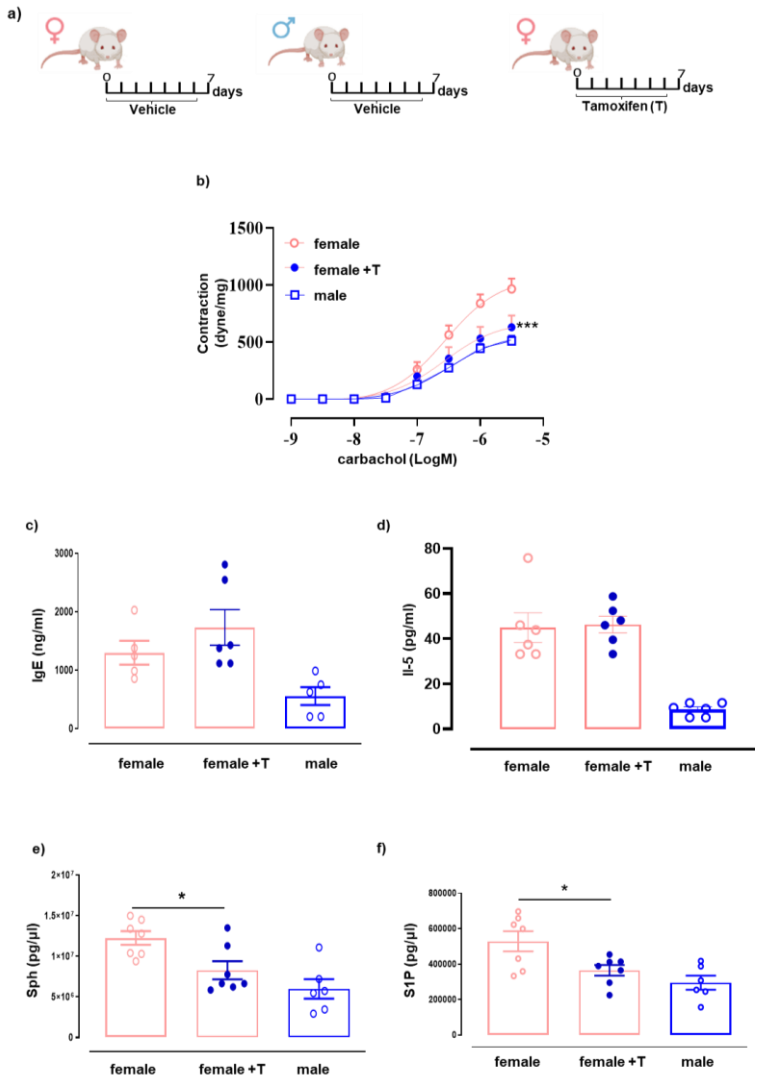


***Figure 4.13: Bronchial reactivity reduction, in female mice, induced by tamoxifen treatment is associated with an alteration of S1P signalling***. a) Female BALB/c mice were subcutaneously treated with tamoxifen (0.4mg/kg per day for 7 days). b) Bronchial reactivity to carbachol was significantly reduced in female mice following tamoxifen injection, abrogating sex difference. The modulation of estradiol signaling in females did not affect c) the plasmatic level of IgE or d) the pulmonary level of IL-5. e) Sph and f) S1P. Data are expressed as mean±SEM. b) n= 6-12; c-e) n=6; f-g) n=6-8. *: $p<0.05$, **: $p<0.01$, ***: $p<0.001$ versus male group, or versus female group

***Sex hormones affect lung Spns2 expression and airway structure.***

Spns2 was evaluated in mice of both sexes following hormonal modulation. Spns2 was upregulated in the bronchi harvested from tamoxifen-treated female and male mice when compared to female or estradiol-treated male mice (figures 4.14a and c). Sirius red staining showed that there was no difference in the amount of peri-bronchial and parenchymal collagen between sexes in BALB/c mice (figure 4.14c panels A, C). After the analysis using a confocal microscope, there seems to be a difference in the organization of peri-bronchial collagen (figure 4.14c panels I, M). This is confirmed by hormonal modulation. Indeed, the peri-bronchial collagen in vehicle-treated females (figure 4.14c panels E-I) showed a neat and compact structure, which is destroyed by tamoxifen treatment (figure 4.14c panels F-L). 17-β- estradiol treatment in male mice enhanced the collagen deposition not only in the peri-bronchial section (figure 4.14c panels H-N) but also in the lung parenchyma (figure 4.14c panel D) compared to vehicle males (figure 4.14c panels C-G). These changes well correlated with the different expression of α-SMA that resulted upregulated in female bronchi (figure 4.14d) and this sex difference was reversed by hormonal modulation with both 17-β- estradiol and tamoxifen.

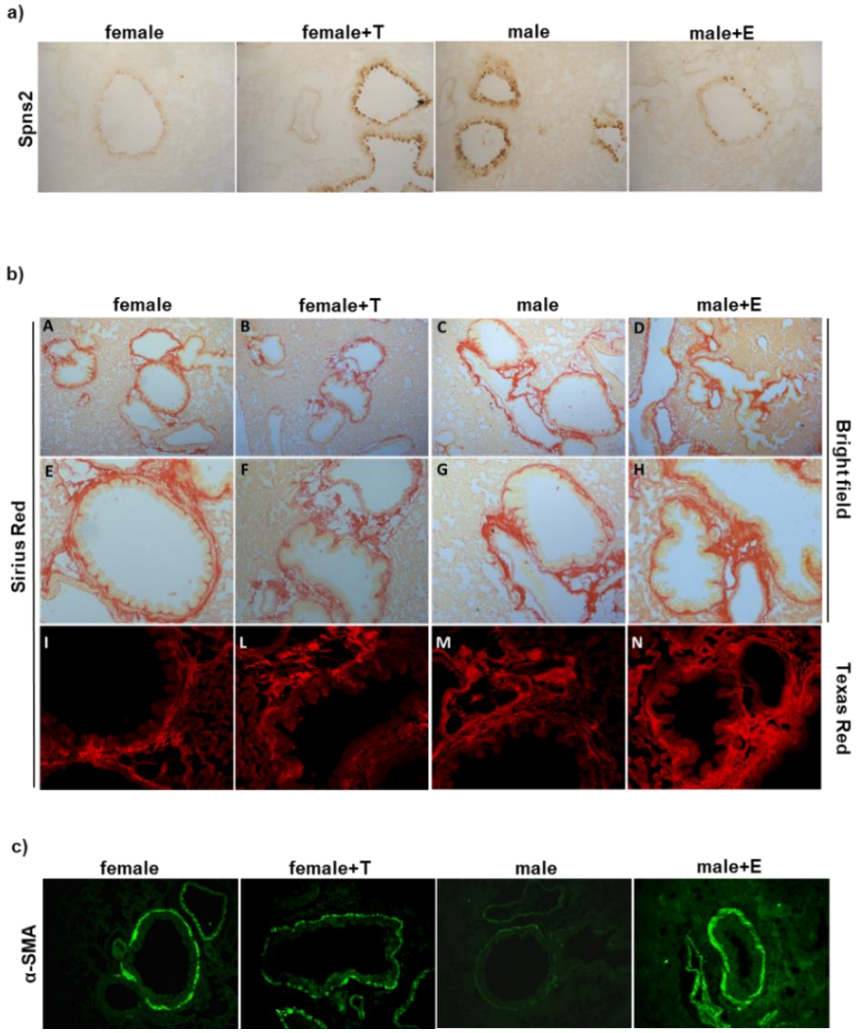


***Figure 4.14: Modulation of sex hormones affects Spns2and α-SMA expression and modulates collagen organization in bronchial sections***. Representative immunohistochemical staining for a) Spns2. There is a sex difference in S1P transporter expression Spns2 is higher in the bronchial epithelium of lung section from males when compared to females. The hormonal modulation in females is enhanced while in males reduces Spns2 expression. b) Representative Sirius Red staining in (A-H) bright field and in a red-fluorescent dye (I-N) Texas Red. The bright field acquisition shows that there was no difference in the amount of collagen deposition in the peri-bronchial section, the red-fluorescent dye acquisition gives detailed information about the organization of collagen fibers. A sex difference

appears in the organization of collagen fibers with an organized bilayer in peri-bronchial section of females (arrow) and disorganized and dispersive fibers in peri-bronchial section of males (*). Hormonal modulation with tamoxifen in females affects this organization (*) making the fibers disorganized and less compact as well as in males. Conversely, estradiol supplementation in males makes the fibers compact tending to form an organized bilayer. c) Representative IF of α-SMA expression which is higher in the peribronchial section from females when compared to males. Modulation of sex hormones through estradiol in males and tamoxifen in females affects α-SMA expression. Data are expressed as Media±SEM. a-d) n=6. *:$p<0.05$, **: $p<0.01$, ***: $p<0.001$. Scale bar = a) 169,6 μm; b, A-D) 169,6 μm; b, E-N) 85,6μm; c) 85,6μm.

***Estradiol upregulates ORMDL/S1P signaling in the model of lung innate immunity.***

Our *in vivo*, data suggest a synergic contribution of sexual hormones and the immune environment related to BALB/c mice in S1P-induced sexual airway dimorphism. To assess this hypothesis, we used *in vitro* cell lines such as human bronchial cells BEAS-2B and an adenocarcinoma human alveolar basal epithelial cell line (A549), both harvested from male subjects. Both cell types were exposed to 17-β-estradiol (figure 4.15a). 17-β-estradiol stimulated in A549 cells a significant upregulation of S1P signaling. All S1P receptors were upregulated as well as SPhK. ASAH1 upregulation also occurred, and it was mostly expressed in its active form following estradiol challenge (figure 4.15b) 17-β-estradiol -treated A549 also showed a significant upregulation of ORLMD3 (figure 4.15b). Conversely when 17-β-estradiol was used to stimulate BEAS-2B cells resulted in insensitivity to hormone challenge when we looked at S1P signaling (figure 4.15c). Indeed, S1P receptors (S1P1, S1P2,

and S1P3), as well as sphingosine kinases, ASAH1 and ORLMD3 were unaltered following 17-β-estradiol exposure (figures 4.15c).

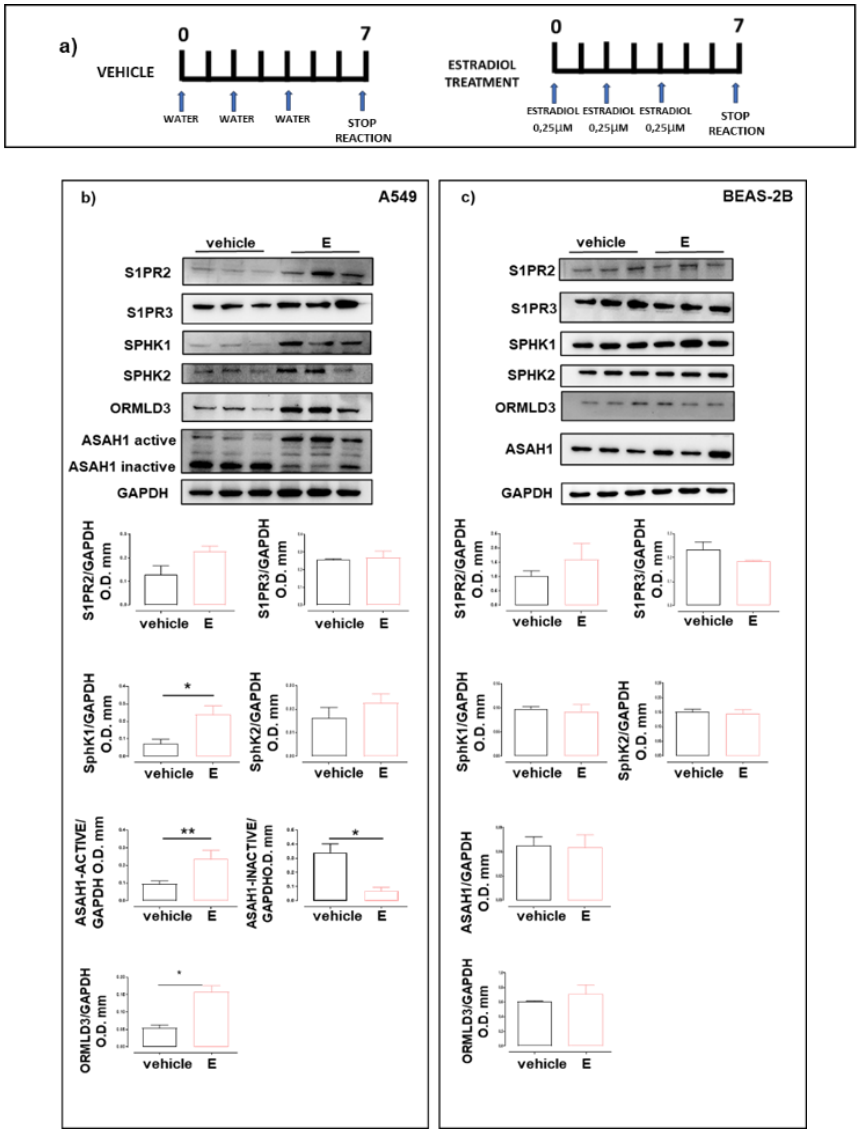


***Figure 4.15: 17β-estradiol (E) enhanced S1P signaling in A549.*** a) human adenocarcinoma epithelial cell line (A549) or human bronchial epithelial cell line (BEAS-2B) were exposed to E (0,25 µM/day for 7 days). Expression of S1PR2,

S1PR3, SphK1, SphK2, ORMDL3 and ASAH1 (active and inactive isoform) were quantified by western blot, Data are expressed as mean ±SEM. b-c) n=3. *:$p<0.05$, **: $p<0.01$.

### 4.2.5 Discussion and Conclusions

The S1P axis holds significant clinical importance, as indicated by extensive research suggesting its crucial role in regulating immune regulatory networks that contribute to human health and several lung disorders [90]. In this study, we investigate the impact of sex on the modulation of sphingolipid metabolism and the role of S1P signaling in driving sex-related differences in asthma features. Our data demonstrate that the sex differences in asthma susceptibility rely on ORMDL/S1P signaling and S1P mediates sexual dimorphism in asthma features. To explore this hypothesis, we employed both animal and cell studies.

Genome-wide association studies (GWAS) have identified a link between alleles within the17q21 asthma-susceptibility locus, childhood asthma, and overexpression of the ORMDL sphingolipid biosynthesis regulator 3 (ORMDL3), an inhibitor of de novo sphingolipid synthesis [89]. Animal models and in vitro studies have connected sphingolipid metabolism to clinical features of asthma, including airway hyperreactivity. ORMDL3 regulates airway smooth muscle hyperplasia, airway smooth muscle contraction, and calcium oscillations in asthma, and contributes to airway remodeling in asthma. Saba et al. have also evidenced that ORMDL3 gene is associated with female asthmatics [91].

Based on this data and taking advantage of animal models, we investigated the interaction among sex, ORMDL3, and asthma features. For the animal studies,

we used mice expressing a Th2-high immunophenotype (BALB/c). BALB/c mice exhibit characteristics of human atopy such as increased levels of IgE and are more susceptible to developing key features of asthma in a sex-dependent manner. First, we evaluated ORMDL3 expression in pulmonary tissues harvested from mice of both sexes. Bronchi harvested from BALB/c female mice overexpress ORMDL3 compared to male. Accordingly, female BALB/c mice exhibit an increased contractility to cholinergic stimuli as compared to males. AHR is also well correlated with enhanced staining to alpha SMA and collagen deposition in bronchi.

S1P regulates different cellular processes involved in immunity and lung inflammation through $S1P_1$ receptors. $S1P_2$ and $S1P_3$ are widely expressed in bronchial smooth muscle and are involved in airway contractility [92]. We found in perfect tune with the functional data an increased expression of S1P receptors such as $S1P_1$, S1P2, and $S1P_3$ in female airways of BALB/c mice. S1P metabolism is regulated by a complex network of enzymes and factors, including ceramidase and sphingosine kinase-1 and -2, which are key enzymes in the balance between sphingosine and its precursor ceramide, determining the S/S1P ratio. On the other hand, the transporter Spns2 plays a key role in maintaining S1P levels and signaling. It has been shown that increased extracellular S1P, achieved through Spns2 transfection, leads to significant downregulation of S1P receptors [93]. In our study, we observe the same inverse correlation between Spns2 expression and S1P levels in the lungs, which changes in response to hormonal stimulation. Additionally, bronchi harvested from female mice show an upregulation of ceramidase (ASAH1). Therefore, the entire pathway involved in S1P synthesis and activity is upregulated in the female airways of BALB/c mice. Functional studies confirm that S1P upregulation contributes to AHR observed in females. Indeed, selective pharmacological inhibition of $S1P_2$ and $S1P_3$ receptors, as

well as sphingosine kinase, resulted in a significant reduction in AHR, only in female mice.

Ongoing investigations reveal that sex hormones can affect airway tone and inflammation and exert effects on different lung cell types. Estrogens potentially influence the outcomes of inflammatory and disease processes by influencing cytokines and inflammatory mediators in the lung. Testosterone is generally proposed to have protective roles because it seems to cause bronchial tissue relaxation, reduce the response to histamine and attenuate airway inflammation. Accordingly, the administration of 17β-estradiol to male BALB/c mice promotes a significant increase in bronchial reactivity. This effect was coupled with a significant rise in both sphingosine and S1P pulmonary levels. Western blot confirms a significant increase in ceramidase in the bronchi of 17β-estradiol-treated male mice when compared to vehicle male mice. Furthermore, AHR induced by 17β-estradiol is reversed by antagonists targeting $S1P_2$ or $S1P_3$ receptors. RT-PCR analysis corroborates a significant increase of all S1P receptors as well as of SPK in bronchi harvested from 17β-estradiol treated male mice. Thus, systemic administration of 17β-estradiol to male BALB/c mice promotes AHR by activating S1P signaling.

Instead, in another set of experiments, tamoxifen treatment significantly reduces bronchial reactivity in females, and decreases the pulmonary levels of sphingosine and S1P. Accordingly, Spns2 exhibits higher expression in the bronchial sections from tamoxifen-treated female and male mice compared to female or estradiol-treated male mice. Confocal microscope results further validate our hypothesis. It seems to be a sex-related difference in the organization of peri-bronchial collagen. Indeed, the peri-bronchial collagen in females shows a neat and compact structure, which is destroyed by tamoxifen treatment. 17-β- estradiol treatment in male mice enhances the collagen deposition not only in the peri-bronchial section, but also in the lung

parenchyma compared to males. These changes well correlate with the different expression of α-SMA that results in upregulated in female bronchi and this sex difference is reversed by hormonal modulation with both 17-β-estradiol and tamoxifen.

Sphingolipid pathway upregulation by 17-β- estradiol was coupled to a significant increase in plasma IgE levels as well as pulmonary IL-5 expression in females. This suggests that female hormones-related sphingolipid pathway upregulation is associated with Th2-type asthma.

To further support our hypothesis, we conducted cellular studies using established models of lung innate immunity, such as human A549 cells and human bronchial cells BEAS-2B cells obtained from male subjects. Both cell lines were exposed to 17β-estradiol, and the effects on S1P signaling were evaluated. The in vitro studies show that 17β-estradiol upregulates S1P signaling, including S1P receptor and SphK, the active form of ASAH1, and ORLMD3 only in A549 cells. A partial upregulation of ORMLD3 has been observed in BEAS-2B cells. Thus, 17β-estradiol and S1P signaling interaction depends on the activated state of the cells and the immune environment.

In conclusion, these data support the hypothesis of sex-related differences in the lung, which contribute to differential susceptibility to the development of asthma. In this context, S1P signaling plays a key role, and its effects are influenced by the cellular environment and direct interactions between stromal cells and immune cells.

# Chapter 5

# 5. Development of new therapeutic strategies in the asthma management

## 5.1 $H_2S$ donor improves therapeutic profile of prednisone in asthma management.

Hydrogen sulfide ($H_2S$) is emerging as an important potential therapeutic option for respiratory inflammatory diseases. In this study, we investigated the effectiveness of a novel corticosteroid derivative, that is chemically linked to an $H_2S$ donor, in asthma features management.

### 5.1.1 Rationale

$H_2S$ is an endogenous gas transmitter and exerts physiological and pathophysiological effects in several systems [94]. Hydrogen sulfide ($H_2S$) is emerging as an important potential therapeutic option for respiratory inflammatory diseases.

Indeed, several studies show that alterations in $H_2S$ levels have been linked with lung disease pathophysiology [94]. Indeed, serum $H_2S$ levels decrease in asthmatic subjects and $H_2S$ levels reduction is accompanied by lower expression of CSE in ovalbumin (OVA)-sensitized mouse and rat lung tissues [95]. On the other hand, CSE deficiency or inhibition of $H_2S$ biosynthesis by inhibiting CSE activity with propargylglycine has been shown to increase

asthma features such as airway reactivity [95]. These pieces of evidence indicate $H_2S$ as a potential therapeutic option for asthmatic subjects.

Airway remodeling is a challenging issue in lung diseases like asthma, causing irreversible loss of lung function [96]. It involves structural changes in the airway walls, which occur due to repeated injury and repair processes. While current therapies can alleviate inflammation, there is no proven treatment to prevent or reverse airway remodeling [96].

Corticosteroids, a key component of anti-inflammatory asthma therapy, effectively manage airway narrowing and asthma attacks [97]. However, their impact on the aspects of remodeling leading to a decline in lung function remains limited. There is compelling evidence suggesting that H2S may have the potential to alleviate airway remodeling [98]. For this study was choose a donor molecule that mimics the slow, gradual, and controlled release of the physiological $H_2S$, such as TBZ, combined with a corticosteroid such as Prednisone [80].

### 5.1.2 Aim

This study aims to investigate the effectiveness of a novel corticosteroid derivative containing an H2S molecule such as TBZ associated to prednisone in controlling asthma-associated airway features.

### 5.1.3 Materials and Methods

Material and methods, and statistical analysis related to these experiments are reported in Chapter3.

### 5.1.4 Results

***TBZ ameliorates the anti-inflammatory effects of PS and modulates the bronchial tone.***

The pharmacological efficacy of PS-TBZ in controlling inflammation was first evaluated *in vitro* on the macrophage cell line J774 (Figure 5.1). Both PS and TBZ, at nontoxic concentrations (Figure 5.1A), exhibited a concentration-dependent anti-inflammatory activity in a concentration-dependent manner, as indicated by the decreased production of LPS-induced nitric oxide (NO), IL-1β, $PGE_2$, and TNF-α (Figure 5.1 B-E). PS and TBZ showed different efficacy among the different mediators, while PS-TBZ clearly showed a synergic effect (Figure 5.1F). To note, the combination achieved an effect at concentrations that were significantly lower than those required when parent compounds were administered alone. Exposure of bronchial rings to TBZ (Figure 5.2A) demonstrated its ability to affect also bronchial tone. TBZ inhibited bronchial contraction induced by carbachol (Figure 5.2B) and potentiated $\beta_2$-receptor mediated bronchorelaxation assessed by exposure of isolate bronchi to salbutamol (Figure 5.2C).

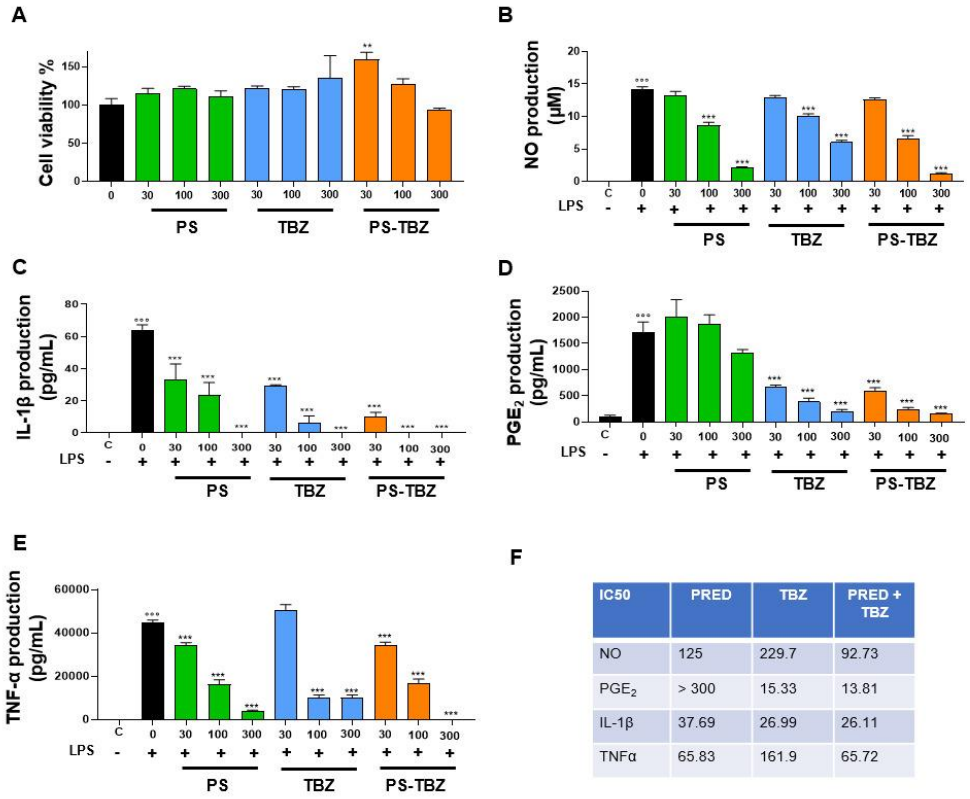


F

| IC50 | PRED | TBZ | PRED + TBZ |
|---|---|---|---|
| NO | 125 | 229.7 | 92.73 |
| $PGE_2$ | > 300 | 15.33 | 13.81 |
| IL-1β | 37.69 | 26.99 | 26.11 |
| TNFα | 65.83 | 161.9 | 65.72 |

***FIGURE 5.1: Effect of PS, TBZ, or PS-TBZ on LPS-stimulated murine macrophages***. A) Cells were pre-treated for 24h with PS, TBZ, or PS-TBZ (30-300µM), and cell viability was evaluated by the mitochondrial-dependent reduction of MTT to formazan. (B, C, D, E): Cells were pretreated for 2h with PS, TBZ, or PS-TBZ (30-300µM) and then stimulated for 24h, with LPS (10µg/mL). The supernatants were collected for the measurement of nitrite (B), IL-1β (C), $PGE_2$, (D), and TNFα (E) levels by ELISA assay. (F) Analysis of $IC_{50}$ has been performed with GraphPad 9 software. Values represent means ± S.E.M.; n = 3 experiments. Data were analyzed by one-way ANOVA plus Bonferroni post-hoc test. Statistical significance is reported as follows °°°$p < 0.001$ vs. unstimulated cells, *$p < 0.05$, **$p<0.01$, and ***$p < 0.001$ *vs.* LPS alone.

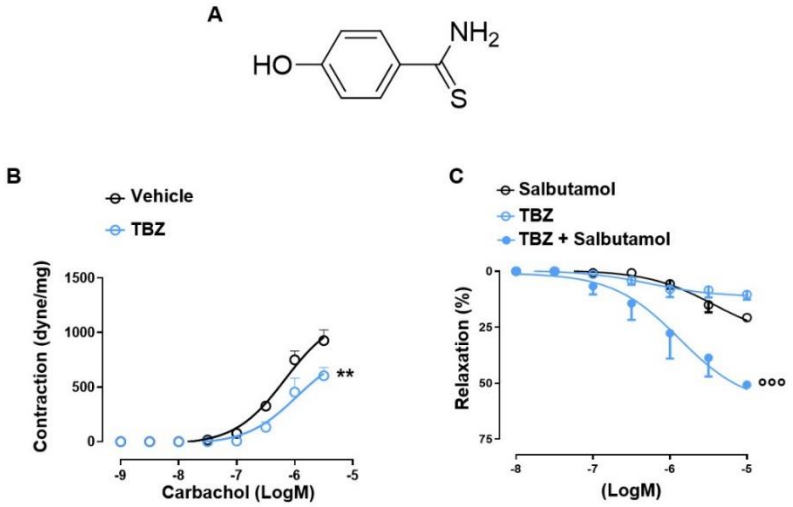


***FIGURE 5.2. TBZ modulates bronchial tone in vitro:*** Chemical structure of TBZ (A). Bronchi harvested from BALB/c mice were incubated on basal tone with TBZ (30μM, 45 minutes) and then stimulated with carbachol (B). Bronchi were stimulated with the $\beta_2$-agonist salbutamol in the presence or absence of TBZ, or with TBZ(C). Values represent means ± S.E.M.; n=6 mice for each group. Data were analyzed by two-way ANOVA plus Bonferroni post-hoc test. Statistical significance is reported as **p<0.01 *vs* vehicle; °°°p<0.001 *vs* salbutamol.

### *PS-TBZ reduces airway hyperresponsiveness (AHR) and restores $\beta_2$-mediated relaxation in OVA-sensitized mice.*

The effect of the parent compounds PS and TBZ, and of the hybrid PS-TBZ was evaluated in an experimental model of asthma induced by OVA (Figure 5.3A). Following OVA exposure, an increase in the plasmatic level of IgE occurred (Figure 5.3B). PS reduced IgE levels, conversely TBZ and PS-TBZ had no effect. Bronchi harvested from OVA-sensitized mice showed increased reactivity to carbachol (AHR). PS partially decreased AHR (Figure 5.3C) while TBZ (Figure 5.3D) and PS-TBZ (Figure 5.3E) reversed AHR. Although

PS-TBZ displayed a similar effect to TBZ on AHR, the association of reducing the dosage of the parent compounds confirms the synergic effect of TBZ with PS (Figure 5.3E).

Further, the allergic inflammation induced by OVA caused an impairment in $\beta_2$-adrenoceptor mediated relaxation as demonstrated by the significant reduction in relaxant effect of salbutamol (Figure 5.3 F-H). However, this effect is restored by both TBZ (Figure 5.3G) and PS-TBZ (Figure 5.3H) treatment, but not by PS alone (Figure 5.3F).

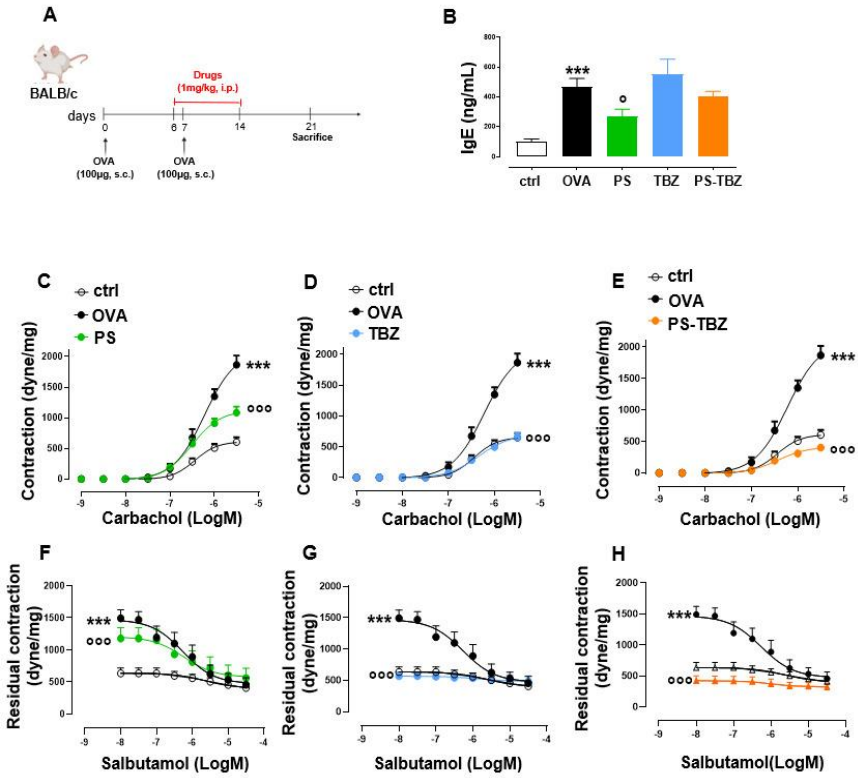


***FIGURE 5.3. Effect of PS, TBZ, or PS-TBZ in an experimental model of asthma:*** (A). Mice were sacrificed to measure the plasmatic level of IgE (B) and evaluate bronchial reactivity to carbachol (C, D, E) or salbutamol (F, G, H). Values represent means ± S.E.M.; n=6 mice for each group. Data were analyzed by two-way ANOVA plus Bonferroni post-hoc test. Statistical significance is reported as ***p<0.001 *vs* ctrl; °°°p<0.001, °p<0.05 *vs* OVA.

***PS-TBZ reverts the OVA-induced epithelial damage.***

Histological examination was performed on the airways of control mice (Figure 5.4A-B), and observed a columnar epithelium lining the airways, with densely packed cells having a basal nucleus (Figure 5.4B). Below the thin basement membrane, a bi/tri-layer of smooth muscle cells were present (Figure 5.4B). The parenchyma contained a net of thin septa, delimiting well-distended alveoli (Figure 5.4A-B, s). Close to the large vessels, the connective thickened, and a bunch of fibers was often visible (Figure 5.4A-B). Following OVA sensitization (Figure 5.4C-D), significant changes occurred. The cells became cylindrical, separated by evident intercellular spaces, and the goblet cells were more evident, protruding into the lumen of the airway (Figure 5.4D). Marked changes also occurred at the level of the parenchyma: the septa were thick, and the alveoli collapsed (Figure 5.4C). Connective fibers were present, close to the large vessels, connecting the structure with the airway (Figure 5.4C). In mice treated with PS (Figure 5.4E), the epithelial cells became columnar, and the apical cytoplasm was irregular and secretory (Figure 5.4E). The smooth muscle layer was hyperplastic (Figure 5.4E), and, in the parenchyma, the septa were thick and delimiting alveoli moderately reduced in volume. After TBZ treatment (Figure 5.4F) the epithelium showed moderately elongated cells, with occasional intercellular spaces. The cell cytoplasm was uniformly dense, the nuclei were basal (Figure 5.4F, inset). The smooth muscle was not hypertrophic, the septa were moderately thickened, and the compressed alveoli were less numerous. The administration of PS-TBZ induced a significant recovery of the epithelium: the cells reduced in height, their cytoplasm returned dense and homogeneous, and the intercellular spaces were almost absent (Figure 5.4G, inset). The parenchyma also returned to normal, with thin septa and large, regularly arranged alveoli (Figure 5.4G).

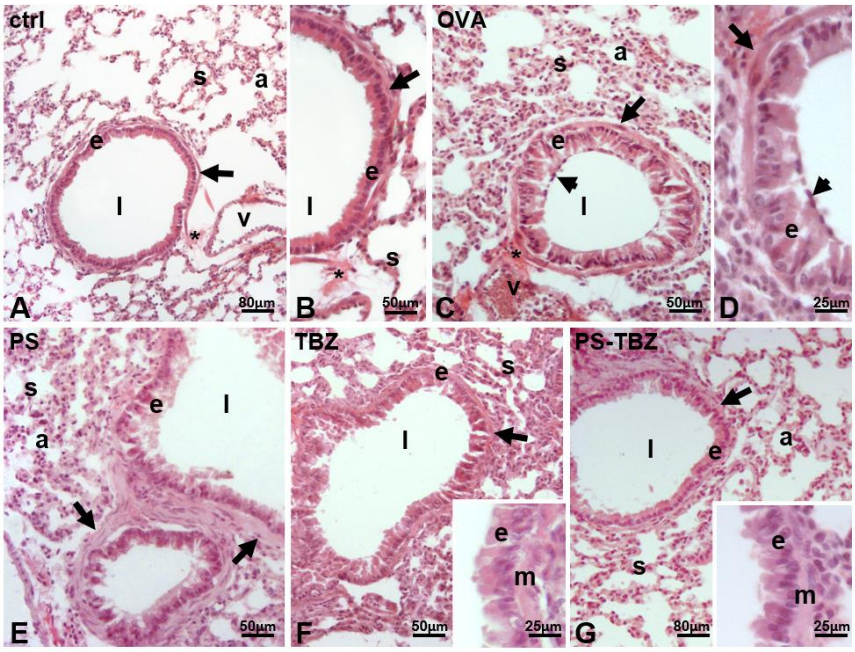


***FIGURE 5.4. Effects of PS, TBZ, or PS-TBZ treatments on lung structure of sensitized mice:*** Lungs harvested from control (A, B), OVA- (C, D), PS- (E), TBZ- (F), and PS-TBZ- (G) treated mice were stained for Hematoxylin &Eosin (H&E) to evaluate the pulmonary structure. (A-B): bronchiolar columnar epithelium enveloped by a thin layer of smooth muscle cells (arrows); thin parenchymal septa line the alveoli. (C-D): disorganized cylindrical epithelium with large intercellular spaces, and numerous goblet cells (arrowhead); thick septa and collapsed alveoli. (E): disorganized epithelium; cylindrical cells have pale, secretory apical cytoplasm and lay on a hypertrophic smooth muscle layer (arrows); moderately thickened septa reduce the alveolar volume. (F): quasi-columnar epithelium with dense cytoplasm, and moderately hypertrophic smooth muscle layer (arrow); thin septa and moderately collapsed alveoli. Inset: detail of the epithelium (e) and smooth muscle layer (m). (G): apparently normal airway with regular epithelium and smooth muscle layer (arrow); thin septa and wide alveoli. Inset: detail of the epithelium (e) and smooth muscle layer (m). Epithelium (e), septa (s), alveoli (a), connective fibers (*), airway lumen (l), vessel (v). Image acquisition with Leica System; Animal for each group n=3; bars: 80µm (A G), 50µm (B, C, E, F), 25µm (D, inset).

***PS-TBZ inhibits airway remodeling in OVA-sensitized mice.***

In the OVA-sensitized mice AHR was correlated with an increase in α-SMA expression (Figure 5.5B) which confirms the activation of myofibroblasts after OVA exposure, as further supported by increased procollagen III production (PIIINP, Figure 5.5G). PS treatment partially reduced the remodeling process as indicated by the reduced α-SMA (Figure 5.5C) and PIIINP expression (Figure 5.5H) in the peri-bronchioles section. In the same way, TBZ treatment partially affected the remodeling process (Figure 5.5D, I). PS-TBZ treatment modified the typical elongated structure of myofibroblasts induced by OVA, and it reduced both α-SMA (Figure 5.5E) and PIIINP (Figure 5.5F) expression.

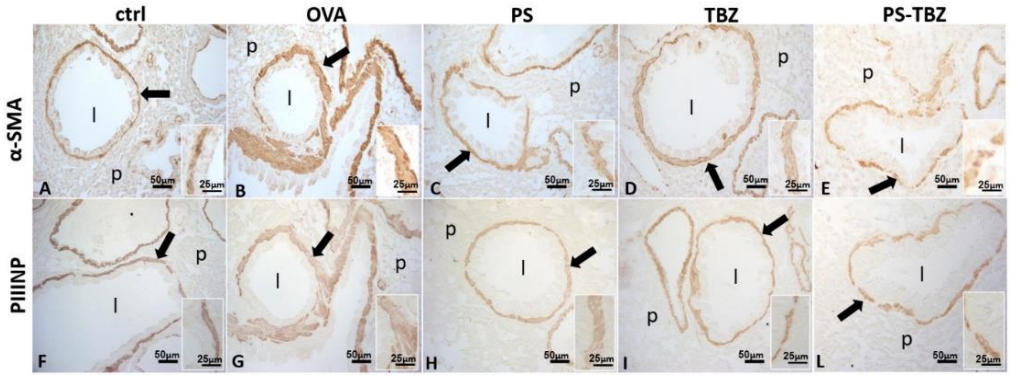


***FIGURE 5.5. Effect of PS, TBZ, or PS-TBZ treatments on airway remodeling in sensitized mice***: Expression of α-Smooth Muscle Actin (α-SMA; A-E) and type III Procollagen Peptide (PIIINP; F-L). was assessed on lung sections as indicated by arrows. Inset: detail of the smooth muscle layer. Airway lumen (l), unstained parenchyma (p). Image acquisition with Leica System; group n=3; bars: 50µm (A-L), 25µm (inset).

***PS-TBZ mitigates the disorganization of peri-bronchioles collagen fibres.***

PSR staining was used to examine collagen distribution in various conditions. In the control group (Figure 6.6A, A1), collagen formed a continuous and uniform layer at the basal membrane level. A second, moderately irregular layer was observed at the base of the smooth muscle layer (indicated by a big arrow in Figure 5.6A). After exposure to OVA (Figure 5.6B), collagen fibers appeared thicker and more dispersed in a specific direction. The typical bilayer organization seen in controls (Figure 5.6A, A1) was less common following OVA exposure (Figure 5.6B, B1b), partly due to irregularities in the basal membrane (Figure 5.6B1a). Furthermore, with PS the situation worsens, causing collagen fibers to become even thicker, curled, and highly disorganized, invading the smooth muscle region and extending into the underlying connective tissue (Figure 5.6C). Following exposure to TBZ (Figure 5.6D, D1), collagen fibers compacted, forming dense amorphous patches at times (Figure 5.6D1). The administration of PS-TBZ resulted in further thickening of the fibrils in some areas (Figure 5.6E), while in other areas, an almost complete restoration of the bilayer organization was observed (Figure 5.6E1).

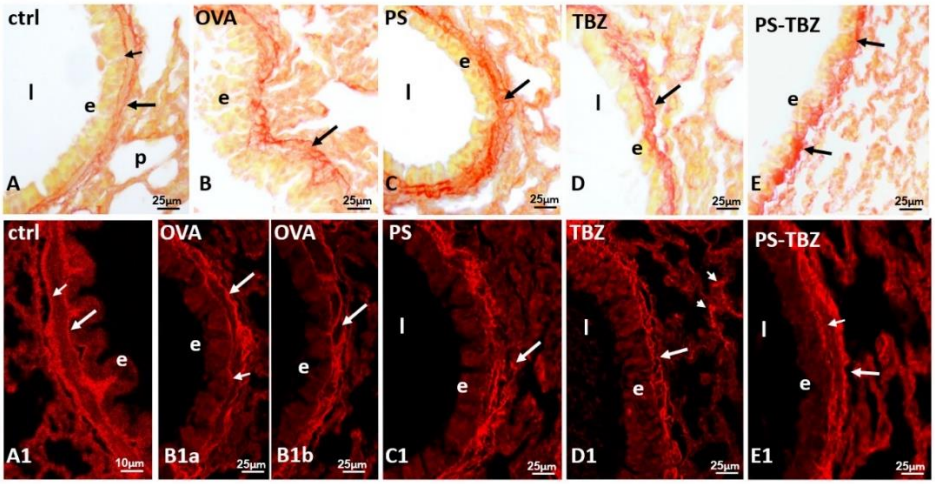


***FIGURE 5.6. Effects of PS, TBZ or PS-TBZ treatments on collagen organization in lungs of sensitized mice:*** PSR staining was performed on lung sections. (A, A1): bronchiole wall with stained basal lamina (small arrow) and a thin layer of collagen (arrow) enveloping the smooth muscle layer. (B, B1a): thick and disorganized fibrils (arrow). (B1b): area of almost regular appearance; basal lamina (small arrow) and collagen under the smooth muscle (arrow). (C, C1): high directional dispersion of thick collagen fibrils (arrow). (D): recompacted fibrils reform a sort of bilayer (arrow). Note in C1 the presence of thick fibrils in septa (arrowheads). (E): compacted fibrils (arrows) from patches with regular bilayer (E1). Airway lumen (l), bronchiolar epithelium (e). Image acquisition with Leica System (A-E) and confocal microscopy Zeiss LSM700 (A1-E1); group n=3; bars: 10µm (A1), 25µm (A-E, B1a-E1).

***PS-TBZ inhibits mucin production.***

PAS+/AB staining (Figure 5.7) was used to detect acid mucins. In the control group (Figure 5.7A, B), there was minimal mucus present. After exposure to OVA (Figure 5.7C), the presence of mucus significantly increased in peri-bronchial and epithelial goblet cells, leading to its release into the airway lumen (Figure 5.7D). PS (Figure 5.7E) and TBZ (Figure 5.7F) treatments

reduced mucin levels at both locations, but the mucus in the airway lumen appeared denser and filamentous. When PS-TBZ was administered in combination (Figure 5.7G), the condition was almost restored to that of the control group, as observed following the single compound treatment, but the new chemical entity achieved the same effect with half dose. Indeed, goblet cells were scattered in the epithelium, submucosal glands remained unstained, and very little mucus was observed in the bronchiole's lumen (Figure 5.7G).

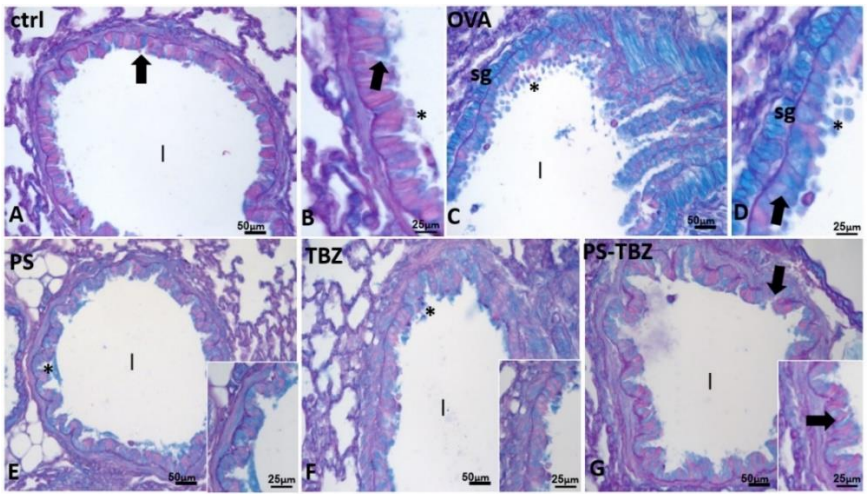


***FIGURE 5.7. Effects of PS, TBZ, or PS-TBZ treatments on mucin production induced by sensitization:*** PAS$^{+}$/AB was performed on lung sections. (A, B): Control airway with scattered goblet cells (arrows) and mucus (*) in the lumen (l). (C, D): increased number of goblet cells (arrows) and mucus (*) in the lumen. Note the positivity of submucosal glands (sg). (E, G): decreased number of positive epithelial goblet cells (arrows), no evident submucosal glands, and almost complete disappearance of mucus in the airway lumen (l). Image acquisition with Leica System; group n=3; bars: 50µm (A, C, E, F, G), 25µm (B, D, inset).

***PS-TBZ modulates changes in carbohydrate composition induced by OVA sensitization.***

Staining with WGA lectin (Figure 5.8) demonstrated that OVA-sensitization caused a decrease in N-Acetyl-glucosamine (glcNAc) in the apical cytoplasm of bronchioles epithelial cells and the basal lamina. In contrast, sensitization significantly increased lectin positivity in goblet cells and, to a lesser extent, in alveolar septa (Figure 5.8B1). After PS treatment (Figure 5.8C, C1), labeled goblet cells were reduced while significant labeling was restored at the level of the basal lamina. TBZ (Figure 5.8D, D1) and PS-TBZ (Figure 5.8E, E1) restored labeling on the apical cytoplasm of the epithelial cells and on the basal membrane. TBZ alone reduced labeling in the alveolar septa while the combination determined a significant increase in such labeling (Figure 5.8E). Vessel, walls that were always labelled (Figure 5.8A1, 8C1) after PS-TBZ appeared completely unstained (Figure 5.8E1).

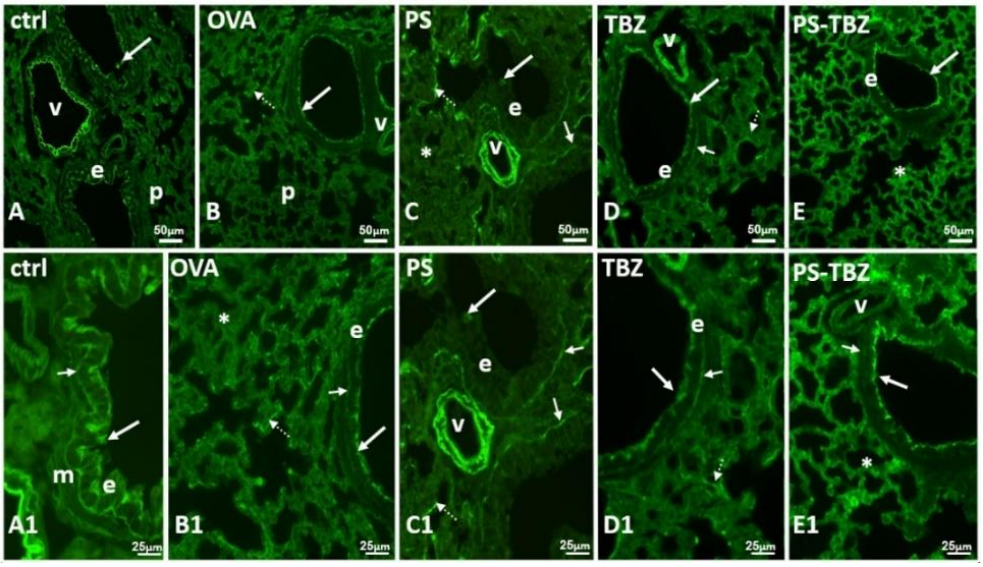


***FIGURE 5.8. Effect of PS, TBZ, or PS-TBZ treatment on N-Ac-glucosamine distribution:*** (A,A1): labeled elastic lamina of the vessels (v), apical cytoplasm (arrows) of the bronchiolar epithelium (e), and basal lamina (small arrow). Muscle (m) is unstained. (B, B1): labeled apical cytoplasm (arrow) of the bronchiolar epithelial cells (e). Notice the irregularity labeled basal membrane (small arrow) and the parenchymal septa containing labeled fibers (dotted arrows). Labelled basal membrane (small arrows), and fibres in parenchymal septa (dotted arrows). Unstained parenchyma (*). (C, C1): unlabelled epithelial cells (e) with occasional stained mucus cells (arrows). Labeled basal membrane (small arrows), and fibers in parenchymal septa (dotted arrows). Unstained parenchyma (*). (D, D1): labeled elastic lamina of the vessels (v), apical cytoplasm (arrow) of the bronchiolar epithelium (e), basal membrane (small arrows) and fibers in parenchymal septa (dotted arrows). (E-E1): labeled apical cytoplasm (arrows) of the bronchiolar epithelium (e), and fibers in all parenchymal septa (*). Unlabeled basal membrane (small arrows) and vessels (v). Image acquisition with Leica System; group n=3; bars: 50µm (A-E), 25µm (A1-E1).

### 5.1.5 Discussion and conclusion

Acute and chronic respiratory diseases constitute a major health burden in both children and adults. Asthma involves many pathophysiologic factors, including airway inflammation, airway remodeling, which refers to structural changes in the airways that eventually lead to airway fibrosis and obstruction, and AHR. Current therapies primarily target inflammation and bronchoconstriction with corticosteroids, but airway remodeling can develop also independently of inflammation, limiting the efficacy of pharmacological treatments. It is becoming increasingly clear that several airway diseases are associated with a state of $H_2S$ deficiency, including asthma. To overcome the limitations of current therapies, we explored the possibility to chemically combining $H_2S$ donors with prednisone. For this purpose, we have chosen a slow $H_2S$ donor such as TBZ. Both PS and TBZ exhibited a concentration-dependent anti-inflammatory activity as indicated by the decreased production of LPS-induced NO, IL-1β, $PGE_2$, and TNF-α. In the same experimental conditions, PS-TBZ clearly showed an enhanced anti-inflammatory action. TBZ exhibited also a weak bronchial relaxant activity and counteracted bronchial reactivity to carbachol. Therefore, TBZ extends the therapeutic efficacy of prednisone in terms of anti-inflammatory action and adds new effects as the ability to directly relax airway smooth muscle. This means that the hybrid compound can achieve a therapeutic effect with smaller doses.

Based on that we conducted *in vivo* experiments using a mouse experimental model of asthma. PS, TBZ, or PS-TBZ have been administered during the sensitization phase. Bronchi harvested from sensitized mice showed increased bronchial reactivity to carbachol that is partially restored by PS treatment. Conversely, TBZ or PS-TBZ completely prevented allergen-induced AHR. The allergic inflammatory reaction induced by sensitization also causes impairment in β2-adrenoceptor-mediated relaxation induced by heterologous

desensitization. Pretreatment with PS-TBZ preserved salbutamol-induced relaxation as well as TBZ, while PS alone had no effect. This means that PS-TBZ shows additional effects in controlling airway dysfunction taking advantage of TBZ action, with a better therapeutic profile than PS alone.

Airway dysfunction correlated with IgE-mediated inflammation, as indicated by increased plasma IgE levels. PS administration as expected significantly reduced IgE increase, while TBZ had no effect.

Histological evaluation of pulmonary sections further demonstrates the enhanced beneficial effects of PS-TBZ treatment. Indeed, allergen sensitization profoundly changes the epithelium structure, and this is an important step in triggering subepithelial mechanisms driving the airway remodeling process. The cells become cylindrical, separated by evident intercellular spaces, and the goblet cells are more evident, protruding into the lumen of the airway. The subepithelial smooth muscle layer appears moderately hypertrophic, appearing bi/tri layered. Marked changes also occur at the level of the parenchyma as evident by alveoli collapse. PS or TBZ treatment partially restored the bronchial epithelium, but PS-TBZ treatment induced a more complete recovery of the epithelium and parenchymal structure.

An active remodeling process is evidenced also by α-SMA expression upregulation following sensitization. The activated state of fibroblasts was confirmed by the increased procollagen III production. PS and TBZ treatments partially affected the remodeling process. In contrast, PS-TBZ significantly reduced the remodeling process compared to treatments alone.

Mice receiving PS or TBZ treatment also showed a significant reduction in acid mucins induced by allergen exposure. This effect exhibited by PS-TBZ is also evident on the whole bronchi as evidenced by lectin staining. The loss of lectin represents a serious event, for any type of cell since it plays

fundamental roles in the extracellular matrix and in cell signaling. In the lungs, it has been related to airway inflammation. Following sensitization collagen fibers frequently appeared thickened and/or showed a high directional dispersion. The typical bilayer organization seen in controls was very hardly visible due to the frequent irregularities in the basal membrane. PS worsened the situation: collagen fibers became thicker, curled, and markedly disorganized, to invade the smooth muscle region, The administration of the PS-TBZ hybrid caused an almost complete restoration of the bilayer.

In conclusion, our data demonstrate the essential role of $H_2S$ in airway function and its contribution to improving asthma features. Moreover, we have demonstrated that PS-TBZ could provide a suitable approach to managing asthma features with a particular impact on airway remodeling. Furthermore, this combination provides an opportunity to optimize the beneficial impact of corticosteroids by reducing dosages and associated side effects [80].

## 5.2 Montelukast preserves β2-agonists rescue therapy avoiding desensitization.

Adrenergic β2-agonists represent a mainstay in asthma management. Their chronic use has been associated with decreased broncho protection and rebound hyperresponsiveness. Here we investigate the possible therapeutic advantage of a pharmacological association of β2-agonists with montelukast, a highly selective leukotriene receptor antagonist, in modulating bronchial reactivity and controlling asthma features.

### 5.2.1 Rationale

Asthma is still one of the main causes of disability since the poor symptoms control [99]. Recently, the beneficial effects of β2-agonists in asthma management have been also ascribed to their ability to control the contractile mechanism of the airway by Inhibition of myosin light chain phosphorylation and lung inflammation by an inhibitory effect on type 2 immune response [100]. For which Adrenergic β2-agonists represent a mainstay in asthma management.

Chronic use represents the major therapeutic limitation of both inhaled and oral β2-agonists because of the induction of decreased broncho protection, rebound hyperresponsiveness, and increased eosinophilic inflammation [101]. Leukotrienes (LTs) are potent lipid mediators involved in airway inflammation and bronchoconstriction. Montelukast is considered a prophylactic agent for asthma demonstrating efficacy in adults with persistent asthma [102].

Interestingly, clinical studies suggest that patients treated with montelukast as an add-on therapy show an improvement in airway function and enhanced response to β2-agonists as compared to patients assuming only β2-agonists [103],[104].

### 5.2.2 Aim

The study aims to individuate the possible functional interaction between β2-agonists and montelukast in modulating bronchial tone and to investigate on the possible therapeutic advantages by using a montelukast-formoterol salt a newly synthesized chemical entity.

### 5.2.3 Materials and Methods

Material and methods, and statistical analysis related to these experiments are reported in Chapter3.

### 5.2.4 Results

***Montelukast preserves $\beta_2$-functional response by preventing homologous desensitization in vitro.***

Montelukast's effect on the regulation of bronchial tone was assessed *in vitro* (Figure 5.9). As shown in Figure 5.9A preincubation of isolated bronchi with montelukast did not affect carbachol-induced contractions. Similarly, relaxation induced by salbutamol was not modified (Figure 5.9B) by

montelukast. Bronchi exposed to two consecutive concentration-response curves to salbutamol develop a lack of the relaxant response to the adrenergic stimuli as also evident in our experimental conditions (Figure 5.9C). However, the in vitro pre-incubation with montelukast preserved salbutamol-induced relaxation (Figure 5.9D). Homologous $\beta_2$ desensitization evokes impaired $\beta_2$-mediated relaxation associated with attenuated cAMP accumulation mediated by PKA/PDE signaling. To assess if this happens in our experimental conditions, we tested the effect of IBMX a pan inhibitor of phosphodiesterase and H89, an inhibitor of PKA on $\beta_2$ desensitization. As evident in Figures 5.9E and 5.9F preincubation with IBMX or H89 prevented desensitization-induced reduced response to salbutamol as observed with montelukast (Figure 5.9B).

To assess if the montelukast effect converged on the desensitization signaling pathway the expression of $\beta_2$, and β arrestin was evaluated in BEAS-2B cells following prolonged exposure to salbutamol and in the presence of montelukast (Figure 5.10 A, B). Immunofluorescence staining evidenced that the salbutamol challenge induced a cytosol translocation of $\beta_2$ (Figure 5.10A) coupled with increased nuclear signaling of β arrestin. Montelukast pretreatment inhibited both $\beta_2$ and β-arrestin upregulation induced by salbutamol (Figure 5.10A, B) confirming its ability to control desensitization mechanisms.

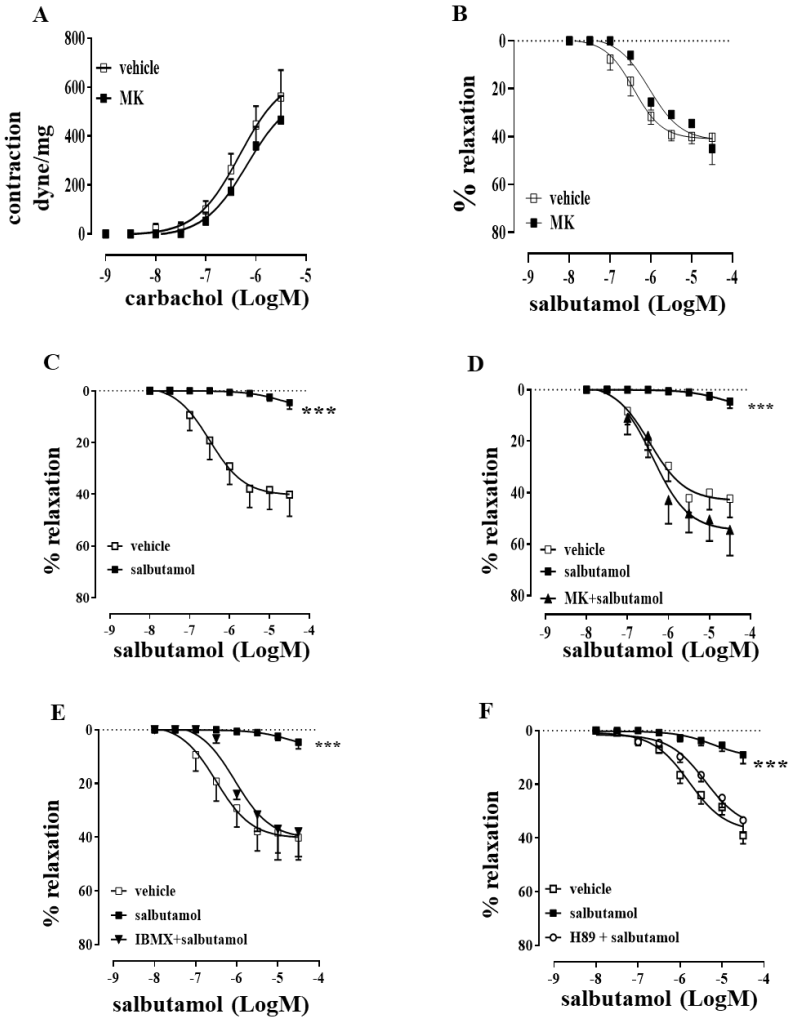


***Figure 5.9: Effect of montelukast on bronchial tone***. Bronchi harvested from BALB/c mice were incubated with MK ($10^{-6}$M, 10 min) and stimulated with carbachol (A) or salbutamol (B). C) Desensitization protocol: bronchi contracted by carbachol were exposed to repetitive salbutamol challenge. Desensitized bronchi were pretreated with MK ($10^{-6}$M, 10 min; D), IBMX ($10^{-7}$M, 10 min; E) or H89 ($10^{-7}$M, 10 min; F) before exposing the bronchi to the following salbutamol challenge. Values represent means ± S.E.M.; n = 6 mice for each group. Data were analyzed by two-way ANOVA plus Bonferroni post-hoc test. Statistical significance is reported as ***P<0.001 vs vehicle.

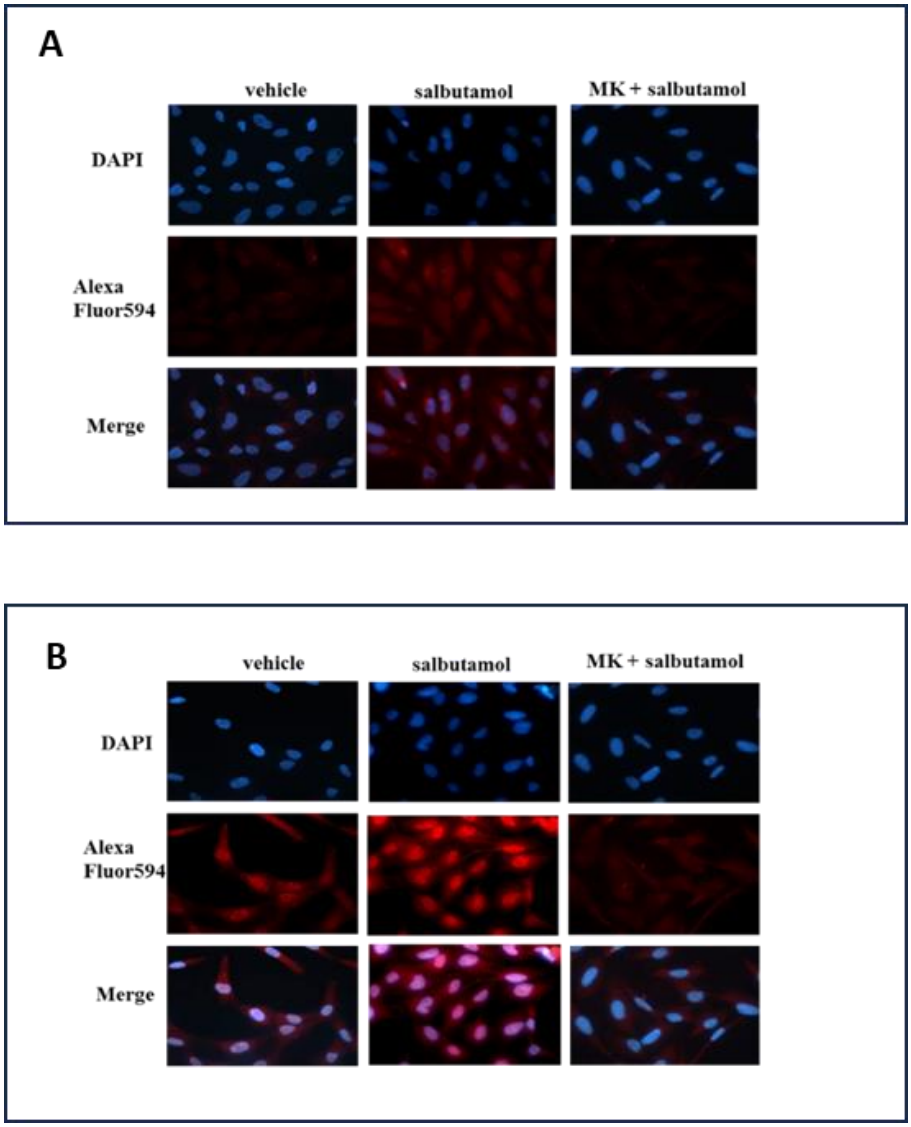


***Figure 5.10: Salbutamol desensitization involves PKA/β-arrestin signaling.*** Immunofluorescence analysis of β2 (A) and β-arrestin 1 (B) on BEAS-2B cells exposed to prolongate salbutamol 30 µM challenge in the absence or presence of MK 30 µM. The image was acquired by using DAPI and AlexaFluor594 staining at 400X magnification with AxioCam MRc5.

***The combination of montelukast with β2 agonist has a synergic effect in modulating the inflammatory response.***

To further investigate the pharmacological relevance of this association we also evaluated its effect on modulating inflammation which is another key asthma feature. For this purpose, formoterol was chosen for in vivo studies considering the more appropriate pharmacokinetic characteristics such as its prolonged half-life compared to salbutamol. First, we confirmed that also in the case of formoterol as observed with salbutamol, prolonged exposure of isolated bronchi induced a lack of $\beta_2$-mediate relaxation (Figure 5.11A) that again was preserved by montelukast. Thus, the advantage of the pharmacological association with the LT-antagonist was class-related rather than drug-specific (Figure 5.11A).

We went on by taking advantage of the synthesis of salt of montelukast with formoterol (MFS; Figure 5.11B). The MFS contains montelukast and formoterol in a ratio of 1:1 (Figure 5.11B). To evaluate if MFS retained its pharmacological activity *in vivo* it was preliminarily tested in the carrageenan mouse paw edema. The three drugs were administered i.p. 30 min before inducing the inflammatory response by sub-plantar injection of carrageenan (Figure 5.11 C-E). Formoterol exhibited a significant inhibitory effect on the first phase of edema (Figure 5.11C), while montelukast inhibited more significantly the second phase (Figure 5.11D). The administration of MFS caused a significant inhibition of both phases indicating that both drugs maintained their pharmacological activity also when administered as salt and in addition, MFS acquired an enhanced activity in controlling both phases of the inflammatory response (Figure 5.11E).

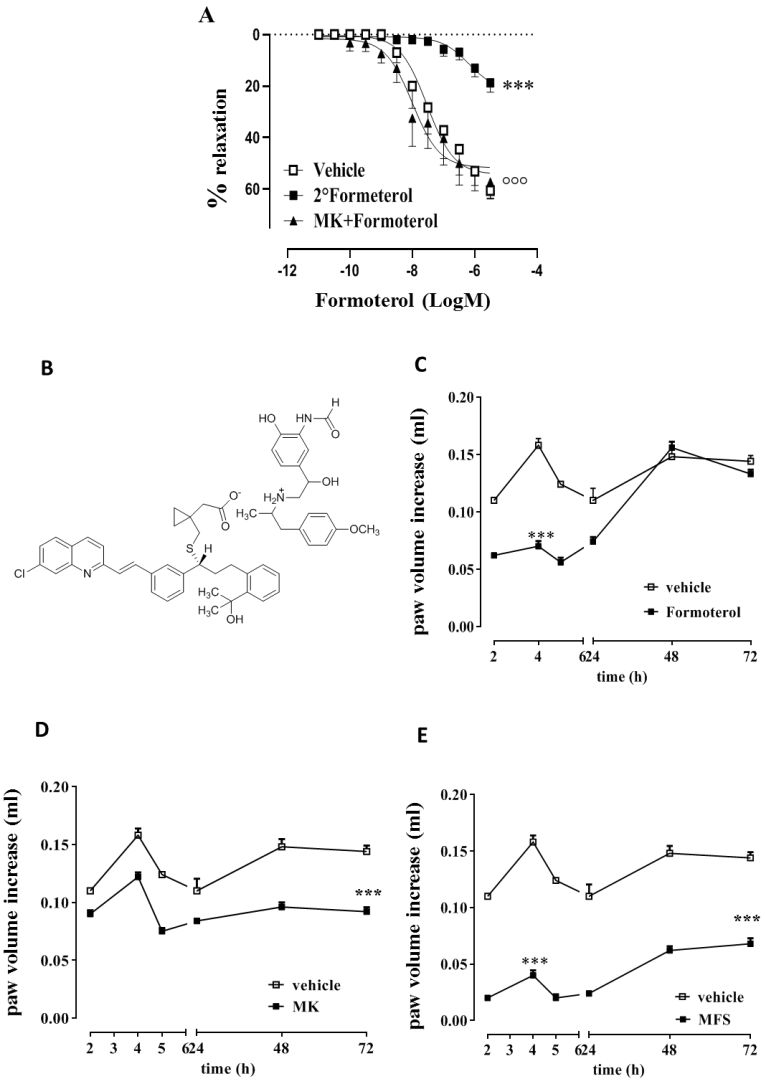


***Figure 5.11: Effect of montelukast and formoterol association***. A) Bronchi desensitized to formoterol were pretreated with MK (10-7M 10 min) before exposing bronchi to the following formoterol challenge. B) Chemical structure of Montelukast formoterol salt (MFS). Effect of formoterol (0.3mg/Kg; C), MK (0.3mg/Kg; D) ) or MFS (0.3mg/Kg; E) on mouse paw edema induced by sub plantar injection of carragenin (1%). Data are expressed as media±SEM. Data were analyzed by two-way ANOVA plus Bonferroni post-hoc test. Statistical significance is reported as ***P<0.001 vs vehicle, °°°P<0.001 vs formoterol.

***MFS inhibits airway hyperresponsiveness and prevents $\beta_2$-adrenoceptor desensitization in vivo.***

The effect of MFS was tested in an experimental model of asthma (Figure 5.12A) and compared to the parent compounds (Figure 5.12 and 5.13). Bronchi harvested from OVA-sensitised mice showed an increased contractile response to carbachol (Figure 4.4B) and a reduced response to salbutamol (Figure 5.12C). Bronchi harvested from mice receiving intraperitoneal administration of formoterol or montelukast showed a significant reduction of the OVA-induced increased contractile effect elicited by carbachol (Figure 5.12D). Following treatment in *vivo* with formoterol, the salbutamol-mediated relaxation of isolated bronchi was further reduced (Figure 5.12E). Montelukast by itself did not affect salbutamol-induced relaxation in vitro (Figure 5.12E).

When Montelukast was associated with formoterol by MFS, we observed a dose-dependent significant inhibition of carbachol-induced contractions in vitro (Figure 5.13A), but also a reversion of OVA-induced reduction in salbutamol response in vitro (Figure 5.13B). Functional data were confirmed by immunohistochemistry. Lung sections obtained from sensitized mice showed that sensitization decreased $\beta_2$ expression and increased β-arrestin expression index of a heterologous desensitization induced by lung inflammatory reaction (Figure 5.13C, D and E). MFS increased β2 and decreased β-arrestin 1 expression (Figure 5.13C, D and E) in perfect tune with the functional data (Figure 5.13B).

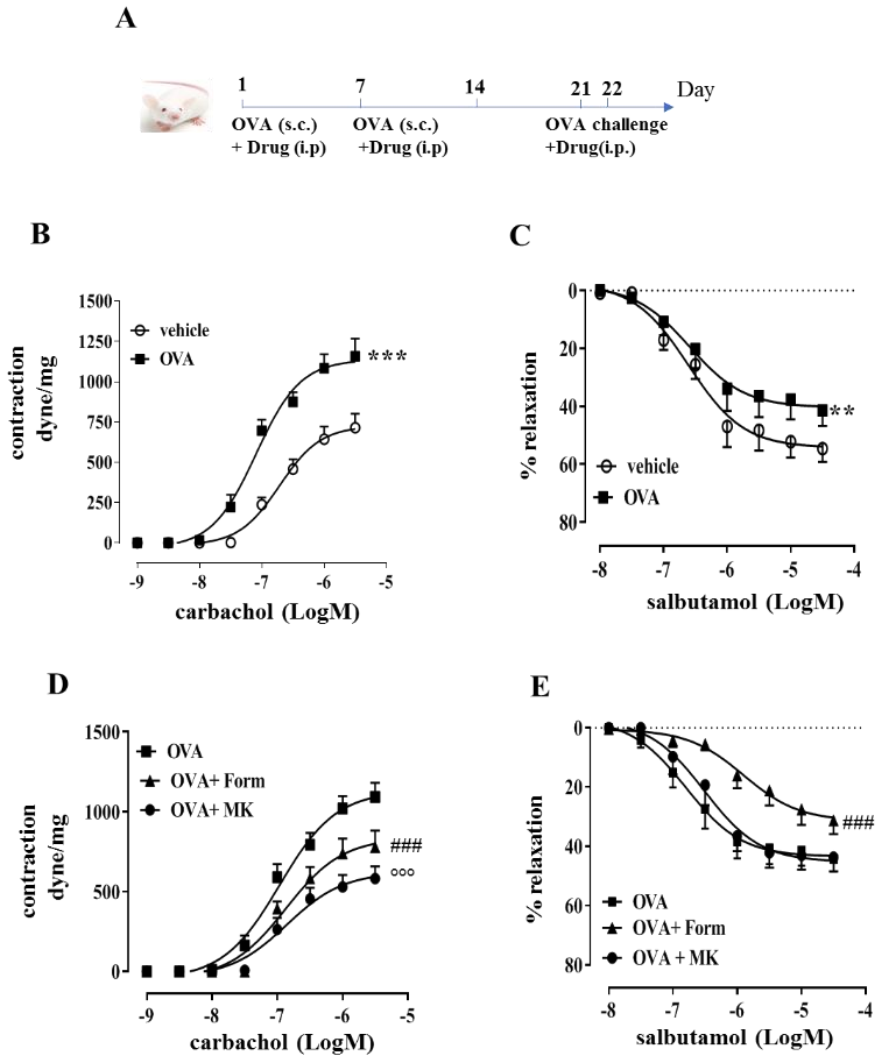


***Figure 5.12: Effect of montelukast or formoterol on OVA-induced bronchial dysfunction.*** A) Scheme of sensitization and treatment. Female mice were pretreated i.p. with formoterol or MK (0.3mg Kg-1) or vehicle (physiologic solution) 30 min before each OVA challenge. Animals were sacrificed to evaluate bronchial reactivity to carbachol (B, D) and salbutamol (C,E). Values represent means ± S.E.M.; n = 6 mice for each group. Data were analyzed by two-way ANOVA plus Bonferroni (C). Statistical significance is reported as follows: ***P < 0.001 vs vehicle; **P < 0.005 vs vehicle; ### P < 0.001 vs OVA; °°° P < 0.001 vs formoterol.

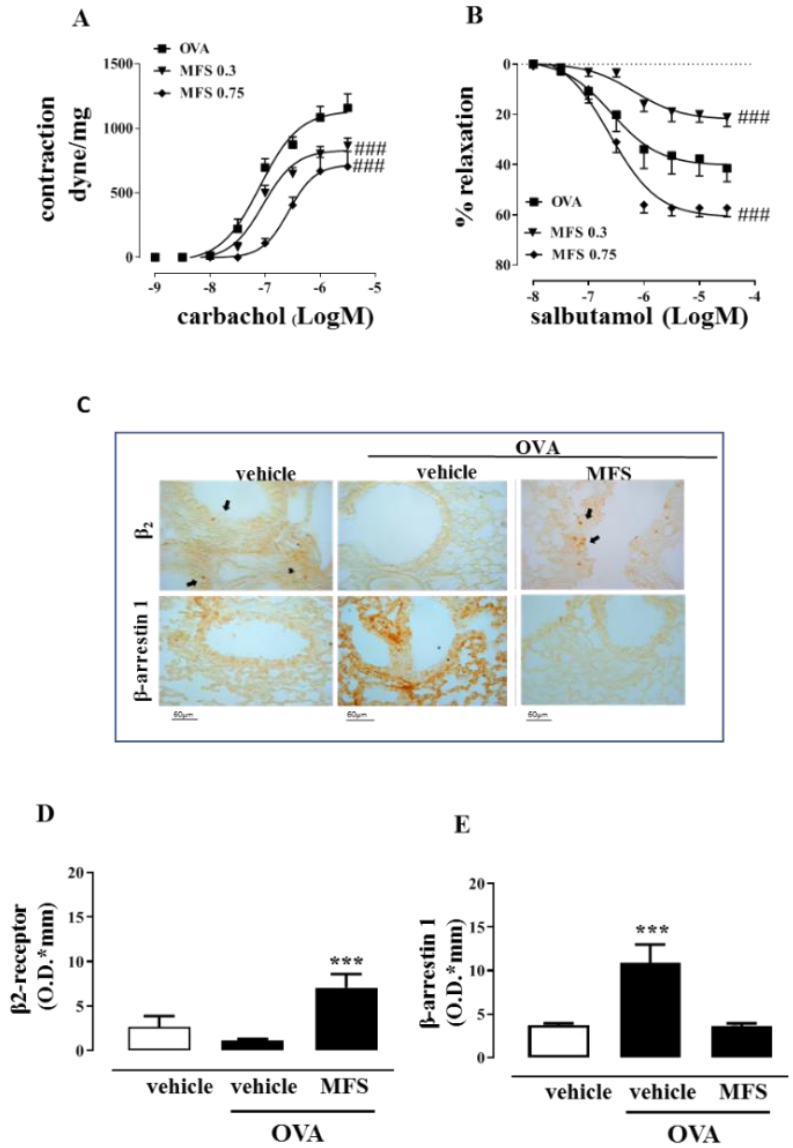


***Figure 5.13: Effect of MFS on OVA-induced bronchial dysfunction.*** Female mice were pretreated i.p. MFS (0.3 and 0.75mg Kg-1) or vehicle (physiologic solution) 30 min before each OVA challenge. Animals were sacrificed to evaluate bronchial reactivity to carbachol (A) and salbutamol (B). Values represent means ± S.E.M.; n = 6 mice for each group. Data were analyzed by two-way ANOVA plus Bonferroni (C). Statistical significance is reported as follows: ###P < 0.001 *vs* OVA. Immunohistochemical analysis for β2-receptor and β-arrestin1 (C) on lung sections

obtained by vehicle, OVA-sensitized, and OVA-sensitized mice pretreated with MFS (0.75mg Kg-1). Semi-quantitative determination of β2-receptor (D) and β-arrestin1 (E) was obtained with ImageJ Fiji. Scale bar =60 μm. N animals for each group 3; Data were analyzed by One-way ANOVA plus Bonferroni post hoc test. Statistical significance is reported as ***P<0.001 *vs* vehicle.

***Synergic effect of MFS in modulating pulmonary inflammation does not involve allergen sensitization mechanisms.***

Histological analysis (Figure 5.14A) of pulmonary sections obtained from sensitized mice showed significant lung damage coupled with an increase in cell infiltration and bronchial epithelial thickness. Treatment with formoterol or montelukast inhibited allergen-induced cell infiltration as confirmed by pulmonary IL-4 cytokine dosage (Figure 5.14A top panel, B and C). However, lung injury was still significantly present when mice were pretreated with formoterol or montelukast (Figure 5.14A and D). Conversely, pretreatment with MFS not only significantly inhibited cell infiltration but also reported lung structure to the basal conditions (Figures 5.14A-D). PAS staining (Figure 5.14A bottom panel) showed increased positive staining in lung sections obtained by sensitized mice that were significantly inhibited by formoterol or MFS (Figures 5.14A and E).

The synergic effect of MFS was confirmed by α-SMA staining. OVA sensitization promoted an increased α-SMA positive staining that was significantly inhibited by formoterol or MFS (Figure 5.15A and B). Inflammatory reaction induced by sensitization is sustained by increased levels of plasma IgE levels. Treatment with all the drugs used did not modify plasma IgE levels indicating that MFS does not affect the systemic immune response (Figure 5.15C) as well as the parent compounds (Figure 5.15C).

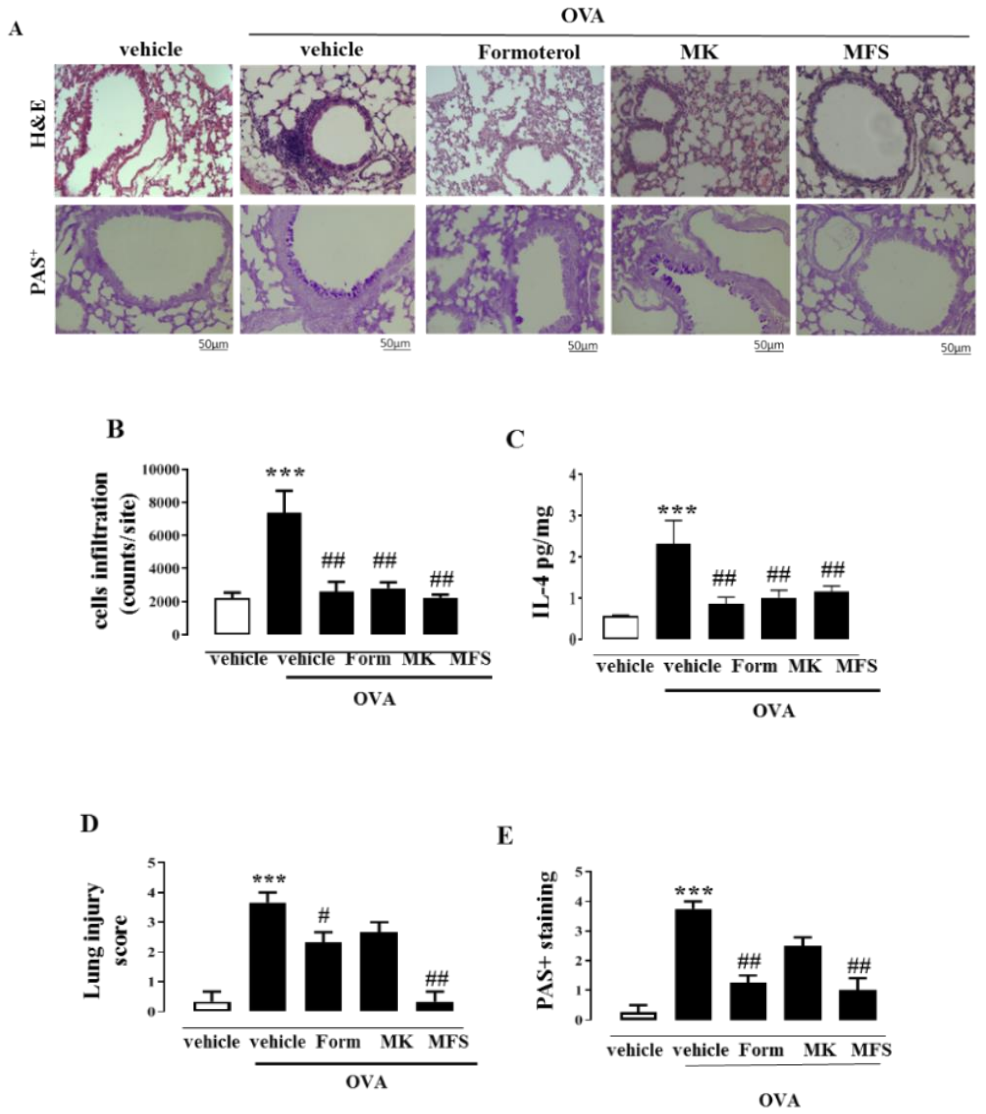


***Figure 5.14: Effect of formoterol, Montelukast or MFS on pulmonary inflammation.*** A) Lung slices obtained from sensitized mice and treated with Form, MK or MFS were stained for Hematoxylin & Eosin (H&E) (top panels) or PAS+ (bottom panels). The pulmonary cell infiltration (C) was evaluated by using ImageJ software. Pulmonary IL-4 was quantified by ELISA (C). The lung injury score (C) was evaluated blindly by scoring from 0 (normal) to 4 (severe) as described in the methods section. PAS+ staining was graded with scores of 0 to 4 (E) as described in the methods section. N animals for each group=3, scale bar=50µm. Data were

analyzed by One-way ANOVA plus Bonferroni post-hoc test. Statistical significance is reported as ***P<0.001 vs vehicle; ## p<0.01vs vehicle-OVA; # p<0.05vs vehicle-OVA.

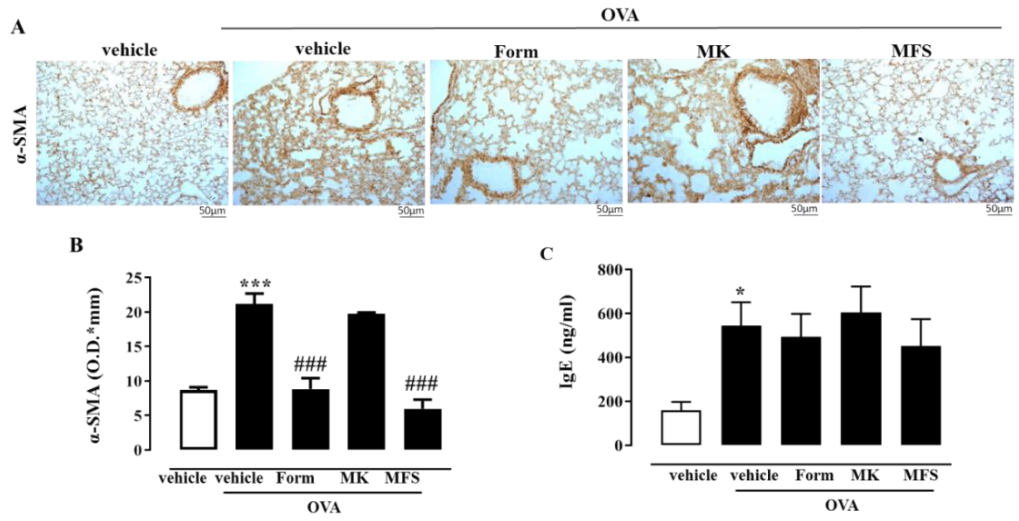


***Figure 5.15: Effect of formoterol, montelukast or MFS on allergic inflammation.*** A) Immunohistochemical staining for α-SMA in non-sensitized mice(vehicle) and OVA-sensitized mice pretreated with vehicle, Form, MK, or MFS. Semi-quantitative determination of α-SMA obtained with ImageJ Fiji software (B). N animals for each group= 3; Scale bar =50 µm. C) Serum levels of IgE. Data were analyzed by One-way ANOVA plus Bonferroni post-hoc test. Statistical significance is reported as ***P<0.001vs vehicle; *P<0.05 *vs* vehicle ###P<0.001 vs vehicle-OVA.

### 5.2.5 Discussion and conclusions

Corticosteroids in association with SABA/LABA are the mainstay in the management of asthma. However, many asthmatics do not reach a total symptom-free condition after the use of this combination. Thus, the Global Initiative for Asthma upgraded the guidelines and included add-on therapy with LT modifiers such as CysLT1R antagonist. Once-daily oral dosage of montelukast significantly improves the airway function in asthmatics. Similarly, it also proves beneficial in delaying the impact on night-time symptoms. Several reasons make montelukast stand out as a part of the treatment regimen of asthma, and the topmost of them is the better compliance for the patient as the recommended posology (once-daily, orally) helps to improve patient adherence to the treatment in comparison with other drugs. Secondly, this also reduces the extended side-effect profile.

Here the therapeutic advantage of montelukast when associated with SABA/LABA in relieving asthma features has been further demonstrated. More interestingly we delineate an additional advantage related to montelukast's ability to provide sustained broncho protection and permit a better rescue bronchodilation response to $\beta_2$-agonists.

Exposure of bronchial rings to montelukast by itself does not affect bronchial tone. Indeed, both carbachol-induced contraction and salbutamol-induced relaxation remain unaltered. However, montelukast preserves adrenergic bronchial response from homologous $\beta_2$-desensitization induced by repeated exposures to salbutamol. Homologous β2 desensitization evokes impaired $\beta_2$-mediated relaxation associated with attenuated cAMP accumulation mediated by PKA/PDE signaling. Indeed, pre-treatment with PDE or PKA inhibitors restores the salbutamol-induced relaxing effect preventing desensitization to the same extent as montelukast. This is in perfect tune with molecular studies

demonstrating that prolonged exposure of bronchial epithelial cells to salbutamol induces an increased expression of β-arrestin-1 and cytosol translocation of $\beta_2$ receptor, which are considered the key cellular elements involved in the desensitization regulatory machinery. Thus, the pharmacological effect displayed by montelukast, and salbutamol association overcomes the desensitization phenomenon that represents an important limitation of $\beta_2$-agonist therapy.

To define if the montelukast effect is limited to SABA we tested, in the same experimental setting, a LABA such as formoterol. Montelukast's rescue effect on formoterol-induced desensitization is indistinguishable from that of salbutamol. Thus, the montelukast effect is class-related.

To further gain insight into the therapeutic advantage of this pharmacological association we have synthesized a montelukast/formoterol salt (MFS) that has allowed us to simultaneously administer the two drugs *in vivo* in comparison to the two-parent compounds.

To define if MFS is adsorbed, we have evaluated its activity in vivo in an experimental model of inflammation such as carrageenan-induced paw edema that is characterized by an acute early response that evolves within 6 hours and a second sub-chronic phase starting after 24h from the administration resolving after 72h. Treatment of mice with formoterol or montelukast shows an inhibitory effect on the inflammatory response as reported in literature. In this mouse model formoterol exhibits a significant effect on the early phase of edema, while montelukast inhibits only the second phase. The administration of MFS causes significant inhibition of both phases, demonstrating that MFS is absorbed and maintains the anti-inflammatory effect, mimics, and optimizes the effect of the two drugs.

Therefore, we tested the efficacy of MFS in an experimental model of asthma. Allergen sensitization induces not only airway hyperresponsiveness but also a

reduction of $\beta_2$ agonist broncho dilating effects (heterologous desensitization) further worsened by pharmacological treatment with LABA (homologous desensitization). Mice sensitized to OVA have been pre-treated by intraperitoneal administration of i) montelukast, ii) formoterol, and iii) MFS before each OVA challenge. The functional study confirms the efficacy of formoterol and montelukast in inhibiting bronchial hyperresponsiveness. A similar effect is obtained by MFS which exhibits a dose-related effect. In addition, MFS treatment rescues salbutamol-induced relaxation counterbalancing both heterologous desensitization and homologous desensitization. Thus, MFS encompasses montelukast and formoterol anti-inflammatory effects and provides sustained broncho protection. Functional data were confirmed by immunohistochemistry. Lung sections obtained from sensitized mice showed that sensitization decreased $\beta_2$ expression and increased the β-arrestin expression index of heterologous desensitization induced by lung inflammatory reaction. MFS restored both β2 and β-arrestin1 expression.

The therapeutic advantage of MFS is not limited to the preserved functional response of airways but is also reflected by a significant modulation of the inflammatory lung response. Therefore, the effect is due to the modulation of inflammatory response within the lungs as demonstrated by the inhibition also of lung Th2 cytokines. Of note, the effect given by MFS is obtained at half of the active dose of the single compounds namely montelukast and formoterol. This same pattern of enhanced activity is highlighted also by the immunohistochemical analysis of lung sections. The analysis of pulmonary sections obtained by sensitized mice shows an increase in cell pulmonary infiltration. Treatment of sensitized mice with formoterol, montelukast, or MFS causes a significant inhibition in cell infiltration. More interesting treatment of sensitized mice with MFS determines further advantage as

demonstrated by a significant inhibition of lung injury and pulmonary metaplasia, not observed with the parent compounds [104].

In conclusion, our data confirm the advantage of a pharmacological association between montelukast and SABA/LABA already suggested by some clinical outcomes. We evidence the importance of coadministration that is guaranteed by a unique chemical entity such as MFS in preventing asthma features such as AHR and lung inflammation, but more interesting in preserving $\beta_2$-agonists rescue therapy [104].

# Chapter 6

# 6. Collaboration: Baylor College of Medicine

During my PhD, I spent one year at Baylor College of Medicine in Houston TX. I carried out a research activity as a visiting student in Professor Francesca Polverino's laboratory at the Department of Medicine, Section of Pulmonary, Critical Care, and Sleep Medicine of Baylor College of Medicine. During this period, I studied the role of sphingolipid metabolism in sexual dimorphism of COPD exacerbation.

## 6.1 Sex-related differences in COPD symptoms are associated to sphingolipids metabolism.

### 6.1.1 Rationale

COPD is identified as a major cause of morbidity and mortality worldwide [31].

In the pathophysiology of COPD, exposure to an irritant risk factor, like cigarette smoke, causes a chronic inflammatory response in the lung; such inflammation can result in: Emphysema, which is one of the structural changes seen in COPD, characterized by the destruction of the alveolar air sacs or could also lead to chronic bronchitis that is characterized by mucous hypersecretion, that results in a chronic productive cough [32].

Cigarette smoke (CS) exposure is a major risk factor in developing this disease. CS causes chronic lung inflammation, chronic bronchitis, and persistent cough. Moreover, CS is also known to induce airway smooth muscle proliferation and airway hyperreactivity (AHR) [105].

Airway smooth muscle is the primary effector cell responsible for controlling airway caliber and thus the resistance to airflow in COPD, particularly in the small airways. Dysfunction in airway smooth muscle plays a crucial role in the pathogenesis and severity of COPD via alterations of inflammatory response and airway smooth muscle proliferation [106].

Several studies demonstrate that the clinical presentation of COPD is different in women and men: it has been shown that in women the exposure to the same amount of cigarette smoke, generates more severe airflow limitation and inflammation at an earlier age than men. On the other hand, at all stages of chronic obstructive pulmonary disease (COPD) severity, men have more severe emphysema than women [31].

Until now, the reasons why women differ from men in cigarette smoking susceptibility and the pathological and clinical expressions of COPD, remain widely unknown [31].

Several studies show that COPD induces dysregulation of sphingolipid metabolism, with an increase in S1P and ceramidase lung levels [107].

Sphingolipids are metabolically active entities involved in the control of inflammation; these molecules have been implicated in COPD, especially in distal lung cell injury and loss of alveolar tissue, the hallmark of emphysema [108].

A proapoptotic second messenger, ceramide, is at the core of the sphingolipid metabolism, serving as a precursor of prosurvival metabolites including sphingosine-1 phosphate (S1P) [69]. The two main pathways of ceramide synthesis are the de novo pathway and the recycling of sphingosine through the salvage pathway [55]. Lung ceramide levels were shown to be higher in human subjects with emphysema compared to those without, and the expression of multiple species of ceramides, was shown to be significantly higher in smokers with COPD than those in non-smokers [62].

Orosomucoid 1-like protein 3 (ORMDL3) and Ceramidase are two important key regulators in the ceramide metabolism, to maintain the right level in the lung, in particular, ORMDL3 is involved in airway inflammation, airway smooth muscle proliferation, and airway hyperreactivity [105].

### 6.1.2 Aim

Based on these findings we hypothesized a contribution of sphingolipids metabolism in sexual dimorphism in COPD presentation. Here we have investigated if the dysregulation of the sphingolipid pathway may drive sex differences in COPD.

### 6.1.3 Materials and Methods

Material and methods, and statistical analysis related to these experiments are reported in Chapter3.

### 6.1.4 Results

***Ceramide metabolism is upregulated in COPD patients mostly in women.***
Immunofluorescent analysis of pulmonary sections from patients never smoker control, smoker control and COPD (GOLD 1-4) were performed to detect ASAH1 and ORMDL3 expression in bronchi and bronchiole (Figures 6.1A, C). ASAH1 and ORMDL3 are both key regulators of sphingolipids

metabolism, ASAH1 is a ceramidase that converts ceramide into sphingosine, while ORMDL3 is a rheostat that regulates ceramide levels.

The staining results showed, in women, an upregulation of both protein ORMDL3 and ASAH1 in COPD patients compared to never-smoker controls and smoker-control patients (Figures 6.1B, 1D); while in men there was an increase of these proteins already in smokers' bronchi compared to never smoker control, with a further significant increase in COPD patients (Figures 6.1B, 1D). These results suggest a higher sphingolipids metabolism in COPD disease, due to a dysregulation of sphingolipids lung levels.

However, the comparison of ORMDL3 and ASAH1 expression levels, between men and women, showed a significantly higher expression of both proteins in women NSC and COPD (GOLD1-4) patients compared to men (Figures 6.1B, D); instead, the smoker control group didn't show sex difference in the expression of these two proteins (Figures 6.1B, D). These results suggest a different involvement of sphingolipids in the development of the disease in men and women and in the presentation of major symptoms.

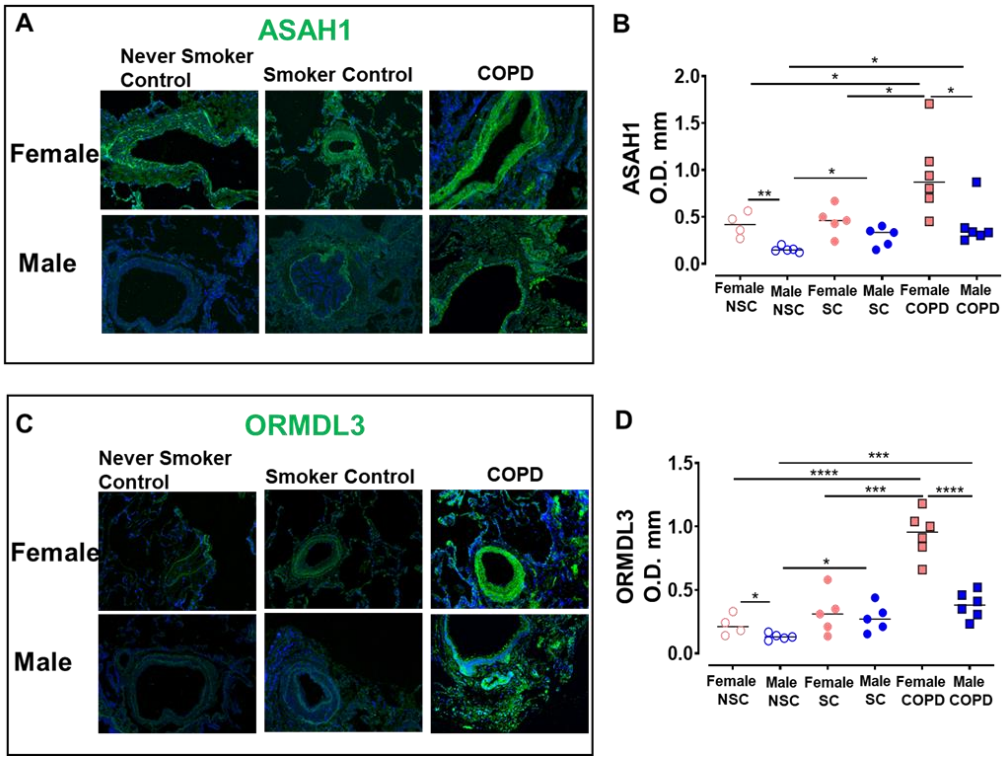


***Figure 6.1: ASAH1 and ORMDL3 lung levels are upregulated in COPD patients***. Representative immunofluorescence staining for a) asah1. There is an upregulation of asah1 in women patients with COPD compared to the nsc and smoker control (b) and an upregulation of asah1 in men patient smokers and with COPD compared to nsc (b). In all three groups women showed higher expression of asah1 compared to men (b). Representative immunofluorescence staining for c) ormdl3. There is an upregulation of ormdl3 in women patients with COPD compared to the nsc and smoker control (d) and an upregulation of ormdl3 in men patient smokers and with COPD compared to nsc (d). In all three groups women showed higher expression of ormdl3 compared to men (d). Data are expressed as Media±SEM. a-d) n=4-6. *:p<0.05, **: p<0.01, ***: p<0.001. Magnification 20X.

***The sexual differences in Ceramide metabolism translate to different systemic levels of sphingolipids.***

As is well known, S1P is involved in different cellular processes such as cell growth, differentiation, proliferation, and immune response [57]. Furthermore, S1P circulating levels increase in chronic inflammation. In perfect tune with ASAH1 (ceramidase) results in lungs, higher level of Sphingosine-1-Phosphate was found in plasma from women COPD patients, with a significantly higher concentration compared to men plasmatic level (Figure 6.2 A).

On the other hand, is well known that an alteration in ceramide lung level has been associated with COPD development, indeed lung ceramide levels were shown to be higher in human subjects with emphysema compared to those without [69]. Confirming that, a higher level of plasmatic ceramide was found in COPD patients compared to NSC levels in both sexes (Figure 6.2 B), but with a significantly higher concentration in men compared to women. In men's plasma ceramide was founded higher already in smoker control compared to NSC, with a further increase in COPD patients. ORMDL3 is known to be involved in sphingolipid metabolism in particular in the de novo sphingolipid synthesis, inhibiting serine palmitoyl-CoA transferase (SPT), in this way it regulates cellular ceramide levels [62]. ORMDL3 was found higher in COPD patients, in perfect tune with ceramide plasma levels results. The significantly higher expression of ORMDL3 in women compared to men, perfectly correlates to the higher ceramide plasma concentration in men (Figure 6.2B-C).

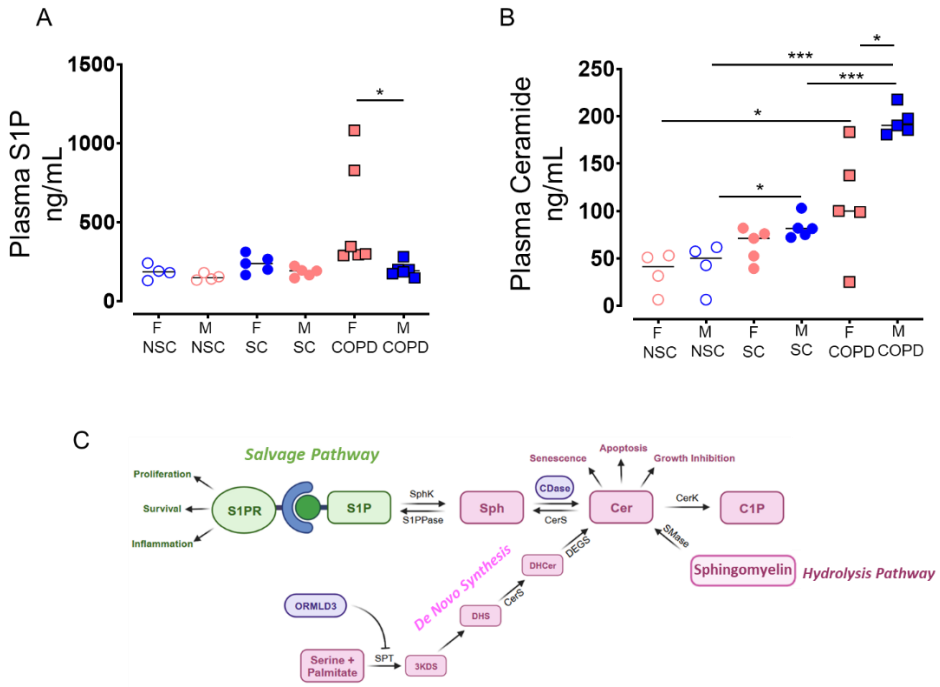


***Figure 6.2: Sphingolipids plasma levels are higher in COPD patients.*** S1P plasma level was measured in men and women with COPD (a). Women showed higher systemic S1P levels than men (a). Ceramide plasma level was measured in men and women with COPD. Ceramide level is higher in COPD patients, male and female, compared to nsc and smoker control. (c) schematic representation of sphingolipid pathway. Data are expressed as Media±SEM. n=5/6. *: $p<0.05$; **: $p<0.005$; *** $p<0.0005$.

***ORMDL3 and ASAH1 bronchi level correlates with the development of emphysema in COPD patients.***

COPD male patients from our cohort present higher levels of emphysema (%LAA) at all the stages of the disease (GOLD1-4) than women (Figure 6.3A); ceramide levels were found higher in plasma from COPD male patients compared to females of our cohort, confirming the evidence for which

ceramide level is higher in human subjects with emphysema compared to those without [62].

The comparison between ORMDL3 and ASAH1 levels and emphysema percentage (LAA%) showed, only in women, an inverse correlation between ASAH1 and ORMLD3 levels and the development of emphysema (Figure 6.3B, C); indeed, higher level of both key regulators of ceramide metabolism translates in lower ceramide production and correlates with lower percentage of emphysema in women. In men, there wasn't any correlation between both protein and LAA%, for which we have a homogeneous protein level for any level of emphysema severity.

***Women patients show higher airway remodeling in COPD exacerbation.***

An active remodeling process is evidenced by α-SMA upregulation in COPD patients compared to smoker and never-smoker control in both men and women patients (Figure 6.3D, E), which underlines an important structural change in the airway exposed to cigarette smoke.

Also, in this case, we found an important difference between women and men in the expression of a-SMA protein: higher level of alfa-sma was detected in women of all three groups, NSC, SC and COPD patients, compared to men (Figures 6.3D, E).

From the moment that α-SMA expression could be correlated with an increase in AHR and bronchi inflammation, this result could suggest a higher incidence of airway remodeling and bronchi inflammation in women with COPD compared to men; these evidence are confirmed also by the higher S1P systemic level in women, an important marker of inflammation. (Figure 6.2A).

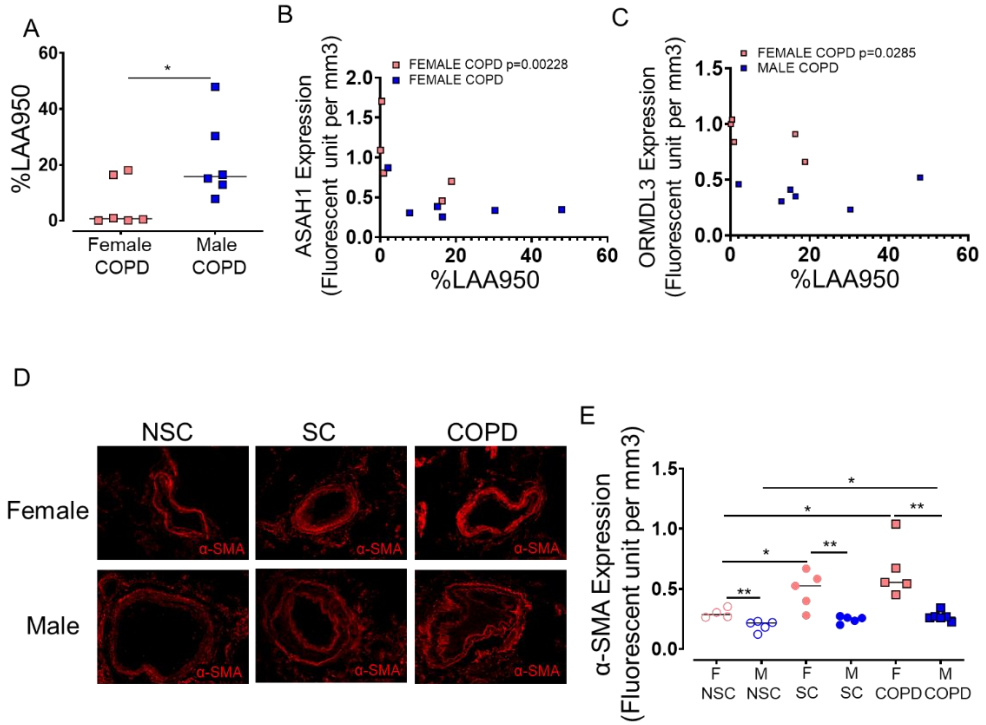


***Figure 6.3: Emphysema is correlated to asah1 and ormdl3 bronchi levels.*** a) %LAA950 is higher in men with COPD at all stages than in women with COPD at all stages. The comparison between asah1 and ormdl3 and %LAA950 showed ad inverse correlation in women but not in men (b,c). ). Data are expressed as Media±SEM. a n=5-6. *: p<0.05. Spearman b-c) n=11. *:p<0,05; **:p<0.005.

***α-SMA bronchial expression is higher in women.*** Representative immunofluorescence staining for d) α-SMA. α-SMA is upregulated in COPD bronchi of both men and women patients (e). In all three groups women showed higher expression of ormdl3 compared to men (e). Data are expressed as Media±SEM. a-h) n=4-6. *:p<0.05, **: p<0.01, ***: p<0.001. Magnification 20X.

***Cigarette smoke extract (CSE) exposure induces bronchi hyperreactivity only in female mice.***

Bronchi harvested from male and female mice c57/B6 were incubated with cigarette smoke extract (CSE) at 2% for 24h at 37 degrees (Figure 6.4A). The airway reactivity measurement conducted in organ bath, showed that the exposure to CSE2% induced bronchial hyperactivity to carbachol in female mice but didn't show any effect in bronchi from male mice (Figure 6.4B).

The incubation of bronchi, exposed to cigarette smoke, with a sphingosine kinase inhibitor (SKI-II), in the organ bath for 1 hour, restored the normal bronchial reactivity in bronchi from female mice; also, SKI-II incubation didn't produce any effect on bronchi from male mice. (Figure 6.4B)

Mice lungs harvested from male and female mice c57/B6 were incubated the same way, with CSE2% for 24h (Figure 6.4C). Western blot performed on the lung tissues showed a significant increase of smooth muscle myosin high chain (SMMHC), a marker of smooth muscle contractility, only in lung from female mice incubated with CSE2% (Figure 6.4D). The pre-incubation of lungs exposed to cigarette smoke with a ceramidase inhibitor (OEA 10uM) restored the basal SMMHC expression, again, only in female lungs (Figure 6.4D).

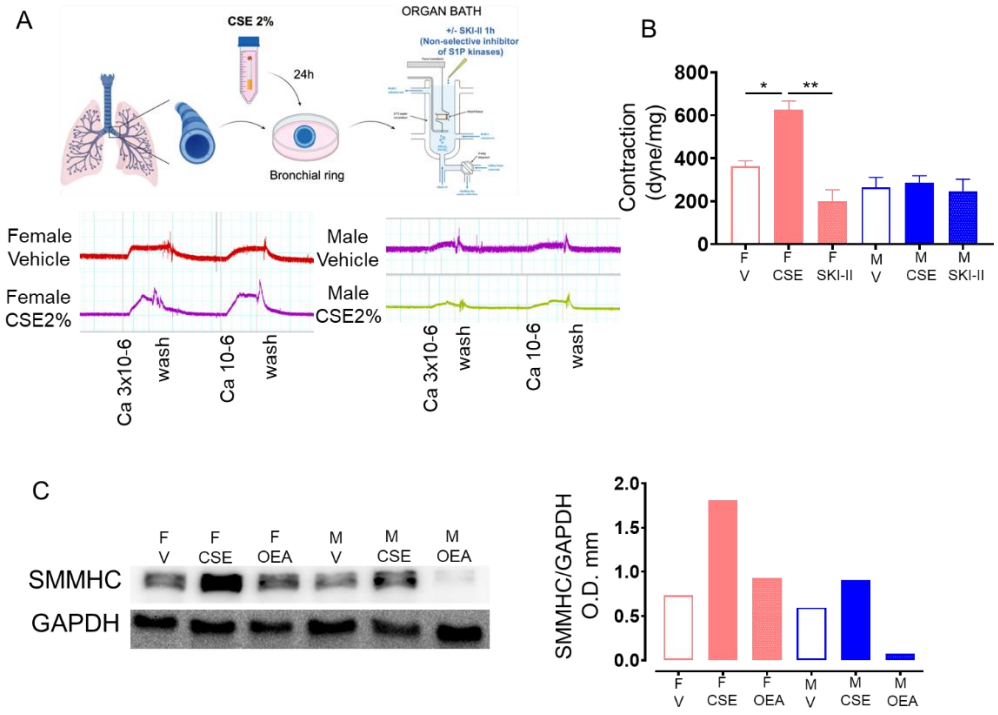


***Figure 6.4: Cigarette smoke extract increases bronchial contraction only in female bronchi.*** a) bronchi harvested from mice C57 B/6 male, and female were incubated for 24h with CSE2% to conduct a functional study on organ bath; a non-selective inhibitor of sphingosine kinases (SKI-II) was incubated for 1h in the organ bath. CSE-induced hyperactivity to carbachol only in female bronchi; SKI-II reduces this hyperactivity in female bronchi (b). c) lungs harvested from mice C57 B/6 male, and female were incubated for 24h with CSE2% to conduct western blot; an inhibitor of ceramidase (OEA) was incubated for 24h. CSE induced an increase in SMMHC expression only in female bronchi; OEA restored the normal expression of SMMHC in lungs from female mice. Data are expressed as Media±SEM. b,c,e) n=3. *: $p<0.05$, **: $p<0.01$.

***CSE treatment induces ORMDL3/ASAH1 upregulation only in Human Bronchial Smooth Muscle cells with estradiol supplementation.***

HBSM cells harvested from male donor were exposed to estradiol solution 25uM or vehicle (water) every other day for 7 days; on the last day the cells (vehicle and exposed to estradiol) were treated for 24h with cigarette smoke extract at 2% (CSE2%) and in part were pretreated with OEA10uM (ceramidase inhibitor) before the exposure to CSE2% (Figure 6.5A). Immunofluorescence staining was performed to measure ORMDL3 and ASAH1 cellular levels after estradiol supplementation and CSE2% treatment (Figure 6.5B, C).

The staining showed that the estradiol supplementation induced an increase of ORMDL3 and ASAH1 protein levels, compared to vehicle (figure 6.5B, 6.5C). Furthermore, the treatment for 24h with CSE2% induced a significantly greater increase of ORMDL3 and ASAH1 compared to control, only in cells exposed to estradiol for one week (Figure 6.5B, 6.5C).

The treatment with estradiol was shown to be capable of increasing the ceramide pathway and consequently, the cells become more susceptible to cigarette smoke exposure.

To confirm the alteration of the pathway driven by estradiol supplementation and Cigarette smoke, S1P levels were detected on cell supernatant using an Elisa Kit (Figure 6.5D). Estradiol supplementations increased the S1P supernatant level compared to vehicle; then the CSE2% treatment further increased the S1P level only in estradiol treated cells; then the OEA pretreatment restored the S1P level seen on estradiol-treated cells (Figure 6.5D). This data confirmed the upregulation of sphingolipids pathway after Cigarette smoke exposure, especially in high estrogen hormone level environment.

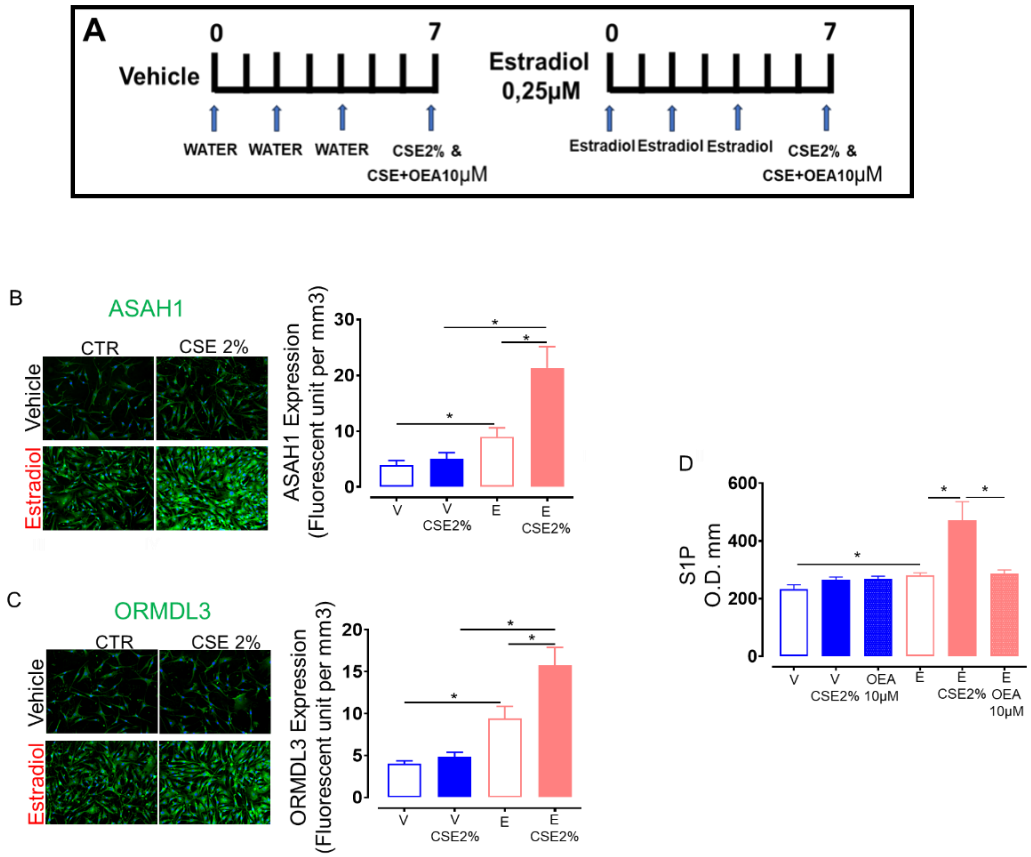


***Figure 6.5: Cigarette smoke extract increases ASAH1 and ORMDL3 expression in Human BSMC.*** a) HBSM were treated every other day with estradiol 0.25µM or water (vehicle), on the last day CSE2%, +/- OEA10µM was incubated for 24h; immunofluorescence staining was conducted on the cells to detect ASAH1 and ORMDL3 expression (b,c). Estradiol treatment increases the expression of both proteins especially with CSE2% treatment (b,c). S1P and Ceramide supernatant level was detected using ELISA assay (d,e); Estradiol increased S1P level in comparison to vehicle, then CSE treatment further increased S1P; OEA treatment restored S1P level (d). Data are expressed as Media±SEM. b,c,e) n=3. *:$p<0.05$. Magnification 20X

**Estradiol and CSE combination result in a synergic effect increasing SMMHC level and cellular proliferation in Human BSMC.**

HBSM cells harvested from male donor were exposed to estradiol solution 25uM or vehicle (water) every other day for 7 days, on the last day the cells were treated, in part, for 24h with CSE2%, and in part were pretreated with OEA10uM (ceramidase inhibitor) before the exposure to cigarette smoke for 24H (Figure 6.6A). Immunofluorescence staining was performed to measure SMMHC cellular level after the treatments (Figure 6.6B).

The estradiol supplementation induced an increase of SMMHC expression compared to vehicle (Figure 6.6B, 6.6C). The incubation for 24h with CSE2% further increased SMMHC level only in cells treated with estradiol (Figure 6.6B, 6.6C). Then, the preincubation with OEA10uM, before CSE2%, abrogates the synergic effect of estradiol and CSE on SMMHC restoring the normal expression of the contractility marker seen in vehicle cells treated with CSE2% (Figure 6.6B, 6.6C).

Estradiol exposure also increased cellular proliferation. Indeed, estradiol-treated cells showed a higher cellular proliferation compared to vehicle cells. Estradiol and CSE2% combination results in a synergic effect on cellular proliferation further increasing the cellular confluency. Also, for those results, the preincubation with OEA10uM abrogates the synergic effect of estradiol and CSE partially restoring the normal proliferation seen in vehicle cells treated with CSE2% (Figure 6.6D).

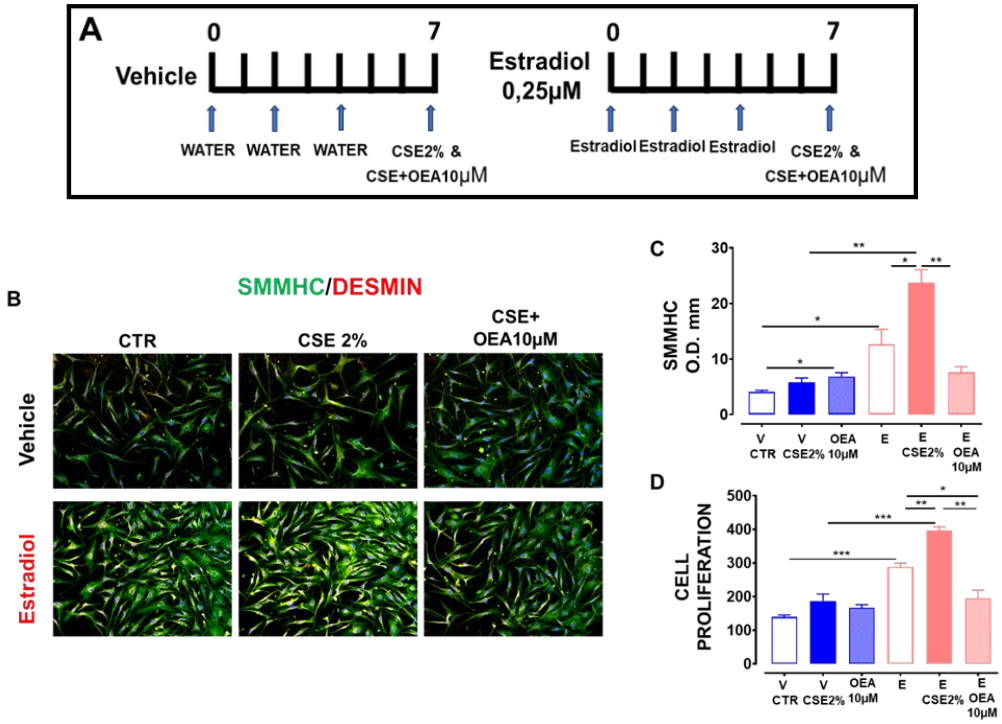


***Figure 6.6: Cigarette smoke extract increases SMMHC expression and cellular proliferation in HBSM cells***. a) HBSM were treated every other day with estradiol 0.25µM or water (vehicle), on the last day CSE2%, +/- OEA10µM was incubated for 24h; immunofluorescence staining was conducted on the cells to detect SMMHC expression (b). Estradiol treatment increases the expression of the protein, especially with CSE2% treatment, but OEA restored the normal expression of SMMHC (c). The counting of the cells stained in the different treatment groups was done to measure the cellular proliferation rate (d). Data are expressed as Media±SEM. b,c,e) n=3. *:p<0.05, **: p<0.01, ***: p<0.001. Magnification 20X.

***Estradiol supplementation altered the effect of CSE on Human BSMC contraction.***

The collagen contraction assay was performed in HBSM cells vehicle and exposed to estradiol, treated with CSE2%, +/-OEA pretreatment. The contraction to carbachol stimulation was measured at the following timepoint: 3h, 6h, 24h, 48h. (Figure 6.5A, 6.7A)

In vehicle cells the CSE2% incubation induced a significant reduction in cellular contraction in 48h; the pretreatment with OEA10uM didn't change the cigarette smoke effect. (Figure 6.7B)

In estradiol treated cells the effect of CSE2% was milder, indeed it only slightly reduced the contractile capacity of the cells, conversely the OEA pretreatment, in this case, further reduced the cellular contraction. (Figure 6.7C)

Estradiol supplementation alone, induces a higher contractility of the cell compared to vehicle cell (derived from a man donor); with cigarette smoke extract treatment these differences in contraction were further increased;(Figure 6.7D, E) these results could underline the different effects of CSE on smooth muscle cell in the presence or not of estradiol.

The treatment with the Ceramidase inhibitor (OEA) abrogates the differences, induced by estradiol, between the two groups and the contraction of vehicle and estradiol treated cells is almost the same (Figure 6.7F).

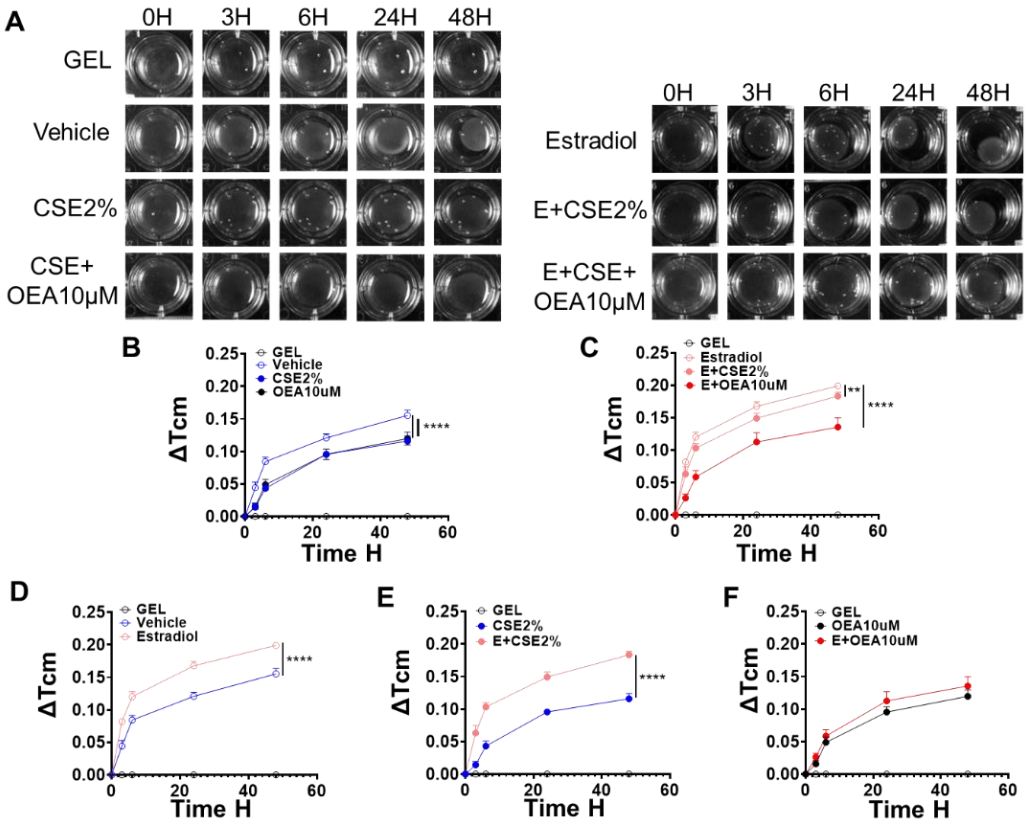


***Figure 6.7: Cigarette smoke extract effect on HBSM contraction.*** a) contraction assay was performed on cells treated with CSE2% and OEA10µM, +/- Estradiol; the picture was taken at time points 3h,6h,24h and 48h. The treatments produce different effects on cell vehicles and on cells treated with estradiol (b,c). The contraction of vehicle cells was significantly lower than estradiol-treated cells in both control group and with CSE2% treatment (d,e); the contraction was the same, for vehicle and estradiol cells, with the OEA treatment (f).

***Estradiol increases the speed migration of Human BSMC and reduces the inhibition of cellular growth caused by CSE treatment.***

The scratch assay was performed in HBSM cells vehicle exposed to estradiol and treated with CSE2% +/-OEA pretreatment. The speed of migration and cellular growth were measured in three different timepoint: 6h, 24h and 48h (Figure 6.5A, 6.8A)

The CSE2% incubation resulted in a decrease in cellular growth and then in the speed migration of bronchial cells; this effect was more marked in vehicle cells than in estradiol-treated cells (Figure 6.8B, C). Instead, the OEA pretreatment resulted in the same effect on both cell groups, reducing the speed of migration and cellular growth (Figure 6.8B, C).

Estradiol supplementation, as for contraction, increases the cellular speed migration and the growth, compared to vehicle. With CSE the differences are further increased. OEA treatment induced in both cellular groups the same speed migration reduction, deleting the estradiol effect on CSE action. (Figure 6.8D, E, F).

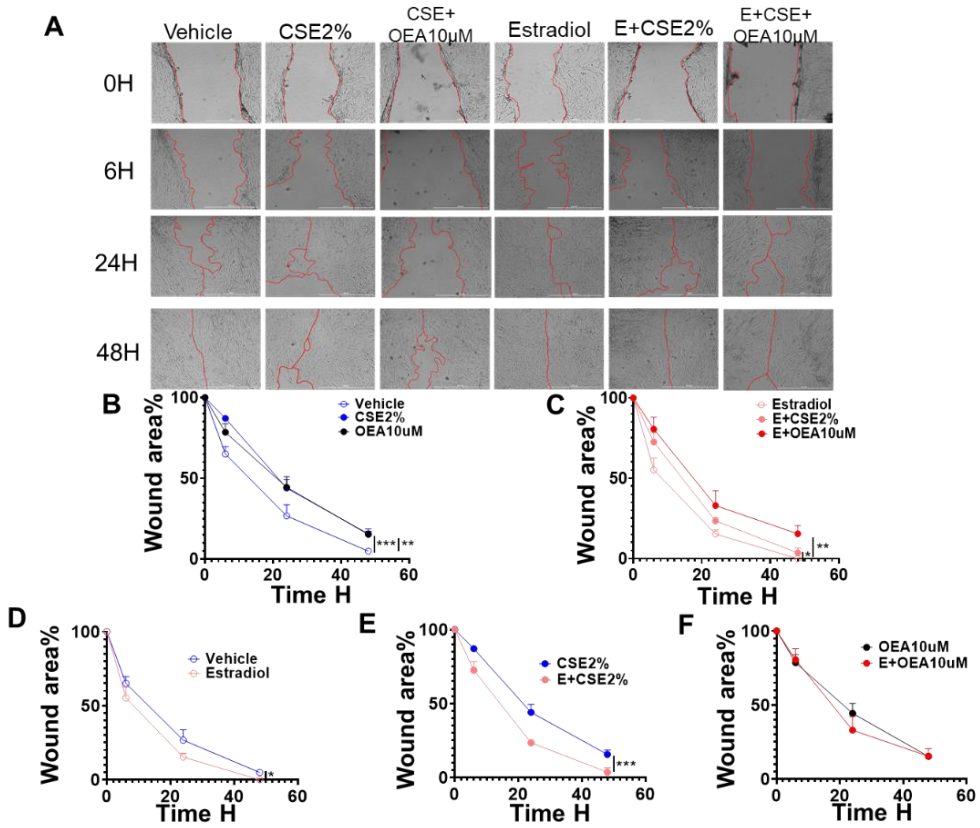


***Figure 6.8: Cigarette smoke extract effect on HBSM migration.*** a) Scratch assay was performed on cells treated with CSE2% and OEA10µM, +/- Estradiol; the picture was taken at time points 6h,24h and 48h. The treatments produce different effects on cell vehicles and cells treated with estradiol (b,c). The speed migration of vehicle cells was significantly lower than estradiol-treated cells in both the control group and with CSE2% treatment (d,e); the speed migration was the same, for vehicle and estradiol cells, with the OEA treatment (f).

### 6.1.5 Discussion and conclusion

This study aims to identify a connection between the dysregulation of the sphingolipid pathway in COPD and the development of the main symptoms of this disease in men and women. We found interesting differences in sphingolipids pathway between men and women already in the patients' controls. These differences increase in the COPD lungs showing a clear correlation between sphingolipids level and presentation of symptoms, as emphysema, AHR and airway remodeling.

We found also clear differences in the response to cigarette smoke in mice bronchi from male and female, and, also in human bronchial smooth muscle cells with and without estradiol supplementation.

In this study we found a link between gender-related symptoms of COPD and sphingolipids, showing a clear crosstalk between sexual hormones and sphingolipids metabolism in the lung.

The clinical presentation of COPD is different in women and men; indeed, it has been shown that women are more likely to develop COPD earlier in life with mainly inflammatory symptoms and airway limitations, while men develop more severe forms of emphysema in any stage of the disease [31].

To confirm these sex differences in COPD exacerbation, some studies in mouse models of chronic cigarette smoke have indicated that sex hormones may contribute to the greater COPD susceptibility in females. Indeed, exposure to cigarette smoke in female mice results in higher peripheral airway inflammation and airway remodeling, but less emphysema than in male mice; this effect is mediated by estrogens [41].

Several clinical and experimental studies aim to understand the contribution of hormones and sex to the biological pathogenesis of COPD [109].

Altered sphingolipid metabolism has been suggested as a possible mechanism in COPD susceptibility in particular, lung ceramide and S1P levels were shown to be higher in human subjects with emphysema compared to those without [69].

Several studies show that exist a correlation between sphingolipids and sexual hormones, in particular estrogens; indeed, estrogen signaling is not limited by the genomic pathway, estrogens have been shown to interact with multiple cytoplasmic signaling networks, including sphingolipids [72].

For these reasons this study aims to study the dysregulation of sphingolipids metabolism in COPD disease, and their interaction with sexual hormones.

First, we focused on two key regulators in the metabolism of sphingolipids, ORMDL3 and ASAH1, using human lung samples, from men and women, Nevers Smoker control, Smoker control and COPD (GOLD1-4). ORMDL3 regulates the de novo pathway of ceramides, blocking the ceramides production when its level results too high in the lung; ASAH1 (ceramidase), regulates the recycling pathway, converting ceramide into sphingosine, the precursor of S1P [110].

Our results show that women present a higher expression of ORMDL3 and ASAH1 in bronchi already in the controls; this upregulation increases in COPD patients. Furthermore, we found higher ceramide plasma levels in COPD patients, significantly higher in men, conversely S1P plasma level was found to be significantly higher in women with COPD.

An increase in Ceramide lung level is associated with higher development of emphysema in COPD exacerbation [69], so an increase in the metabolism of the latter could be associated with lower emphysema. Indeed, our results confirmed a higher percentage of emphysema in male patients at all stages of COPD; furthermore, an inverse correlation between ASAH1 and ORMDL3 level and %LAA950, was found in women with COPD.

From this evidence we may suppose that higher levels of the key regulators of ceramide metabolism, could have a protective role in women in the development of emphysema.

On the other hand, higher metabolism of ceramide translates to higher S1P level, as shown by S1P plasmatic level results (higher in women samples). The S1P is an inflammatory marker that has been associated with chronic inflammation and remodeling [60]. To support this, bronchi from women samples, showed enhanced expression of alfa-SMA, a marker of AHR and lung inflammation, as well as ORMDL3 that regulates airway smooth muscle hyperplasia, airway smooth muscle contraction, and contributes to airway remodeling [91]; all these results could be correlated with higher hyperreactivity and airway remodeling as COPD symptoms in women.

Starting from these human results, we conducted animal studies using C57Bl/6 mice male and female, to test Cigarette smoke effect on mice's bronchi and lungs.

In perfect tune with human results, only bronchi and lungs harvested from female mice showed a higher reactivity to carbachol and SMMHC expression after CSE incubation; the pharmacological inhibition of sphingolipids pathway restored the normal reactivity and SMMHC expression in female mice; this result underlines the different effect of cigarette smoke exposure in male and female airways, derived from a different interaction with sphingolipid, due to sexual hormones.

The interaction between sexual hormones and sphingolipid signaling was confirmed by further in vitro studies on human bronchial smooth muscle cells generated from a male donor.

Human BSMC were sensitized for 1 week with medium supplemented with estradiol 0,25µM. The estradiol induced an upregulation of the sphingolipids pathway and an increase in contraction, growth, and speed migration of the

cell and in S1P supernatant level. Indeed, is well known that estrogen signaling is not limited by the genomic pathway but has been shown to interact with multiple cytoplasmic signaling networks, [72] and these results confirm the interaction with sphingolipids pathway.

CSE2% treatment induced different effects in vehicle and estradiol treated cells; indeed, CSE further increased the ceramide metabolism in estradiol treated cells but didn't induce any significant effect on vehicle cells. Furthermore, higher levels of S1P were found in supernatant from cells treated with estradiol exposed to CSE. The increase in ceramide metabolism to S1P translates in higher cell survivor, proliferation, and inflammation susceptibility [111]. In perfect tune, with these results, the CSE treatment further increases SMMHC and cell proliferation levels, only in estradiol treated cells, and highlights even more the difference in contraction and speed migration between vehicle and estradiol cells.

Confirming this relationship between sphingolipids and estrogens, we used a ceramidase inhibitor OEA10μM, before CSE stimulation in both, vehicle and estradiol treated cells; OEA decreased S1P levels in cells treated with estradiol restored the normal effect of CSE in reactivity and migration of Human BSMC treated with estradiol and reduced the S1P supernatant level, so the treatment abrogates the estradiol effect, suggesting that these functional changes, founded after cigarette smoke exposure, in estradiol treated cells, were correlated to the changes in sphingolipids pathway.

In conclusion, we saw that females present an upregulation of sphingolipids pathway in the lungs, compared to men. This upregulation is associated with a lower incidence of developing emphysema in COPD but higher inclination to develop lung inflammation, AHR and bronchi remodeling. For these findings, sex differences observed in COPD symptoms might be associated with an estrogen-dependent dysregulation of sphingolipid metabolism.

We believe this study, although with its limitation due to the lack of a clear molecular mechanism suggesting the interaction between sphingolipids and estrogens, will increase our understanding of COPD pathogenesis, and provide a starting point to develop personalized approaches for treating COPD even in the earliest phases, taking account of sphingolipids as possible markers to diagnose different exacerbation of the disease.

# Chapter 7

# 7. Conclusions

In conclusion, this thesis project highlighted the important role of sphingolipids in the development of chronic respiratory diseases, such as asthma and COPD; particularly we demonstrated that S1P is an inducer of an important asthma feature, such as EMT, through regulation of TGF-β. Furthermore, we found an important connection between sphingolipids and sexual hormones, suggesting that the hormone's role in the development of chronic lung disease and sex-related symptoms, is due to the interaction with sphingolipids. Indeed, our data support the hypothesis of sex-related differences in the lung, which contribute to differential susceptibility to the development of asthma and COPD.

Another important goal was to synthesize new drugs that could optimize the pharmacological activity of drugs already used for the treatment of lung diseases such as β2-agonists and corticosteroids. In this context, we demonstrated the efficacy of the combination of beta-agonist formoterol with Montelukast, an anti-leukotriene used for asthma therapy, in overcoming the β2 receptor desensitization and preserving the rescue therapy as well as reducing AHR and lung inflammation. Another drug combination that resulted positively in the management of asthma features, was, Prednisone, a common anti-inflammatory drug, combined with TBZ, an H2S slow-releasing molecule; this hybrid provides a suitable approach to managing asthma features with a particular impact on airway remodeling.

**Table 1**

| Antibody Target | CAT# | Source | Working Dilution |
|---|---|---|---|
| ASAH1 | 11274-1-AP | Rabbit | 1:200-1:1000 |
| ORMDL3 | ab211522 | Rabbit | 1:200-1:1000 |
| α-SMA | SC-53142 | Mouse | 1:100 |
| SMMHC | 21404-1-AP | Rabbit | 1:50-1:1000 |
| S1P1/EDG1 | Ab11424 | Rabbit | 1:1000 |
| S1PR2 | orb319083 | Rabbit | 1:1000 |
| SPHK1 | EPR4293(2) | Rabbit | 1:1000 |
| SPHK2 | Ab37977 | Rabbit | 1:1000 |
| Beta Arrestin 1 | Ab31868 | Rabbit | 1:100 |
| ADRB2 | TA323758 | Rabbit | 1:50 |

**Table 1: Antibodies details. Target, Catalogue number, Company, source, and working dilution for Western Blot, IHC, and conventional IF.**

# Chapter 8

# 8. Synthesis

## Aim 1 & 2

Airway dysfunction is a common denominator of chronic lung diseases including asthma. Alteration in sphingolipid metabolism has been suggested as a possible mechanism in Asthma susceptibility and exacerbation.
Sphingosine 1-phosphate (S1P) is a potent bioactive molecule involved in a variety of cellular processes, including cell differentiation, proliferation, and migration. Many studies have shown the crucial role of S1P in driving molecular mechanisms involved in pulmonary diseases among which a significant positive correlation between S1P levels and epithelial-mesenchymal transition (EMT), AHR and inflammation [83]. In asthma-features development the contribution of S1P as an inducer of EMT happens through the regulation of TGF-β signaling has been demonstrated. Thus, targeting the S1P/TGF-β axis may hold promise as a feasible therapeutic target to prevent lung dysfunction in pulmonary diseases associated with EMT such as asthma [75].

Sex differences in the anatomy and physiology of the respiratory system have been widely known and reported by various studies. From birth to adult life, significant differences exist between male and female lungs. Changes in sex hormone levels during development, puberty, and physiological events such as pregnancy and menopause, also influence lung function and health [41].
These differences in the respiratory system can therefore contribute to a different predisposition to the development, progression, and pharmacological response in respiratory diseases, like Asthma and COPD. The involvement of sphingolipids in the development of asthma has been widely discussed, and

several studies show that exists a correlation between sphingolipids and sexual hormones such as estrogens [72].

Starting from this evidence, the first aim of the study was to identify the role of sphingolipid metabolism in the development of chronic lung disease and the interaction with sexual hormones.

In the first study we investigated the sphingosine-1-phosphate (S1P) role in EMT and its involvement in asthma-related airway dysfunction. Our data showed that, following incubation with TGF-β or S1P, A549 acquired a fibroblast-like morphology associated with an increase of mesenchymal markers and down-regulation of the epithelial. These effects are reversed by treatment with the TGF-β receptor antagonist LY2109761. On the other hand, systemic administration of S1P to BALB/c mice induces asthma-like disease characterized by mucous cell metaplasia and increased levels of TGF-β, IL-33 and FGF-2 within the lung. The bronchi harvested from S1P-treated mice display bronchial hyperresponsiveness associated with overexpression of the mesenchymal and fibrosis markers and reduction of the epithelial. The S1P-induced switch from the epithelial toward the mesenchymal pattern correlates to a significant increase of lung resistance and fibroblast activation. TGF-β blockade, in S1P-treated mice, abrogates these effects. Finally, inhibition of sphingosine kinases by SK1-II in OVA-sensitized mice, abrogates EMT, pulmonary TGF-β up-regulation, fibroblasts recruitment and airway hyperresponsiveness.
These data demonstrate how targeting S1P/TGF-β axis may hold promise as a feasible therapeutic target to control airway dysfunction in asthma [75].

In the second study, we investigate the impact of sex on the modulation of sphingolipid metabolism and the role of S1P signaling in driving sex-related differences in asthma features. Our data demonstrate that the sex differences in asthma susceptibility depend on ORMDL/S1P signaling, upregulated in females already in the controls, that could be correlated to the higher predisposition, in women, to develop asthma; indeed, female BALB/c mice showed a pulmonary ORMDL3 upregulation compared to males. This difference was coupled to the highest levels of pulmonary interleukin-5 and plasma IgE levels in female BALB/c mice. Accordingly, female BALB/c-derived bronchi exhibited airway hyperresponsiveness (AHR), S1P signaling upregulation and downregulation of its transporter SpnS2 compared to males. Furthermore, we found that S1P signaling effects were influenced by sexual hormones, indeed pharmacological blockage of S1P signaling or tamoxifen supplementation to females abrogated sexual dimorphism in airway function and S1P signaling. Conversely, estradiol supplementation in male BALB/c mice induced AHR as well as S1P signaling upregulation. Histological and immunohistochemical analysis showed concomitant sex differences in airway structure, ORMDL3, and SpnS2 expression that were reversed by hormonal modulation. In vitro experiments confirmed estradiol's capacity to upregulate S1P signaling and transcription of the ORMDL3 gene in human airway epithelium.

These data support the hypothesis of sex-related differences in the lung, which contribute to differential susceptibility to the development of asthma. Furthermore, sex is also a crucial determinant of sphingolipid metabolism and S1P role in airway function. Therefore, S1P signaling could represent a target in sex-tailored drug therapy in asthma.

Subsequently, in the last study, we investigated the effect of the dysregulation of sphingolipids in the development of the major symptoms of COPD in men and women. Our data demonstrate that women with COPD showed a higher level of a-SMA, ORMDL3 and ASAH1 in their lungs, than men. That translates in higher level of ceramide in men, which is associated with higher incidence of developing emphysema in COPD exacerbation, and higher level of S1P in women which is associated to a lower incidence of emphysema but higher AHR and lung inflammation. In vivo study confirmed the higher incidence of female mice developing AHR after Cigarette smoke exposure. The pharmacological blockade of ceramide pathway abrogates this hyperreactivity. Also, the cellular studies underlined the interaction between sexual hormones and sphingolipids pathway after cigarette smoke exposure. CSE increases ASAH1 and ORMDL3 expression and so S1P production, only after estradiol treatment. The increase in S1P translates in higher cellular proliferation, speed migration and contraction, while, the inhibition of ceramidase, abrogates the effect of estradiol on cellular functionality and proliferation.

For these reasons, sex differences observed in COPD symptoms might be associated with an estrogen-dependent dysregulation of sphingolipid metabolism.

## Aim 3

Chronic respiratory diseases, like asthma and COPD, are one of the main causes of morbidity and mortality worldwide. For these diseases doesn't exist a resolving treatment but just medication for the control of the symptoms, aiming to improve the quality of patient's life. The most common drugs used

in therapy are bronchodilators and corticosteroids with chronic use. Unfortunately, a prolonged use of these drugs induces a reduction in receptor responsiveness, that is caused by a prolonged stimulation of β2 -agonists or by the interaction of many pro-inflammatory mediators with β2 -AR, this process is known as desensitization [27].

Furthermore, the chronic use of corticosteroids (especially the oral one) could also cause systemic side effects including osteoporosis, bone fractures, diabetes, ocular disorders, and respiratory infections.

These limits suggest the need to develop new therapeutic strategies that aim to find advanced combinations to delay the desensitization process, and to reduce the dosage of corticosteroids to be taken, as much as possible, obtaining the same therapeutic result [26].

T third aim of the study was to identify new therapeutic strategies for asthma treatments, that could overcome the major limits of the usual treatment.

In the first study, our data demonstrate the essential role of $H_2S$ in airway function and its contribution to improving asthma features. A drug's combination resulted positively in the management of asthma features, that is, Prednisone, a common anti-inflammatory drug, and TBZ, an $H_2S$ donor molecule with slow release; this combination could provide a suitable approach to manage asthma features with a particular impact on airway remodeling.

In the *in vitro* study we found that PS-TBZ exhibited an increased effect compared to the individual parent compounds in modulating the production of inflammatory mediators. TBZ also significantly reduced bronchial contractility and enhanced bronchial relaxation. In the *in vivo* experiments, where we administered PS, TBZ, or PS-TBZ to ovalbumin-sensitized BALB/c mice, we confirmed that PS-TBZ had a significantly better action in

controlling airway hyperreactivity as compared to TBZ or PS alone. Moreover, PS-TBZ was more effective in restoring salbutamol-induced relaxation. The immunohistochemistry analysis demonstrated a significant reduction in the production of α-SMA and procollagen III, indicating the efficacy of PS-TBZ in controlling airway remodeling. Moreover, PS-TBZ also promoted epithelial repair, and recovery of the bronchial and parenchyma structure and inhibited mucin production. In conclusion, PS-TBZ provides an opportunity to optimize the beneficial impact of corticosteroids by reducing dosages and associated side effects [80].

In the second study we showed that the combination of beta-agonist SABA/LABA with Montelukast, an anti-leukotriene used for asthma therapy, could overcome one of the major limits of $\beta_2$-agonists rescue therapy, avoiding the desensitization on the $\beta_2$ receptor and preserving the rescue therapy as well as reducing AHR and lung inflammation.

The study has been conducted in vitro and in vivo and takes advantage of the synthesis of a salt that gave us the possibility to simultaneously administer in vivo formoterol and montelukast (MFS). In vitro studies demonstrate that montelukast (1) preserves β2-agonist response in isolated bronchi by preventing homologous β2-adrenoceptor desensitization; (2) reduces desensitization by modulating β2-receptor translocation in bronchial epithelial cells. In vivo studies demonstrate that sensitized mice receiving formoterol or montelukast display a significant reduction in airway hyperresponsiveness, but the β2-agonist relaxing response is still impaired. Allergen challenge causes $\beta_2$ heterologous desensitization that is further increased by treatment in vivo with formoterol. MFS not only inhibits airway hyperresponsiveness, but it rescues the β2-agonist response. Histological analysis confirms the functional data, demonstrating an enhanced therapeutic efficiency of MSF in

controlling also pulmonary metaplasia and lung inflammation. MFS is efficacious also when sensitized mice receive the drug by local administration. In conclusion, our data evidenced a therapeutic advantage in the association of β2-agonists with montelukast in the control of asthma-like features and a better rescue bronchodilation response to β2-agonists [104].

# Publications

- Cerqua, I., Granato, E., Petti, A., Pavese, R., Costa, S. K. P., Feitosa, K. B., Soares, A. G., Muscara, M., Camerlingo, R., Rea, G., Fiorino, F., Santagada, V., Frecentese, F., Cirino, G., Caliendo, G., Severino, B., & Roviezzo, F. (2022). Enhanced efficacy of formoterol-montelukast salt in relieving asthma features and in preserving β2-agonists rescue therapy. *Pharmacological research*, *186*, 106536. https://doi.org/10.1016/j.phrs.2022.106536

- Cerqua, I., Granato, E., Corvino, A., Severino, B., D'Avino, D., Simonelli, M., Perissutti, E., Scognamiglio, A., Mirra, D., D'Agostino, B., Caliendo, G., Rossi, A., Cirino, G., Motta, C. M., & Roviezzo, F. (2023). Prednisone-hydrogen sulfide releasing hybrid shows improved therapeutic profile in asthma. *Frontiers in pharmacology*, *14*, 1266934. https://doi.org/10.3389/fphar.2023.1266934

- Riemma, M. A., Cerqua, I., Romano, B., Irollo, E., Bertolino, A., Camerlingo, R., Granato, E., Rea, G., Scala, S., Terlizzi, M., Spaziano, G., Sorrentino, R., D'Agostino, B., Roviezzo, F., & Cirino, G. (2022). Sphingosine-1-phosphate/TGF-β axis drives epithelial mesenchymal transition in asthma-like disease. *British journal of pharmacology*, *179*(8), 1753–1768. https://doi.org/10.1111/bph.15754

- Corvino, A., Cerqua, I., Lo Bianco, A., Caliendo, G., Fiorino, F., Frecentese, F., Magli, E., Morelli, E., Perissutti, E., Santagada, V., Cirino, G., Granato, E., Roviezzo, F., Puliti, E., Bernacchioni, C., Lavecchia, A., Donati, C., & Severino, B. (2021). Antagonizing $S1P_3$ Receptor with Cell-Penetrating Pepducins in Skeletal Muscle Fibrosis. *International journal of molecular sciences*, *22*(16), 8861. https://doi.org/10.3390/ijms22168861

- Cerqua, I., Musella, S., Peltner, L. K., D'Avino, D., Di Sarno, V., Granato, E., Vestuto, V., Di Matteo, R., Pace, S., Ciaglia, T., Bilancia, R., Smaldone, G., Di Matteo, F., Di Micco, S., Bifulco, G., Pepe, G., Basilicata, M. G., Rodriquez, M., Gomez-Monterrey, I. M., Campiglia, P., Bertamino, A. (2022). Discovery and Optimization of Indoline-Based Compounds as Dual 5-LOX/sEH Inhibitors: *In Vitro* and *In Vivo* Anti-Inflammatory Characterization. *Journal of medicinal chemistry*, *65*(21), 14456–14480. https://doi.org/10.1021/acs.jmedchem.2c00817

- D'Avino, D., Cerqua, I., Ullah, H., Spinelli, M., Di Matteo, R., Granato, E., Capasso, R., Maruccio, L., Ialenti, A., Daglia, M., Roviezzo, F., & Rossi, A. (2023). Beneficial Effects of *Astragalus membranaceus* (Fisch.) Bunge Extract in Controlling Inflammatory Response and Preventing Asthma Features. *International journal of molecular sciences*, *24*(13), 10954. https://doi.org/10.3390/ijms241310954

- Mirra, D., Cione, E., Spaziano, G., Esposito, R., Sorgenti, M., Granato, E., Cerqua, I., Muraca, L., Iovino, P., Gallelli, L., & D'Agostino, B. (2022). Circulating MicroRNAs Expression Profile in Lung Inflammation: A Preliminary Study. *Journal of clinical medicine*, *11*(18), 5446. https://doi.org/10.3390/jcm11185446

- Cerqua, I., Neukirch, K., Terlizzi, M., Granato, E., Caiazzo, E., Cicala, C., Ialenti, A., Capasso, R., Werz, O., Sorrentino, R., Seraphin, D., Helesbeux, J. J., Cirino, G., Koeberle, A., Roviezzo, F., & Rossi, A. (2022). A vitamin E long-chain metabolite and the inspired drug candidate α-amplexichromanol relieve asthma features in an experimental model of allergen sensitization. *Pharmacological research*, *181*, 106250. https://doi.org/10.1016/j.phrs.2022.106250

# References

[1] Hansen-Flaschen, J. and Bates, . David V. (2023, November 26). respiratory disease. Encyclopedia Britannica. https://www.britannica.com/science/respiratory-disease

[2] Cukic, V., Lovre, V., Dragisic, D., & Ustamujic, A. (2012). Asthma and Chronic Obstructive Pulmonary Disease (COPD) - Differences and Similarities. *Materia socio-medica*, *24*(2), 100–105. https://doi.org/10.5455/msm.2012.24.100-105

[3] Mims J. W. (2015). Asthma: definitions and pathophysiology. *International forum of allergy & rhinology*, *5 Suppl 1*, S2–S6. https://doi.org/10.1002/alr.21609

[4] National Heart, Lung, and Blood Institute. Guide-lines for the Diagnosis and Management of Asthma (EPR-3). 2007. http://www.nhlbi.nih.gov/guidelines/ asthma/index.htm.

[5] Ober, C., & Yao, T. C. (2011). The genetics of asthma and allergic disease: a 21st century perspective. *Immunological reviews*, *242*(1), 10–30. https://doi.org/10.1111/j.1600-065X.2011.01029.x

[6] Holloway, J. W., Yang, I. A., & Holgate, S. T. (2010). Genetics of allergic disease. *The Journal of allergy and clinical immunology*, *125*(2 Suppl 2), S81–S94. https://doi.org/10.1016/j.jaci.2009.10.071

[7] Jackson, D. J. (2008). Wheezing rhinovirus illnesses in early life predict asthma development in high-risk children. *American journal of respiratory and critical care medicine*, *178*(7), 667–672. https://doi.org/10.1164/rccm.200802-309OC

[8] Harb, H., & Renz, H. (2015). Update on epigenetics in allergic disease. *The Journal of allergy and clinical immunology*, *135*(1), 15–24. https://doi.org/10.1016/j.jaci.2014.11.009

[9] Busse, W. W., & Lemanske, R. F., Jr (2001). Asthma. *The New England journal of medicine*, *344*(5), 350–362. https://doi.org/10.1056/NEJM200102013440507)

[10] Stevenson, D. D., & Szczeklik, A. (2006). Clinical and pathologic perspectives on aspirin sensitivity and asthma. *The Journal of allergy and clinical immunology*, *118*(4), 773–788. https://doi.org/10.1016/j.jaci.2006.07.024

[11] National Asthma Education and Prevention Program: Guidelines for the Diagnosis and Management of Asthma. Bethesda (MD): National Heart, Lung, and Blood Institute (US); 2007 Aug. https://www.ncbi.nlm.nih.gov/books/NBK7223/

[12] Holgate, S. T., & Polosa, R. (2006). The mechanisms, diagnosis, and management of severe asthma in adults. *Lancet (London, England)*, *368*(9537), 780–793. https://doi.org/10.1016/S0140-6736(06)69288-X)

[13] Fahy J. V. (2015). Type 2 inflammation in asthma--present in most, absent in many. *Nature reviews. Immunology*, *15*(1), 57–65. https://doi.org/10.1038/nri3786

[14] Bunyavanich, S., & Schadt, E. E. (2015). Systems biology of asthma and allergic diseases: a multiscale approach. *The Journal of allergy and clinical immunology*, *135*(1), 31–42. https://doi.org/10.1016/j.jaci.2014.10.015

[15] Djuric-Filipovic, I., Caminati, M., Filipovic, D., Salvottini, C., & Zivkovic, Z. (2017). Effects of specific allergen immunotherapy on biological markers and clinical parameters in asthmatic children: a controlled-real life study. *Clinical and molecular allergy : CMA*, *15*, 7. https://doi.org/10.1186/s12948-017-0064-5

[16] Gans, M. D., & Gavrilova, T. (2020). Understanding the immunology of asthma: Pathophysiology, biomarkers, and treatments for asthma endotypes. *Paediatric respiratory reviews*, *36*, 118–127. https://doi.org/10.1016/j.prrv.2019.08.002

[17] Mansur, A. H., Srivastava, S., Mitchell, V., Sullivan, J., & Kasujee, I. (2017). Longterm clinical outcomes of omalizumab therapy in severe allergic asthma: Study of efficacy and safety. *Respiratory medicine*, *124*, 36–43. https://doi.org/10.1016/j.rmed.2017.01.008

[18] Dweik, R. A., Boggs, P. B., Erzurum, S. C., Irvin, C. G., Leigh, M. W., Lundberg, J. O., Olin, A. C., Plummer, A. L., Taylor, D. R., & American Thoracic Society Committee on Interpretation of Exhaled Nitric Oxide Levels (FENO) for Clinical Applications (2011). An official ATS clinical practice guideline: interpretation of exhaled nitric oxide levels (FENO) for clinical applications. *American journal of respiratory and critical care medicine*, *184*(5), 602–615. https://doi.org/10.1164/rccm.9120-11ST

[19] Kaur, R., & Chupp, G. (2019). Phenotypes and endotypes of adult asthma: Moving toward precision medicine. *The Journal of allergy and clinical immunology*, *144*(1), 1–12. https://doi.org/10.1016/j.jaci.2019.05.031

[20] Bateman, E. D., Hurd, S. S., Barnes, P. J., Bousquet, J., Drazen, J. M., FitzGerald, J. M., Gibson, P., Ohta, K., O'Byrne, P., Pedersen, S. E.,

Pizzichini, E., Sullivan, S. D., Wenzel, S. E., & Zar, H. J. (2008). Global strategy for asthma management and prevention: GINA executive summary. *The European respiratory journal*, *31*(1), 143–178. https://doi.org/10.1183/09031936.00138707

[21] Zöllner, E. W., Lombard, C. J., Galal, U., Hough, F. S., Irusen, E. M., & Weinberg, E. (2012). Hypothalamic-pituitary-adrenal axis suppression in asthmatic school children. *Pediatrics*, *130*(6), e1512–e1519. https://doi.org/10.1542/peds.2012-1147

[22] Naqvi, M., Tcheurekdjian, H., DeBoard, J. A., Williams, L. K., Navarro, D., Castro, R. A., Rodriguez-Santana, J. R., Chapela, R., Watson, H. G., Meade, K., Rodriguez-Cintron, W., LeNoir, M., Thyne, S. M., Avila, P. C., Choudhry, S., & Burchard, E. G. (2008). Inhaled corticosteroids and augmented bronchodilator responsiveness in Latino and African American asthmatic patients. *Annals of allergy, asthma & immunology : official publication of the American College of Allergy, Asthma, & Immunology*, *100*(6), 551–557. https://doi.org/10.1016/S1081-1206(10)60055-5

[23] Levin, A. M., Gui, H., Hernandez-Pacheco, N., Yang, M., Xiao, S., Yang, J. J., Hochstadt, S., Barczak, A. J., Eckalbar, W. L., Rynkowski, D., Samedy, L. A., Kwok, P. Y., Pino-Yanes, M., Erle, D. J., Lanfear, D. E., Burchard, E. G., & Williams, L. K. (2019). Integrative approach identifies corticosteroid response variant in diverse populations with asthma. *The Journal of allergy and clinical immunology*, *143*(5), 1791–1802. https://doi.org/10.1016/j.jaci.2018.09.034

[24] Busse, W. W., Bateman, E. D., Caplan, A. L., Kelly, H. W., O'Byrne, P. M., Rabe, K. F., & Chinchilli, V. M. (2018). Combined Analysis of Asthma

Safety Trials of Long-Acting $\beta_2$-Agonists. *The New England journal of medicine*, *378*(26), 2497–2505. https://doi.org/10.1056/NEJMoa1716868

[25] Pacheco, Y., Freymond, N., & Devouassoux, G. (2014). Impact of montelukast on asthma associated with rhinitis, and other triggers and co-morbidities. *The Journal of asthma : official journal of the Association for the Care of Asthma*, *51*(1), 1–17. https://doi.org/10.3109/02770903.2013.822081

[26] Vianna, E. O., & Martin, R. J. (1998). Bronchodilators and corticosteroids in the treatment of asthma. *Drugs of today (Barcelona, Spain : 1998)*, *34*(3), 203–223. https://doi.org/10.1358/dot.1998.34.3.485166

[27] Shore, S. A., & Moore, P. E. (2003). Regulation of beta-adrenergic responses in airway smooth muscle. *Respiratory physiology & neurobiology*, *137*(2-3), 179–195. https://doi.org/10.1016/s1569-9048(03)00146-0

[28] Agarwal AK, Raja A, Brown BD. Chronic Obstructive Pulmonary Disease. [Updated 2023 Aug 7]. In: StatPearls [Internet]. Treasure Island (FL): StatPearls Publishing; 2023 Jan-. Available from: https://www.ncbi.nlm.nih.gov/books/NBK559281/

[29] Singh, D., Agusti, A., Anzueto, A., Barnes, P. J., Bourbeau, J., Celli, B. R., Criner, G. J., Frith, P., Halpin, D. M. G., Han, M., López Varela, M. V., Martinez, F., Montes de Oca, M., Papi, A., Pavord, I. D., Roche, N., Sin, D. D., Stockley, R., Vestbo, J., Wedzicha, J. A., … Vogelmeier, C. (2019). Global Strategy for the Diagnosis, Management, and Prevention of Chronic Obstructive Lung Disease: the GOLD science committee report 2019. *The European respiratory journal*, *53*(5), 1900164. https://doi.org/10.1183/13993003.00164-2019

[30] Lareau, S. C., Fahy, B., Meek, P., & Wang, A. (2019). Chronic Obstructive Pulmonary Disease (COPD). *American journal of respiratory and critical care medicine*, *199*(1), P1–P2. https://doi.org/10.1164/rccm.1991P1

[31] Polverino, M., Capuozzo, A., Cicchitto, G., Ferrigno, F., Mauro, I., Santoriello, C., Sirignano, E., Aliverti, A., Celli, B., & Polverino, F. (2020). Smoking Pattern in Men and Women: A Possible Contributor to Sex Differences in Smoke-related Lung Diseases. *American journal of respiratory and critical care medicine*, *202*(7), 1048–1051. https://doi.org/10.1164/rccm.202004-1472LE

[32] MacNee W. Pathology, pathogenesis, and pathophysiology. BMJ. 2006 May 20;332(7551):1202–4. PMCID: PMC1463976

[33] Qaseem, A., Wilt, T. J., Weinberger, S. E., Hanania, N. A., Criner, G., van der Molen, T., Marciniuk, D. D., Denberg, T., Schünemann, H., Wedzicha, W., MacDonald, R., Shekelle, P., American College of Physicians, American College of Chest Physicians, American Thoracic Society, & European Respiratory Society (2011). Diagnosis and management of stable chronic obstructive pulmonary disease: a clinical practice guideline update from the American College of Physicians, American College of Chest Physicians, American Thoracic Society, and European Respiratory Society. *Annals of internal medicine*, *155*(3), 179–191. https://doi.org/10.7326/0003-4819-155-3-201108020-00008

[34] ATS Committee on Proficiency Standards for Clinical Pulmonary Function Laboratories (2002). ATS statement: guidelines for the six-minute

walk test. *American journal of respiratory and critical care medicine*, *166*(1), 111–117. https://doi.org/10.1164/ajrccm.166.1.at1102

[35] Shaker, S. B., Dirksen, A., Bach, K. S., & Mortensen, J. (2007). Imaging in chronic obstructive pulmonary disease. *COPD*, *4*(2), 143–161. https://doi.org/10.1080/15412550701341277

[36] Melani A. S. (2015). Long-acting muscarinic antagonists. *Expert review of clinical pharmacology*, *8*(4), 479–501. https://doi.org/10.1586/17512433.2015.1058154

[37] Ram, F. S., Jones, P. W., Castro, A. A., De Brito, J. A., Atallah, A. N., Lacasse, Y., Mazzini, R., Goldstein, R., & Cendon, S. (2002). Oral theophylline for chronic obstructive pulmonary disease. *The Cochrane database of systematic reviews*, *2002*(4), CD003902. https://doi.org/10.1002/14651858.CD003902

[38] Nannini, L. J., Lasserson, T. J., & Poole, P. (2012). Combined corticosteroid and long-acting beta (2)-agonist in one inhaler versus long-acting beta (2)-agonists for chronic obstructive pulmonary disease. *The Cochrane database of systematic reviews*, *2012*(9), CD006829. https://doi.org/10.1002/14651858.CD006829.pub2

[39] Rabe K. F. (2011). Update on roflumilast, a phosphodiesterase 4 inhibitor for the treatment of chronic obstructive pulmonary disease. *British journal of pharmacology*, *163*(1), 53–67. https://doi.org/10.1111/j.1476-5381.2011.01218.x

[40] Albert, R. K., Connett, J., Bailey, W. C., Casaburi, R., Cooper, J. A., Jr, Criner, G. J., Curtis, J. L., Dransfield, M. T., Han, M. K., Lazarus, S. C., Make,

B., Marchetti, N., Martinez, F. J., Madinger, N. E., McEvoy, C., Niewoehner, D. E., Porsasz, J., Price, C. S., Reilly, J., Scanlon, P. D., … COPD Clinical Research Network (2011). Azithromycin for prevention of exacerbations of COPD. *The New England journal of medicine*, *365*(8), 689–698. https://doi.org/10.1056/NEJMoa1104623

[41] Silveyra, P., Fuentes, N., & Rodriguez Bauza, D. E. (2021). Sex and Gender Differences in Lung Disease. *Advances in experimental medicine and biology*, *1304*, 227–258. https://doi.org/10.1007/978-3-030-68748-9_14

[42] Carrel, L., & Willard, H. F. (2005). X-inactivation profile reveals extensive variability in X-linked gene expression in females. *Nature*, *434*(7031), 400–404. https://doi.org/10.1038/nature03479

[43] Rysavy, M. A., Horbar, J. D., Bell, E. F., Li, L., Greenberg, L. T., Tyson, J. E., Patel, R. M., Carlo, W. A., Younge, N. E., Green, C. E., Edwards, E. M., Hintz, S. R., Walsh, M. C., Buzas, J. S., Das, A., Higgins, R. D., & Eunice Kennedy Shriver National Institute of Child Health and Human Development Neonatal Research Network and Vermont Oxford Network (2020). Assessment of an Updated Neonatal Research Network Extremely Preterm Birth Outcome Model in the Vermont Oxford Network. *JAMA pediatrics*, *174*(5), e196294. https://doi.org/10.1001/jamapediatrics.2019.6294

[44] GBD 2016 Disease and Injury Incidence and Prevalence Collaborators (2017). Global, regional, and national incidence, prevalence, and years lived with disability for 328 diseases and injuries for 195 countries, 1990-2016: a systematic analysis for the Global Burden of Disease Study 2016. *Lancet (London, England)*, *390*(10100), 1211–1259. https://doi.org/10.1016/S0140-6736(17)32154-2

[45] Chowdhury, N. U., Guntur, V. P., Newcomb, D. C., & Wechsler, M. E. (2021). Sex and gender in asthma. *European respiratory review : an official journal of the European Respiratory Society*, *30*(162), 210067. https://doi.org/10.1183/16000617.0067-2021

[46] Moore, W. C., Bleecker, E. R., Curran-Everett, D., Erzurum, S. C., Ameredes, B. T., Bacharier, L., Calhoun, W. J., Castro, M., Chung, K. F., Clark, M. P., Dweik, R. A., Fitzpatrick, A. M., Gaston, B., Hew, M., Hussain, I., Jarjour, N. N., Israel, E., Levy, B. D., Murphy, J. R., Peters, S. P. National Heart, Lung, Blood Institute's Severe Asthma Research Program (2007). Characterization of the severe asthma phenotype by the National Heart, Lung, and Blood Institute's Severe Asthma Research Program. *The Journal of allergy and clinical immunology*, *119*(2), 405–413. https://doi.org/10.1016/j.jaci.2006.11.639

[47] Loisel, D. A., Tan, Z., Tisler, C. J., Evans, M. D., Gangnon, R. E., Jackson, D. J., Gern, J. E., Lemanske, R. F., Jr, & Ober, C. (2011). IFNG genotype and sex interact to influence the risk of childhood asthma. *The Journal of allergy and clinical immunology*, *128*(3), 524–531. https://doi.org/10.1016/j.jaci.2011.06.016

[48] Yung, J. A., Fuseini, H., & Newcomb, D. C. (2018). Hormones, sex, and asthma. *Annals of allergy, asthma & immunology : official publication of the American College of Allergy, Asthma, & Immunology*, *120*(5), 488–494. https://doi.org/10.1016/j.anai.2018.01.016

[49] Fuseini, H., & Newcomb, D. C. (2017). Mechanisms Driving Gender Differences in Asthma. *Current allergy and asthma reports*, *17*(3), 19. https://doi.org/10.1007/s11882-017-0686-1

[50] Blanquart, E., Mandonnet, A., Mars, M., Cenac, C., Anesi, N., Mercier, P., Audouard, C., Roga, S., Serrano de Almeida, G., Bevan, C. L., Girard, J. P., Pelletier, L., Laffont, S., & Guéry, J. C. (2022). Targeting androgen signaling in ILC2s protects from IL-33-driven lung inflammation, independently of KLRG1. *The Journal of allergy and clinical immunology*, *149*(1), 237–251.e12. https://doi.org/10.1016/j.jaci.2021.04.029

[51] Aryal, S., Diaz-Guzman, E., & Mannino, D. M. (2013). COPD and gender differences: an update. *Translational research: the journal of laboratory and clinical medicine*, *162*(4), 208–218. https://doi.org/10.1016/j.trsl.2013.04.003

[52] Tam, A., Morrish, D., Wadsworth, S., Dorscheid, D., Man, S. F., & Sin, D. D. (2011). The role of female hormones on lung function in chronic lung diseases. *BMC women's health*, *11*, 24. https://doi.org/10.1186/1472-6874-11-24

[53] Hannun, Y. A., & Obeid, L. M. (2008). Principles of bioactive lipid signalling: lessons from sphingolipids. *Nature reviews. Molecular cell biology*, *9*(2), 139–150. https://doi.org/10.1038/nrm2329

[54] Larry R. Engelking. (2015). Chapter 59 - Sphingolipids, Textbook of Veterinary Physiological Chemistry (Third Edition),Pages 378-383, https://doi.org/10.1016/B978-0-12-391909-0.50059-1.

[55] Turpin-Nolan, S. M., & Brüning, J. C. (2020). The role of ceramides in metabolic disorders: when size and localization matters. *Nature reviews. Endocrinology*, *16*(4), 224–233. https://doi.org/10.1038/s41574-020-0320-5

[56] Mendelson, K., Evans, T., & Hla, T. (2014). Sphingosine 1-phosphate signalling. *Development (Cambridge, England)*, *141*(1), 5–9. https://doi.org/10.1242/dev.094805

[57] Strub, G. M., Maceyka, M., Hait, N. C., Milstien, S., & Spiegel, S. (2010). Extracellular and intracellular actions of sphingosine-1-phosphate. *Advances in experimental medicine and biology*, *688*, 141–155. https://doi.org/10.1007/978-1-4419-6741-1_10

[58] Renault, A. D., Kunwar, P. S., & Lehmann, R. (2010). Lipid phosphate phosphatase activity regulates dispersal and bilateral sorting of embryonic germ cells in Drosophila. *Development (Cambridge, England)*, *137*(11), 1815–1823. https://doi.org/10.1242/dev.046110

[59] Ghidoni, R., Caretti, A., & Signorelli, P. (2015). Role of Sphingolipids in the Pathobiology of Lung Inflammation. *Mediators of inflammation*, *2015*, 487508. https://doi.org/10.1155/2015/487508

[60] Uhlig, S., & Yang, Y. (2013). Sphingolipids in acute lung injury. *Handbook of experimental pharmacology*, (216), 227–246. https://doi.org/10.1007/978-3-7091-1511-4_11

[61] Anderson G. P. (2008). Endotyping asthma: new insights into key pathogenic mechanisms in a complex, heterogeneous disease. *Lancet (London, England)*, *372*(9643), 1107–1119. https://doi.org/10.1016/S0140-6736(08)61452-X

[62] Ono, J. G., Worgall, T. S., & Worgall, S. (2015). Airway reactivity and sphingolipids-implications for childhood asthma. *Molecular and cellular pediatrics*, *2*(1), 13. https://doi.org/10.1186/s40348-015-0025-3

[63] Nishiuma, T., Nishimura, Y., Okada, T., Kuramoto, E., Kotani, Y., Jahangeer, S., & Nakamura, S. (2008). Inhalation of sphingosine kinase inhibitor attenuates airway inflammation in asthmatic mouse model. *American journal of physiology. Lung cellular and molecular physiology*, *294*(6), L1085–L1093. https://doi.org/10.1152/ajplung.00445.2007

[64] Blé, F. X., Cannet, C., Zurbruegg, S., Gérard, C., Frossard, N., Beckmann, N., & Trifilieff, A. (2009). Activation of the lung S1P (1) receptor reduces allergen-induced plasma leakage in mice. *British journal of pharmacology*, *158*(5), 1295–1301. https://doi.org/10.1111/j.1476-5381.2009.00391.x

[65] Roviezzo, F., D'Agostino, B., Brancaleone, V., De Gruttola, L., Bucci, M., De Dominicis, G., Orlotti, D., D'Aiuto, E., De Palma, R., Rossi, F., Sorrentino, R., & Cirino, G. (2010). Systemic administration of sphingosine-1-phosphate increases bronchial hyperresponsiveness in the mouse. *American journal of respiratory cell and molecular biology*, *42*(5), 572–577. https://doi.org/10.1165/rcmb.2009-0108OC

[66] Jolly, P. S., Bektas, M., Olivera, A., Gonzalez-Espinosa, C., Proia, R. L., Rivera, J., Milstien, S., & Spiegel, S. (2004). Transactivation of sphingosine-1-phosphate receptors by FcepsilonRI triggering is required for normal mast cell degranulation and chemotaxis. *The Journal of experimental medicine*, *199*(7), 959–970. https://doi.org/10.1084/jem.20030680

[67] Ammit, A. J., Hastie, A. T., Edsall, L. C., Hoffman, R. K., Amrani, Y., Krymskaya, V. P., Kane, S. A., Peters, S. P., Penn, R. B., Spiegel, S., & Panettieri, R. A., Jr (2001). Sphingosine 1-phosphate modulates human airway smooth muscle cell functions that promote inflammation and airway remodeling in asthma. *FASEB journal: official publication of the Federation of American Societies for Experimental Biology*, *15*(7), 1212–1214. https://doi.org/10.1096/fj.00-0742fje

[68] Oyeniran, C., Sturgill, J. L., Hait, N. C., Huang, W. C., Avni, D., Maceyka, M., Newton, J., Allegood, J. C., Montpetit, A., Conrad, D. H., Milstien, S., & Spiegel, S. (2015). Aberrant ORM (yeast)-like protein isoform 3 (ORMDL3) expression dysregulates ceramide homeostasis in cells and ceramide exacerbates allergic asthma in mice. *The Journal of allergy and clinical immunology*, *136*(4), 1035–46. e6. https://doi.org/10.1016/j.jaci.2015.02.031

[69] Petrache, I., Natarajan, V., Zhen, L., Medler, T. R., Richter, A. T., Cho, C., Hubbard, W. C., Berdyshev, E. V., & Tuder, R. M. (2005). Ceramide upregulation causes pulmonary cell apoptosis and emphysema-like disease in mice. *Nature medicine*, *11*(5), 491–498. https://doi.org/10.1038/nm1238

[70] Bowler, R. P., Jacobson, S., Cruickshank, C., Hughes, G. J., Siska, C., Ory, D. S., Petrache, I., Schaffer, J. E., Reisdorph, N., & Kechris, K. (2015). Plasma sphingolipids are associated with chronic obstructive pulmonary disease phenotypes. *American journal of respiratory and critical care medicine*, *191*(3), 275–284. https://doi.org/10.1164/rccm.201410-1771OC

[71] Lucki, N. C., & Sewer, M. B. (2008). Multiple roles for sphingolipids in steroid hormone biosynthesis. *Sub-cellular biochemistry*, *49*, 387–412. https://doi.org/10.1007/978-1-4020-8831-5_15

[72] Guo, S., Yu, Y., Zhang, N., Cui, Y., Zhai, L., Li, H., Zhang, Y., Li, F., Kan, Y., & Qin, S. (2014). Higher level of plasma bioactive molecule sphingosine 1-phosphate in women is associated with estrogen. *Biochimica et biophysica acta*, *1841*(6), 836–846. https://doi.org/10.1016/j.bbalip.2014.02.005

[73] Kilkenny, C., Browne, W. J., Cuthill, I. C., Emerson, M., & Altman, D. G. (2010). Improving bioscience research reporting: the ARRIVE guidelines for reporting animal research. *PLoS biology*, *8*(6), e1000412. https://doi.org/10.1371/journal.pbio.1000412

[74] Cerqua, I., Granato, E., Petti, A., Pavese, R., Costa, S. K. P., Feitosa, K. B., Soares, A. G., Muscara, M., Camerlingo, R., Rea, G., Fiorino, F., Santagada, V., Frecentese, F., Cirino, G., Caliendo, G., Severino, B., & Roviezzo, F. (2022). Enhanced efficacy of formoterol-montelukast salt in relieving asthma features and in preserving β2-agonists rescue therapy. *Pharmacological research*, *186*, 106536. https://doi.org/10.1016/j.phrs.2022.106536

[75] Riemma, M. A., Cerqua, I., Romano, B., Irollo, E., Bertolino, A., Camerlingo, R., Granato, E., Rea, G., Scala, S., Terlizzi, M., Spaziano, G., Sorrentino, R., D'Agostino, B., Roviezzo, F., & Cirino, G. (2022). Sphingosine-1-phosphate/TGF-β axis drives epithelial mesenchymal transition in asthma-like disease. *British journal of pharmacology*, *179*(8), 1753–1768. https://doi.org/10.1111/bph.15754.

[76] Rossi, A., Roviezzo, F., Sorrentino, R., Riemma, M. A., Cerqua, I., Bilancia, R., Spaziano, G., Troisi, F., Pace, S., Pinto, A., D'Agostino, B., Werz, O., & Cirino, G. (2019). Leukotriene-mediated sex dimorphism in murine asthma-like features during allergen sensitization. *Pharmacological research*, *139*, 182–190. https://doi.org/10.1016/j.phrs.2018.11.024

[77] Cerqua, I., Terlizzi, M., Bilancia, R., Riemma, M. A., Citi, V., Martelli, A., Pace, S., Spaziano, G., D'Agostino, B., Werz, O., Ialenti, A., Sorrentino, R., Cirino, G., Rossi, A., & Roviezzo, F. (2020). 5α-dihydrotestosterone abrogates sex bias in asthma like features in the mouse. *Pharmacological research*, *158*, 104905. https://doi.org/10.1016/j.phrs.2020.104905

[78] Roviezzo, F., Sorrentino, R., Terlizzi, M., Riemma, M. A., Iacono, V. M., Rossi, A., Spaziano, G., Pinto, A., D'Agostino, B., & Cirino, G. (2017). Toll-Like Receptor 4 Is Essential for the Expression of Sphingosine-1-Phosphate-Dependent Asthma-Like Disease in Mice. *Frontiers in immunology*, *8*, 1336. https://doi.org/10.3389/fimmu.2017.01336

[79] Krenacs, L., Krenacs, T., Stelkovics, E., & Raffeld, M. (2010). Heat-induced antigen retrieval for immunohistochemical reactions in routinely processed paraffin sections. *Methods in molecular biology (Clifton, N.J.)*, *588*, 103–119. https://doi.org/10.1007/978-1-59745-324-0_14

[80] Cerqua, I., Granato, E., Corvino, A., Severino, B., D'Avino, D., Simonelli, M., Perissutti, E., Scognamiglio, A., Mirra, D., D'Agostino, B., Caliendo, G., Rossi, A., Cirino, G., Motta, C. M., & Roviezzo, F. (2023). Prednisone-hydrogen sulfide releasing hybrid shows improved therapeutic profile in asthma. *Frontiers in pharmacology*, *14*, 1266934. https://doi.org/10.3389/fphar.2023.1266934

[81] Polverino, F., Lu, B., Quintero, J. R., Vargas, S. O., Patel, A. S., Owen, C. A., Gerard, N. P., Gerard, C., & Cernadas, M. (2019). CFTR regulates B cell activation and lymphoid follicle development. *Respiratory research*, *20*(1), 133. https://doi.org/10.1186/s12931-019-1103-1

[82] Igari K, Kelly MJ, Yamanouchi D. Cigarette Smoke Extract Activates Tartrate-Resistant Acid Phosphatase-Positive Macrophage. J Vasc Res. 2019;56(3):139-151. doi: 10.1159/000498893. Epub 2019 May 7. PMID: 31064000; PMCID: PMC6764454.

[83] Roviezzo, F., Di Lorenzo, A., Bucci, M., Brancaleone, V., Vellecco, V., De Nardo, M., Orlotti, D., De Palma, R., Rossi, F., D'Agostino, B., & Cirino, G. (2007). Sphingosine-1-phosphate/sphingosine kinase pathway is involved in mouse airway hyperresponsiveness. *American journal of respiratory cell and molecular biology*, *36*(6), 757–762. https://doi.org/10.1165/rcmb.2006-0383OC

[84] Roviezzo, F., Sorrentino, R., Bertolino, A., De Gruttola, L., Terlizzi, M., Pinto, A., Napolitano, M., Castello, G., D'Agostino, B., Ianaro, A., Sorrentino, R., & Cirino, G. (2015). S1P-induced airway smooth muscle hyperresponsiveness and lung inflammation in vivo: molecular and cellular mechanisms. *British journal of pharmacology*, *172*(7), 1882–1893. https://doi.org/10.1111/bph.13033

[85] Slager, R. E., Hawkins, G. A., Li, X., Postma, D. S., Meyers, D. A., & Bleecker, E. R. (2012). Genetics of asthma susceptibility and severity. *Clinics in chest medicine*, *33*(3), 431–443. https://doi.org/10.1016/j.ccm.2012.05.005

[86] Martinez F. D. (2007). Genes, environments, development and asthma: a reappraisal. *The European respiratory journal*, *29*(1), 179–184. https://doi.org/10.1183/09031936.00087906

[87] Matteis, M., Polverino, F., Spaziano, G., Roviezzo, F., Santoriello, C., Sullo, N., Bucci, M. R., Rossi, F., Polverino, M., Owen, C. A., & D'Agostino, B. (2014). Effects of sex hormones on bronchial reactivity during the menstrual cycle. *BMC pulmonary medicine*, *14*, 108. https://doi.org/10.1186/1471-2466-14-108

[88] Fuerst, E., Foster, H. R., Ward, J. P., Corrigan, C. J., Cousins, D. J., & Woszczek, G. (2014). Sphingosine-1-phosphate induces pro-remodelling response in airway smooth muscle cells. *Allergy*, *69*(11), 1531–1539. https://doi.org/10.1111/all.12489

[89] Moffatt, M. F., Kabesch, M., Liang, L., Dixon, A. L., Strachan, D., Heath, S., Depner, M., von Berg, A., Bufe, A., Rietschel, E., Heinzmann, A., Simma, B., Frischer, T., Willis-Owen, S. A., Wong, K. C., Illig, T., Vogelberg, C., Weiland, S. K., von Mutius, E., Abecasis, G. R., Cookson, W. O. (2007). Genetic variants regulating ORMDL3 expression contribute to the risk of childhood asthma. *Nature*, *448*(7152), 470–473. https://doi.org/10.1038/nature06014

[90] Baeyens, A. A. L., & Schwab, S. R. (2020). Finding a Way Out: S1P Signaling and Immune Cell Migration. *Annual review of immunology*, *38*, 759–784. https://doi.org/10.1146/annurev-immunol-081519-083952

[91] Saba, N., Yusuf, O., Rehman, S., Munir, S., Noor, A., Saqlain, M., Mansoor, A., & Raja, G. K. (2018). Single nucleotide polymorphisms in asthma candidate genes *TBXA2R, ADAM33 FCER1B* and *ORMDL3* in

Pakistani asthmatics a case control study. *Asthma research and practice*, *4*, 4. https://doi.org/10.1186/s40733-018-0039-4

[92] Hannun, Y. A., & Obeid, L. M. (2008). Principles of bioactive lipid signalling: lessons from sphingolipids. *Nature reviews. Molecular cell biology*, *9*(2), 139–150. https://doi.org/10.1038/nrm2329

[93] Hisano, Y., Kobayashi, N., Yamaguchi, A., & Nishi, T. (2012). Mouse SPNS2 functions as a sphingosine-1-phosphate transporter in vascular endothelial cells. *PloS one*, *7*(6), e38941. https://doi.org/10.1371/journal.pone.0038941

[94] Cirino, G., Szabo, C., & Papapetropoulos, A. (2023). Physiological roles of hydrogen sulfide in mammalian cells, tissues, and organs. *Physiological reviews*, *103*(1), 31–276. https://doi.org/10.1152/physrev.00028.2021

[95] Chen, Y. H., Yao, W. Z., Gao, J. Z., Geng, B., Wang, P. P., & Tang, C. S. (2009). Serum hydrogen sulfide as a novel marker predicting bacterial involvement in patients with community-acquired lower respiratory tract infections. *Respirology (Carlton, Vic.)*, *14*(5), 746–752. https://doi.org/10.1111/j.1440-1843.2009.01550.x

[96] Hirota, N., & Martin, J. G. (2013). Mechanisms of airway remodeling. *Chest*, *144*(3), 1026–1032. https://doi.org/10.1378/chest.12-3073

[97] Alangari A. A. (2014). Corticosteroids in the treatment of acute asthma. *Annals of thoracic medicine*, *9*(4), 187–192. https://doi.org/10.4103/1817-1737.140120

[98] Guan, R., Wang, J., Cai, Z., Li, Z., Wang, L., Li, Y., Xu, J., Li, D., Yao, H., Liu, W., Deng, B., & Lu, W. (2020). Hydrogen sulfide attenuates cigarette smoke-induced airway remodeling by upregulating SIRT1 signaling pathway. *Redox biology*, *28*, 101356. https://doi.org/10.1016/j.redox.2019.101356

[99] Côté, A., Godbout, K., & Boulet, L. P. (2020). The management of severe asthma in 2020. *Biochemical pharmacology*, *179*, 114112. https://doi.org/10.1016/j.bcp.2020.114112

[100] Rossi, A., Khirani, S., & Cazzola, M. (2008). Long-acting beta2-agonists (LABA) in chronic obstructive pulmonary disease: efficacy and safety. *International journal of chronic obstructive pulmonary disease*, *3*(4), 521–529. https://doi.org/10.2147/copd.s1353

[101] Okunishi, K., & Peters-Golden, M. (2011). Leukotrienes and airway inflammation. *Biochimica et biophysica acta*, *1810*(11), 1096–1102. https://doi.org/10.1016/j.bbagen.2011.02.005

[102] Hon, K. L., Leung, T. F., & Leung, A. K. (2014). Clinical effectiveness and safety of montelukast in asthma. What are the conclusions from clinical trials and meta-analyses?. *Drug design, development and therapy*, *8*, 839–850. https://doi.org/10.2147/DDDT.S39100

[103] Pein, H., Ville, A., Pace, S., Temml, V., Garscha, U., Raasch, M., Alsabil, K., Viault, G., Dinh, C. P., Guilet, D., Troisi, F., Neukirch, K., König, S., Bilancia, R., Waltenberger, B., Stuppner, H., Wallert, M., Lorkowski, S., Weinigel, C., Rummler, S., Koeberle, A. (2018). Endogenous metabolites of vitamin E limit inflammation by targeting 5-lipoxygenase. *Nature communications*, *9*(1), 3834. https://doi.org/10.1038/s41467-018-06158-5

[104] Cerqua, I., Granato, E., Petti, A., Pavese, R., Costa, S. K. P., Feitosa, K. B., Soares, A. G., Muscara, M., Camerlingo, R., Rea, G., Fiorino, F., Santagada, V., Frecentese, F., Cirino, G., Caliendo, G., Severino, B., & Roviezzo, F. (2022). Enhanced efficacy of formoterol-montelukast salt in relieving asthma features and in preserving β2-agonists rescue therapy. *Pharmacological research*, *186*, 106536. https://doi.org/10.1016/j.phrs.2022.106536

[105] Chen, R., Michaeloudes, C., Liang, Y., Bhavsar, P. K., Chung, K. F., Ip, M. S. M., & Mak, J. C. W. (2022). ORMDL3 regulates cigarette smoke-induced endoplasmic reticulum stress in airway smooth muscle cells. *The Journal of allergy and clinical immunology*, *149*(4), 1445–1457.e5. https://doi.org/10.1016/j.jaci.2021.09.028

[106] Jia, M., Zhang, Y., Zhang, H., Qin, Q., & Xu, C. B. (2019). Cigarette Smoke Particles-Induced Airway Hyperreactivity in Vivo and in Vitro. *Biological & pharmaceutical bulletin*, *42*(5), 703–711. https://doi.org/10.1248/bpb.b18-00736

[107] Siegfried J. M. (2022). Sex and Gender Differences in Lung Cancer and Chronic Obstructive Lung Disease. *Endocrinology*, *163*(2), bqab254. https://doi.org/10.1210/endocr/bqab254

[108] Berdyshev, E. V., Serban, K. A., Schweitzer, K. S., Bronova, I. A., Mikosz, A., & Petrache, I. (2021). Ceramide and sphingosine-1 phosphate in COPD lungs. *Thorax*, thoraxjnl-2020-215892. Advance online publication. https://doi.org/10.1136/thoraxjnl-2020-215892

[109] Barnes P. J. (2016). Sex Differences in Chronic Obstructive Pulmonary Disease Mechanisms. *American journal of respiratory and critical care medicine*, *193*(8), 813–814. https://doi.org/10.1164/rccm.201512-2379ED

[110] Quinville, B. M., Deschenes, N. M., Ryckman, A. E., & Walia, J. S. (2021). A Comprehensive Review: Sphingolipid Metabolism and Implications of Disruption in Sphingolipid Homeostasis. *International journal of molecular sciences*, *22*(11), 5793. https://doi.org/10.3390/ijms22115793

[111] Hait, N. C., & Maiti, A. (2017). The Role of Sphingosine-1-Phosphate and Ceramide-1-Phosphate in Inflammation and Cancer. *Mediators of inflammation*, *2017*, 4806541. https://doi.org/10.1155/2017/4806541